SKI Report 2006:24

Research

Crack Characterisation for In-service Inspection Planning – An Update

Jan Wåle

May 2006

ISSN 1104-1374
ISRN SKI-R-06/24-SE

SKI

SKI perspective

Background

The need to qualify non-destructive testing systems (NDT systems) for pre- and in-service inspection has been recognised to a greater or lesser extent for many years in many countries engaged in nuclear power generation. However, NDT in general and qualification of NDT systems in particular are multidisciplinary and complex tasks. Development of NDT systems and demonstration of their effectiveness by qualifications require good knowledge in the NDT methods and techniques that are to be used as well as the influence from component geometry, material structure, defect morphologies, NDT operator (personnel) performance in different situations.

The representativeness of defects in the qualification test blocks is a key point in any practical assessment of NDT systems. The response of the defects used, with respect to the actual NDT system, must therefore adequately represent the response of the expected or observed real defects.

In 1994, SKI therefore initiated a work to characterize a number of morphology parameters for common crack mechanisms. The analysis was structured in a certain way to obtain consistency in future reporting as well as make further statistical evaluations and comparisons possible.

In 2005, this project was initiated to follow up the first project and to obtain even better statistical data.

Purpose of the project

The purpose of the project is to obtain better statistical analysis results of the most common morphology parameters for crack mechanisms primary for nuclear environments.

SKI believe such information is important for,

- work with qualifications of NDT systems
- work to simulate defects in qualification mock-ups in a realistic way
- developing NDT techniques suitable for different degradation mechanisms

It is also useful for evaluation of the leak flow rate for cracked nuclear components.

Results

The result of the survey gives an good overview of the most common morphology parameters for different crack mechanisms. The result confirms a lot of statements in the first report (SKI 95:70) but also present some new interesting results concerning the morphology of defects such as Interdendritic Stress Corrosion Cracking (IDSCC).

The results can consequently be used in In-Service Inspection planning as well as for NDT system developments and NDT qualifications. The results can also be used in leak flow rate calculations for developing leak detection systems.

SKI would also like to make some comments about the parameters surface roughness and the number of turns per mm which are important for the evaluation of the leak flow rate through

leaking cracks. The magnitudes of these parameters are determined by the way they are measured, particularly the magnification of the micro-graphs and the measuring length is important. A detailed explanation is given in the report how these values are measured. In the report, a magnification between 20 and 100 times has been used with a typical value of 50. The measuring length used has been 1-2 mm. In comparing the crack morphology values in this report with other published results, this information should be remembered.

Project information

Responsible for the project at SKI has been Peter Merck.
SKI reference: 14.43-200543105

SKI Report 2006:24

Research

Crack Characterisation for In-service Inspection Planning – An Update

Jan Wåle

Inspecta Technology AB
P.O. Box 30100
SE-104 25 Stockholm

May 2006

Summary

One important factor to optimize the NDT equipment and NDT procedure is to know the characteristics of the specific defects being sought for in each case. Thus, access is necessary to reliable morphology data of defects from all possible degradation mechanisms in all existing materials of the components that are subject to the NDT. In 1994 the Swedish Nuclear Power Inspectorate (SKI) initiated a project for compiling crack morphology data based on systematic studies of cracks that have been observed in different plants (nuclear and non-nuclear) in order to determine typical as well as more extreme values of e.g. orientation, width and surface roughness. Although, a large number of identified cracking incidents was covered by the work it was recognised that further studies were needed to increase the data base, and thereby getting more confidence in the use of different crack characteristic data for NDT development and qualification purposes. That is the major reason why the present work was initiated.

A thorough review of the SKI archives was performed aiming to find useful material from the time period between 1994 and today to compile complementary data and produce an update. Furthermore, older material was collected and evaluated. Thus, the data cover cracking found within the time period 1977-2003. In addition, useful material was supplied by the Swedish nuclear power plants.

The evaluation and presentation of the results are similar to the 1994 study, with a few exceptions. The base for the evaluation is failure analysis reports, where the crack morphology parameters were measured from photografies on cracked surfaces or cross-sections through cracks. The resulting data were divided into seven groups depending on the cracking mechanism/material group combination. The data groups are:

- IGSCC in austenitic stainless steels
- IGSCC in nickel base alloys
- IDSCC in nickel base weld metal
- TGSCC in austenitic stainless steels
- Thermal fatigue in austenitic stainless steels
- Mechanical fatigue
- Solidification cracking in weld metal

The evaluated parameters were divided into visually detectable and metallurgical parameters, which need to be evaluated from a cross-section. The visually detectable parameters are; location, orientation and shape in surface direction and finally the number of cracks in the cracked region. The metallurgical parameters are; orientation and shape in the through thickness direction, macroscopic branching, crack tip radius, crack surface roughness, crack width and finally discontinuous appearance.

The morphology parameters were statistically processed and the results are presented as minimum, maximum, mean, median and scatter values for each data group, both in tables and in various graphs. Finally each morphology parameter is compared between the seven data groups. A brief description of typical characteristics of each data group is given below.

IGSCC in austenitic stainless steels

Most IGSCC develop next to welds with straight or winding cracks oriented almost parallel to the weld. Single cracking is most common but occasionally two cracks are

formed on each side of the weld. In the through thickness direction IGSCC is typically winding or lightly bend and macroscopic branching is rare. The surface roughness is normally on a grain size magnitude and the cracks are particularly narrow providing secondary corrosion is small.

IGSCC in nickel base alloys

Similar characteristics to IGSCC in austenitic stainless steels may be expected. However, cracking close to weld are less frequent and macroscopic branching is more common for IGSCC in nickel base alloys compared to austenitic stainless steels.

IDSCC in nickel base alloy weld metal

Typically IDSCC is winding or straight, single cracking in the weld metal transverse to the weld. In the through thickness direction IDSCC cause typically winding, non-branched cracks with large surface roughness due to course solidification micro-structure. The crack width often shows large variation along the crack and a width close to zero at the surface intersection is common.

TGSCC in austenitic stainless steels

Typically, TGSCC is branched both in surface and through thickness direction. The crack orientation shows a random distribution and the number of cracks is large. The crack surface roughness show low values and the crack width is typically medium range compared with the other groups.

Thermal fatigue in austenitic stainless steels

A large number of randomly oriented cracks are typical for thermal fatigue. However, single or few cracks with similar orientation occur. In the through thickness direction straight, non-branched cracking oriented in right angle to the surface is most common. The crack surface roughness is of medium range and larger than for mechanical fatigue.

Mechanical fatigue

Typically straight, single cracking oriented parallel with stress raisers is common for mechanical fatigue. In the through thickness direction most cracks are straight, non-branched and oriented in right angle to the surface. The crack surface roughness is the smallest and the correlation length the highest of all groups.

Solidification cracking (Hot cracking)

Solidification cracks occur equally frequent parallel as well as transversal to the weld. A large number of cracks are common. In the through thickness direction the cracks seldom show branching and is most often oriented close to 90º to the surface. The crack surface roughness is in the medium range and far below the one for IDSCC, which was not expected.

Sammanfattning

En viktig faktor för att optimera utrustning och procedurer för oförstörande provning är att känna till egenskaper och utseende hos de defekter som provningen avser att detektera. Därför är det nödvändigt att ha tillgång till morfologiska data för defekter från alla de skademekanismer som kan förväntas och de material som förekommer i de objekt som avses att provas. Under 1994 startades ett projekt på initiativ av Statens Kärnkraftinspektion (SKI) med målet att sammanställa typiska, men även avvikande värden hos morfologiska sprickparametrar på ett systematiskt sätt. Fastän arbetet ledde fram till en väsentlig databas insågs redan då att en utökad mängd data skulle medföra större tillförlitlighet när databasen användes för utveckling och kvalificering av teknik för oförstörande provning. Det är den viktigaste anledningen till att det nu genomförda arbetet startades.

En genomsökning av SKIs arkiv genomfördes för att identifiera användbara data för perioden efter 1994. Syftet var även att fånga upp äldre material som inte täcktes in av det tidigare arbetet. Den uppdaterade databasen innehåller därför material under från perioden 1977 – 2003.

Arbetet genomfördes på liknande sätt som 1994. Både sättet att utvärdera och att presentera resultaten gjordes på liknande sätt som 1994. Syftet var här att kunna addera nya data till de gamla med bibehållna definitioner av enskilda parametrar. Underlaget utgjordes av rapporter från skadutredningar där ingående foton användes för utvärdering av morfologi parametrarna. Resultaten delades in i sju datagrupper beroende på skademekanism och materialtyp enligt följande:

- IGSCC i austenitiska rostfria stål
- IGSCC i nickelbaslegeringar
- IDSCC i svetsgods av nickelbaslegeringar
- TGSCC i austenitiska rostfria stål
- Termisk utmattning i austenitiska rostfria stål
- Mekanisk utmattning
- Stelningssprickor i svetsgods

Utvärderade morfologiparametrar delades in I visuellt detekterbara parametrar och metallurgiska parametrar. De senare måste utvärderas från ett tvärsnitt genom sprickan. De visuellt detekterbara parametrarna är: läge, orientering och form I ytled samt antal sprickor I det skadade området. De metallurgiska parametrarna är: orientering och form i djupled, makroskopisk förgreningsgrad, sprickspetsradie, ytjämnhet, sprickbredd och obrutna ligament. En översiktlig sammanfattning av typiska egenskaper för respektive datagrupp redovisas nedan.

IGSCC i austenitiska rostfria stål

De flesta IGSC-sprickor bildas nära svetsar. Den vanligaste formerna är rak eller slingrande medan orienteringen ofta är parallell med svetsen. Enstaka sprickor är vanligast men en spricka på vardera sidan om svetsen förekommer även. I djupled har sprickorna vanligen slingrande form och är ofta lätt böjda mot svetsen. Makroskopiska förgreningar är ovanliga. Sprickprofilens ytjämnhet är ofta av samma storleksordning som kornstorleken, 10–100 μm och sprickbredden liten, förutsett att sekundär korrosion inte förekommer i sprickan.

IGSCC i nickelbaslegeringar

Liknande egenskaper som IGSCC I austenitiska rostfria stål kan förväntas. Det kan dock konstateras att sprickor nära svetsar är mindre vanligt och att förgreningar är mer vanliga hos IGSCC I nickelbaslegeringar.

IDSCC i svetsgods av nickelbaslegeringar

Typisk form hos IDSC-sprickor är rak och de förekommer vanligen som enstaka sprickor i svetsgods tvärs svetsen. I djupled har IDSC-sprickor en slingrande form, de är ogrenade och har höga värden på ytjämnhet på grund av grov stelningsstruktur. Sprickbredden är ofta kraftigt varierande längst sprickan och det är inte ovanligt med mycket låga värden nära skärningen med ytterytan.

TGSCC i austenitiska rostfria stål

Typisk form hos TGSC-sprickor är förgrenad både i ytled och djupled. Orienteringen är slumpmässig och antalet sprickor är stort. Sprickprofilens ytjämnhet visar låga värden och sprickbredden är medelstor jämfört med andra datagrupper.

Termisk utmattning i austenitiska rostfria stål

Ett stort antal slumpvist orienterade sprickor i ytled är typiskt för termisk utmattning. Dock förekommer enstaka sprickor och flera sprickor som är orienterade parallellt. I djup led är sprickorna normalt raka, ogrenade och orienterade i rät vinkel mot ytan. Ytjämnheten är medelstor och normalt större jämfört med mekanisk utmattning.

Mekanisk utmattning

Typisk sprickform är rak, där sprickorna förekommer som enstaka sprickor ofta parallella med spänningsförhöjande ojämnheter i ytan. I djupled är sprickformen rak, ogrenad och orienterad i rät vinkel mot ytan. Ytjämnheten uppvisar normalt lägst värden och korrelationslängden högst jämfört med övriga grupper.

Stelningssprickor (varmsprickor)

Stelningssprickor uppträder både parallellt och tvärs svetsen. Ett stort antal sprickor är vanligt. I djupled är sprickorna sällan förgrenade och är ofta orienterade vinkelrätt mot ytan. Ytjämnheten är av medelhög nivå och väsentligt lägre än för IDSC-sprickor, viket kan betraktas som oväntat.

1 Introduction

Reliable inspections of nuclear components throughout all manufacturing stages and later during their service life, play a significant role in preventing structural failures. Reliable inspections also play an important role in plant life management and component residual life assessment of nuclear power plants as they get older. The effectiveness of these inspections can, however, be affected by many different aspects, such as the objective of the inspections, timing of the inspections, acceptance criteria to be used as well as the capability and reliability of non destructive testing (NDT) systems that are applied.

The capability and reliability of NDT systems depends upon a wide range of factors, such as the nature of structure under examination, the types of defects being sought and the choice of NDT technique to be employed. Other aspects are the reliability of inspection equipment, the ergonomics of the use of the equipment in power plants, and the performance of the NDT personnel, including physiological and psychological factors. All these factors must consequently be taken into account during the NDT system development stage, as well as, during the subsequent validation and qualification stage.

The optimization of the NDT equipment and NDT procedure with respect to the component that shall be inspected and to the type of defects being sought is fundamental. While, the optimization to the component and its geometry, material structure and surface structure, normally is relatively straightforward when the fabrication specification is known, the optimization with respect to the defects being sought can be problematic. The main reason for this is that quantitative data not always is available as to which crack characteristics depend on underlying degradation mechanisms.

In 1994 the Swedish Nuclear Power Inspectorate (SKI) initiated a project for assembling crack characteristics based on systematic studies of cracks that have been observed in different plants (nuclear and non-nuclear) in order to determine typical as well as more extreme values of e.g. orientation, width and surface roughness.

The results of that project were presented in /1/, which has been given the form of a data handbook that can be used by NDT engineers working with development and qualification of NDT systems. The major part of the report is a record of the evaluated crack parameters.

Although, /1/ was based on a fairly large number of identified cracking incidents it was recognised that further studies were needed to increase the data base, and thereby getting more confidence in the use of different crack characteristic data for NDT development and qualification purposes. That is the major reason why the present work was initiated. One important source of information used for the present work is the SKI archives, which were not available at the preparing of /1/. Therefore, a thorough review of the SKI archives was performed aiming to find useful material from the time period between /1/ and today to compile complementary data and produce an update of /1/. Furthermore, older material that was not covered by /1/ was collected and evaluated. Thus, the data cover cracking found within the time period 1977-2003. In addition, useful material was supplied by the Swedish nuclear power plants.

2 Scope of work

This work is focused on defects found within the nuclear power area and on the most common cracking mechanisms/material type combinations, namely IGCSS and thermal fatigue of austenitic stainless steels and IDSCC in weld metal of Nickel-base alloys. During the collecting of data several solidification cracks were found and were included in the study. They cover austenitic stainless steels, ferritic low alloy steels, nickel as well as cobalt base alloys. In addition, a small number of mechanical fatigue and TGSCC were included in the study. In the case of mechanical fatigue all material groups are covered as one data group to extend the data; austenitic stainless steels and ferritic low alloy steels.

The number of evaluated defects in this work is displayed in Table 3.1 and compared with evaluated defects from the nuclear industry covered by /1/.

Material group	*Mechanical fatigue*	*Thermal fatigue*	*IGSCC*	*TGSCC*	*IDSCC*	*Weld flaws*	*Total*
Austenitic stainless steels	3/(2)	16/(22)	38/(39)	5/(19)	0/(0)	0/(5)	62/(87)
Nickel base alloys	0/(0)	0/(0)	3/(16)	0/(3)	17/(13)	13/(0)	33/(32)
Others	1/(1)	0/(0)	1/(1)	0/(0)	0/(0)	1/(1)	3/(3)
Total	4/(3)	16/(22)	42/(56)	5/(22)	17/13)	14/(6)	98/(122)

Table 3.1 Number of evaluated cracks of the present work divided into crack mechanism and material group. Figures in brackets are from /1/

3 Objective

The major objective of the present work is to characterise critical morphology parameters of the most common crack mechanism/material group combinations to provide necessary data from real cracking for use within the process of qualifying non-destructive testing systems. The data are presented as typical values and scatter, as well as relevant extreme values.

4 Nomenclature

The following commonly recognised abbravations are used in this report:

IGSCC – Inter-Granular Stress Corrosion Cracking

TGSCC – Trans-Granular Stress Corrosion Cracking

IDSCC – Inter-Dendritic Stress Corrosion Cracking (IGSCC in weld metal)

Skew is commonly used for the crack orientation along the surface. In this work skew is designated crack orientation in surface direction.

Tilt is commonly used for the crack orientation in the through thickness direction. In this work skew is designated crack orientation in through thickness direction.

Functions for statistical evaluation of data are defined below.

n = number of data points

$\bar{x}$ = mean of the data

x_i = current data value (from 1 to n)

Mean

$$\frac{1}{n}\sum_{i=1}^{n} x_i$$

RMS (Root Mean Square)

$$\sqrt{\frac{1}{n}\sum_{i=1}^{n} x_i^2}$$

Standard Deviation

$$\sqrt{\frac{\sum_{i=1}^{n} x_i^2 - n(\bar{x})^2}{n-1}}$$

Standard Error

$$\frac{\text{Standard Deviation}}{\sqrt{n}}$$

Variance

$$\frac{\sum_{i=1}^{n} x_i^2 - n(\bar{x})^2}{n-1}$$

For the comparison of data in section 13 two types of graphs are used.

In the **box plot** each box comprise 50% of the data with the median value of the variable displayed as a line. The top and bottom of the box mark the limits of ± 25% of the variable population. The lines extending from the top and bottom of each box mark the 95% and 5% limits, repectively. Any value outside of this range, called an outlier, is displayed as an individual point.

A **percentile plot** represents each variable as a separate box. The Y axis displays the range of the data and the X axis displays the names of each variable. Each box compriese 90% of the data. The bottom and top of each box represent 5% and 95% of the data. Three lines are drawn inside each box. The middle line represents the median value of the data (50%), while the lower and upper dashed lines represent 25% and 75% of the data, respectively.

5 Evaluation methodology

Crack parameter data was collected and evaluated from failure analysis reports. Measurements were made on photographs of the reports, displaying the crack appearance on the surface or in cross-sections along the cracks. All records are from failures within the nuclear power industry. The data are divided in three categories;

- General data; Normally used for reference only, but occasionally used as a plotting parameter (wall thickness, material Grade etc)
- Visually detectable parameters; Features detectable by NDT surface testing methods, such as VT, PT, ET etc
- Metallurgical parameters; Crack features evaluated from cross-sections of cracks

All data of /1/ is incorporated in the evaluation of this work. An identical evaluation methodology was employed as defined in /1/. However, a number of new parameters were added. For the IDSCC in nickel base weld metal three discontinuity parameters were defined. They are identical with those evaluated in /2/ and they are defined in 5.3. During the evaluation of the crack surface roughness two new parameters were considered; i) number of intersections between the crack profile and a medium line and, ii) number of turns of the crack over the measuring length. Both parameters are given as intersections/mm and turns/mm. In addition, information if weld repair ever was performed in the cracked area was recorded. All data and evaluated parameters are defined below.

5.1 General data

The recorded parameters are:

Identification: The system or component and power plant where the crack was found

Reference: Reference number or other identity of the failure report

Cracking mechanism: IGSCC, IDSCC, TGSCC, mechanical fatigue or thermal fatigue

Crack location: For example; in a pipe bend, close to a weld, in a fitting etc.

Material grade: Standard designation of the material

Material group: The material grades were divided into two groups: austenitic stainless steels and nickel base alloys

Condition: The condition of the material, such as, solution annealed, cold worked, normalised, as welded etc.

Delivery form: plate, pipe, pipe bend, forging etc.

$\mathbf{D_y}$: Outside diameter of pipe or similar

T: Wall thickness of component

Loading conditions: Information on the loading conditions in the vicinity of the crack that can affect the crack morphology, for example internal pressure, residual stresses, alternating thermal loads etc.

5.2 Visually detectable parameters

The recorded parameters are:

Crack dimensions: Crack length on the surface.

Distance to...: Distance from the crack to a weld, pipe bend or similar feature affecting the crack initiation or propagation.

Orientation in surface direction: This angle describes the direction of the crack on the surface. If the crack is far away from a weld, then 0° is in the longitudinal direction of the pipe and 90° is perpendicular to the pipe. If the crack is close to a weld, then 0° is parallel to the weld and 90° is perpendicular to the weld.

Macroscopic shape in surface direction: The expressions used are straight, winding, bend, bilinear and branched. The different shapes are illustrated in Figure 5-1.

Number of cracks: The number of visible cracks in the cracked area. A numerical value in the range of 1-5 was recorded. If the number of cracks was larger than five, then >5 was recorded.

5.3 Metallurgical parameters

The crack dimension parameters length, depth and width is defined by Figure 5-1.

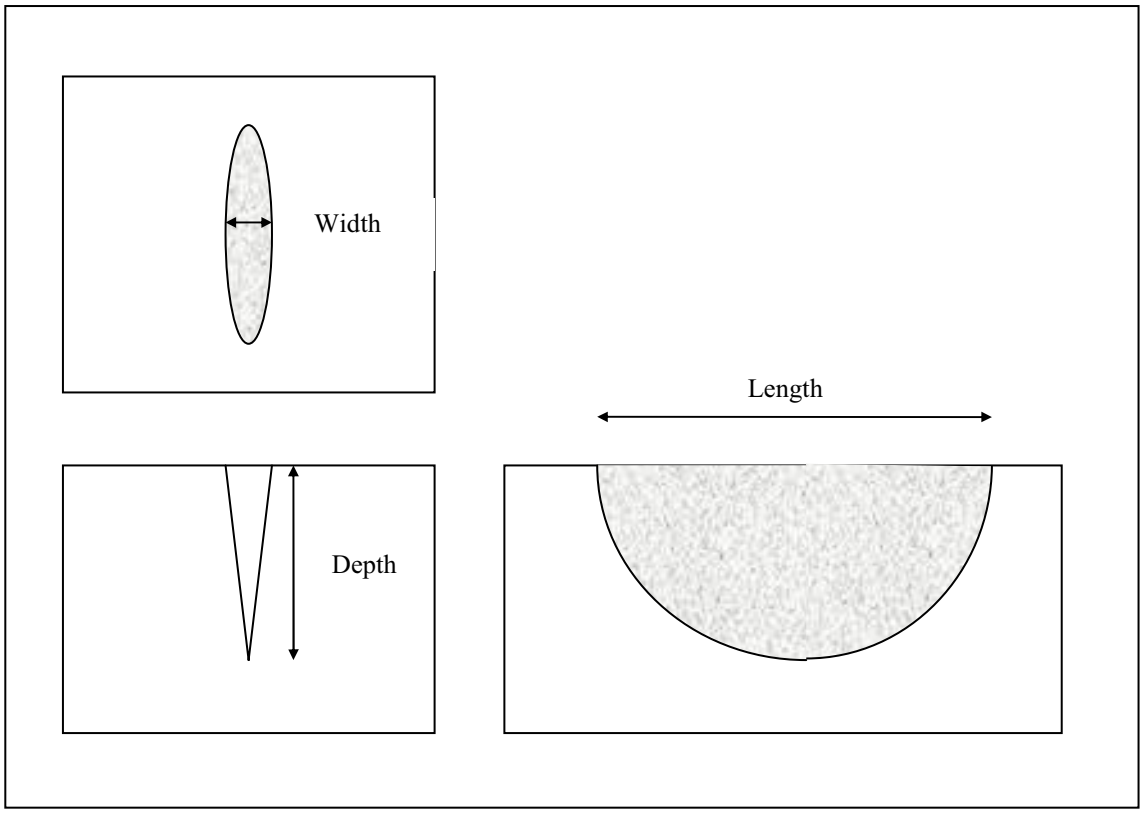

Figure 5-1 Definitions of crack length, depth and width

Crack dimensions: Crack depth. The crack depth/wall thickness ratio was also recorded.

Orientation in through thickness direction: The angle is measured in relation to the surface. If the crack is located close to a weld, then the angle is < 90° if the crack grows towards the weld or > 90° if it grows away from the weld. The definition of the through thickness angle is given in Figure 5-2. If the crack is located far away from a weld then the angle is always in the range of 0-90°.

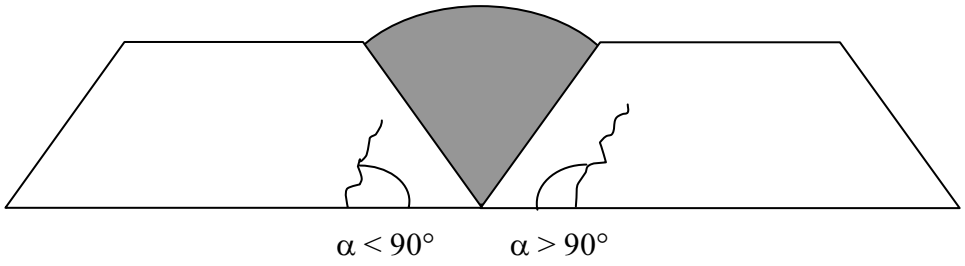

Figure 5-2 Definition of angles when the crack is located close to a weld

Macroscopic shape in the through thickness direction: The expressions used are straight, winding, bend, bilinear and branched. The different shapes are illustrated in Figure 5-3.

Cobble stone pattern distance: Cobble stone pattern is common as a surface pattern for cracking caused by thermal fatigue. A value of the mean distance between the cracks at the surface was recorded. A typical cobble stone pattern is shown in section 10.2.

Macroscopic branching: This parameter describes the amount of branching in the through thickness direction. Only branches longer than five grain diameters were recorded. The number of branches per mm crack length was recorded. Crack branches shorter than five grain diameters, approximately 100 μm, were regarded as microscopic branching.

Grain size: The grain size adjacent to the evaluated crack was recorded. The grain size was measured with the intercept method, and given as a mean grain diameter.

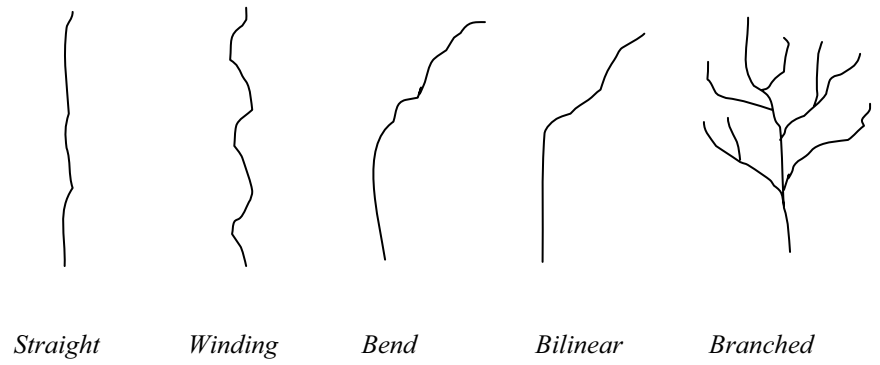

Figure 5-3 Schematic illustration of typical crack features used to categorise crack shape in surface and through thickness direction

Micro-structure: The micro-structure in terms of the shape of the grains close to the crack was recorded. The following expressions were used: equiaxed grains, column formed grains (weld metal), cold worked stretched grains, cast micro-structure etc.

Crack surface roughness: The surface roughness of a crack is a not a straightforward parameter to measure, particularly if the measurements are made on photos. Thus, a sufficiently accurate but still a robust method must be used. The definition of the

roughness parameter should therefore be rather simple and the required number of measurements should be reasonably low. A well known roughness parameter that is quite simple to evaluate is the "ten point height of irregularities", R_Z. The definition of R_Z is given in Figure 5-4. To determine R_Z, the five highest peaks and the five lowest valleys on the crack profile, within a certain length of the crack, are measured. This makes R_Z an appropriate parameter to use in this type of evaluation. Furthermore, R_Z, can easily be converted to other, well known surface roughness parameter, such as, "the arithmetical mean deviation of the profile", R_a. The relation between R_a and R_Z is, $R_a \approx R_Z / 4$. This relation is valid for R_Z-values in the range of 12-1000 μm.

The crack surface roughness that is of interest is the one on a macro scale and not smaller than the grain size level. Therefore, a measurement length, L, in a range of 1-2 mm and micro-graphs at magnifications between 20 and 100 times, were used when ever possible.

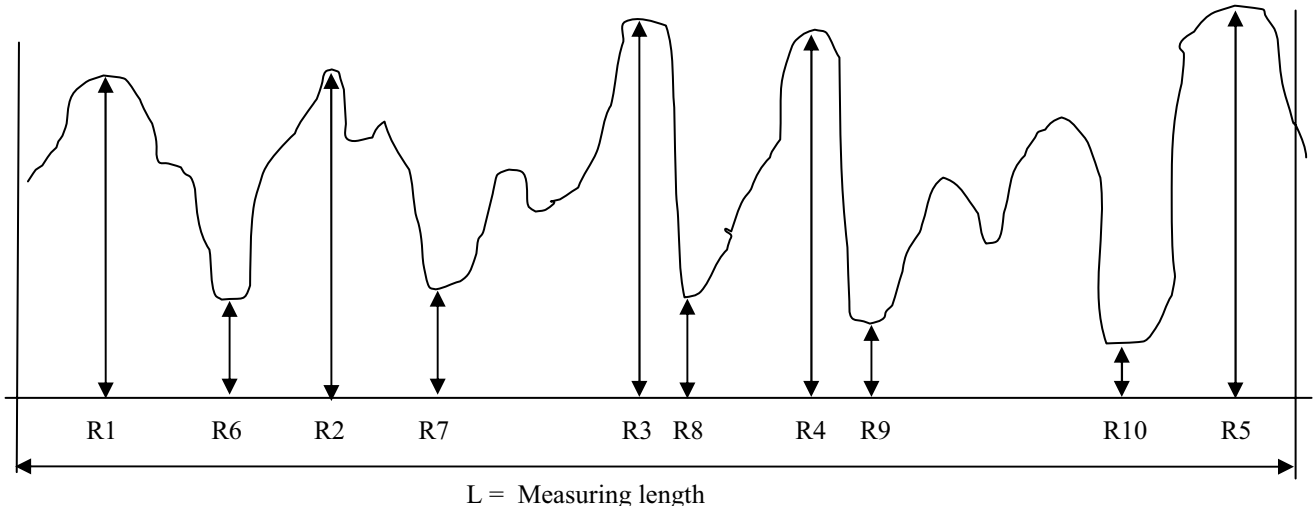

$$Rz = \{ (R1 + R2 + R3 + R4 + R5) - (R6 + R7 + R8 + R9 + R10) \} / 5$$

Figure 5-4 Definition of the crack surface roughness parameter, R_Z

Correlation length: The correlation length, λ_0, is a measure of the rate of change of surface height with distance along the surface. To calculate λ_0 from its theoretical definition is complicated and involves a large number of measurements. In this work an empirical formula for the correlation length was used, as defined by Figure 5-5. Two examples of how this measurement was applied on real cracks is shown by Figure 5-6.

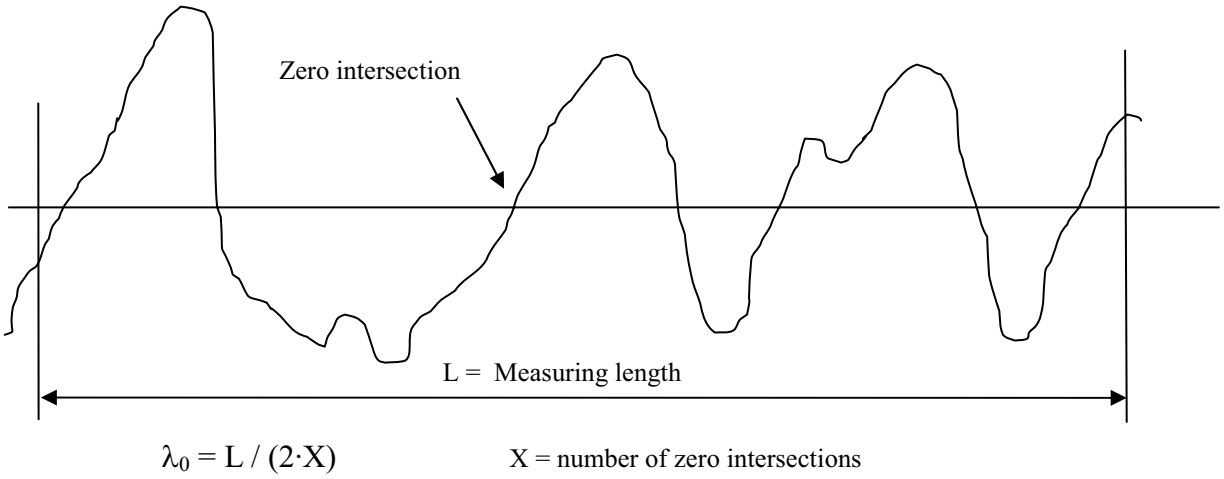

Figure 5-5 Definition of correlation length, λ_0

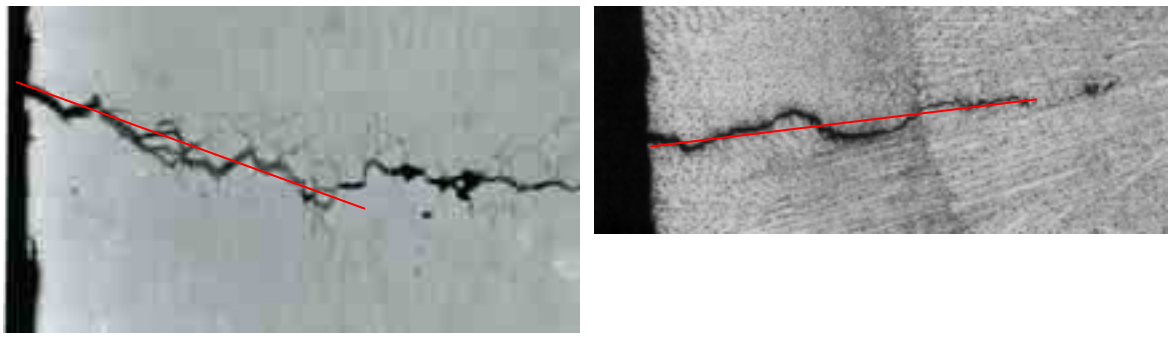

Figure 5-6 Two examples of crack profiles and median lines adjusted to the crack

Measurement length: The crack length used for the determination of R_Z, see Figure 5-4 and 5-5, was, whenever possible, in the range of 1-2 mm.

Intersections: The number of intersections within the measuring length (X in Figure 5-5) was evaluated. The result is given as number of intersections/mm.

Turns: When the crack profile change direction more than 30° this was defined as a turn. The number of turns within the measuring length was evaluated. The result is given as number of turns/mm.

Crack width: The crack width was recorded at three locations for each crack, at the surface, at half the distance between the surface and the crack tip and at the crack tip. The crack width at the crack tip normally is twice the crack tip radius and is, thus, often too small for measuring. Therefore, the crack width at the crack tip is in this report only occasionally given.

Influence of sampling: The method of cutting out samples for failure investigations can have a great influence on the measured crack width. An attempt was made to estimate the influence by assigning a number between 1 and 3, where 1 is negligible influence, 2 is minor influence and 3 is a large influence on the crack width. The lowest number represents a large sample, including the whole wall thickness, not in connection

to a weld. The intermediate number represents a large sample close to a weld or a small sample far away from welds, and finally, the highest number was assigned to small samples close to a weld.

Crack tip radius: The crack tip radius was measured and recorded for those cracks where such a measuring was possible.

Amount of oxides: The amount of oxides at the crack tip, halfway between the surface and the crack tip and at the surface was recorded. A number from one to three was used to represent the amount of oxides, where the number, in increasing order, represents, no oxide, a small amount of oxide, and a heavily oxidised crack surface, respectively. Due to lack of micro-graphs at sufficient magnification the amount of oxides could only be evaluated in a few cases. Therefore, this parameter is not reported in this work.

Discontinuities: If the crack show a discontinuous appearance on the cross-section used for evaluation the number of discontinuities were recorded. Furthermore, the length of each discontinuity, i.e. the distance between the partial crack tips, as well as the length of each partial crack were measured and recorded. An example is shown in figure 5-7, where four discontinuities of an IDSCC in nickel base weld metal are indicated.

Weld repair: If weld repair ever was performed in the cracked area this is recorded.

Sketch over crack features: A sketch of each evaluated crack was made showing the crack shape.

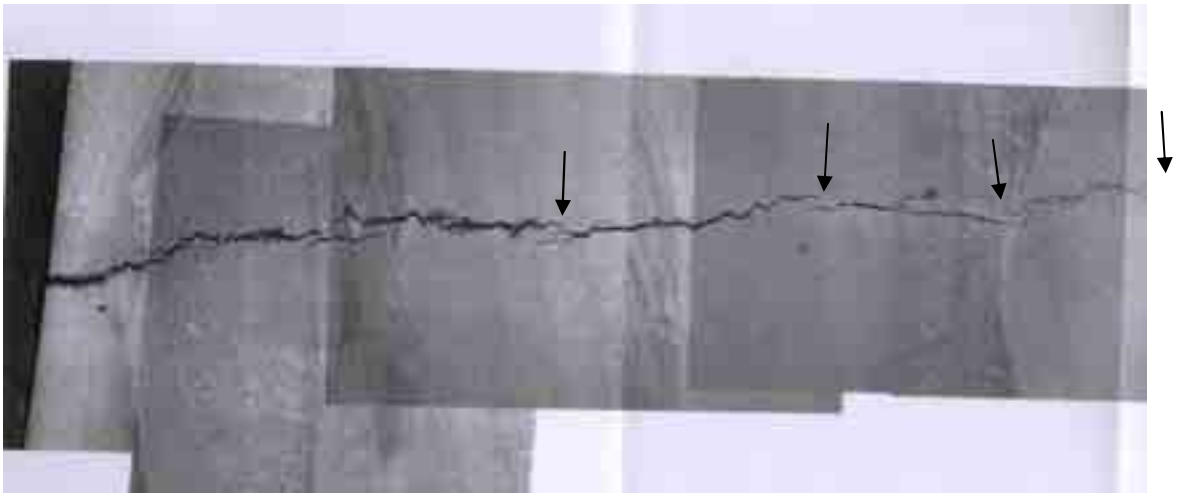

Figure 5-7 Example of IDSCC in nickel base weld metal. Apparent discontinuities marked by arrows.

5.4 Limitations

The basis for this work was failure analysis reports. The purpose with such investigations is generally to identify and explain the failure mechanism, for each specific case. A detailed description of the crack shape and location is often of less importance. Therefore, the amount of useful information varies between different failure reports. In very few cases all the parameters sought for in this work could be evaluated from one single failure report. This means that the number of data points for each parameter is not as many as the number of evaluated cracks of each data group.

A crack is a three-dimensional defect. The specified parameters in this work do not cover a complete description of a three dimensional crack. The reason for this is of course lack of information in the evaluated failure reports. The information extracted in this work, over the crack characteristics, must therefore be treated in the light of these shortcomings. For example, the crack width at the surface of course varies along the crack length. The crack width measurements are made on micro-graphs showing the crack in the through thickness direction. These photos are taken from a cross section of the sample somewhere along the crack length. Thus, the registered cracks widths are dependent on were the cross sections were made. The lack of information appears as a large scatter in the registered crack width values. Large scatter in other parameters can be explained similarly.

6 IGSCC in austenitic stainless steels

6.1 General comments

Necessary factors to develop inter-granular stress corrosion cracking (IGSCC) are tensile stresses, a sensitive material condition and sufficiently corrosive environment. The evaluated cases contain two types of sensitisation; one from welding and another from cold deformation. Out of totally 77 cases 51 are cracking close to welds, i.e. in weld sensitised material and 13 are cracking of parent metal of cold formed pipe bends or at surface deformation of straight pipes.

Out of 77 IGSCC cases 50 occurred in Steel grade 304 or similar (1.4301, SS-steel 23 33), that is, high carbon content without molybdenum (Mo). Eleven cases are in 316, high carbon with Mo and three in 316L, low carbon with Mo. 2 are in 304L and 7 in Nb-stabilised type 347. For remaining cases the steel grade were not specified. It is obvious that most of the IGSCC occurred in grade 304. Similar findings on the influence of the carbon content are reported in /2/.

6.2 Visually detectable parameters

6.2.1 Location (distance to weld fusion line)

Totally 77 cases of IGSCC in austenitic stainless steels were evaluated. In 51 cases the cracks occur close to welds. In 13 cases the cracks are located in cold formed pipe bends or straight pipes far away from any weld. In the remaining 13 cases the crack location is in various other non-welded components or is not documented.

Due to maximum sensitization the cracks typically are oriented parallel to welds and located in the heat affected zone. The crack is expected to form in the region of most severe sensitisation. Thus, the distance between the crack and the weld fusion line is dependent on the welding parameters, number of weld beads, wall thickness etc. Furthermore, the heat input is a crucial parameter. The typical distance found in this work is between 0 and 10 mm, see Figure 6-1. For single run welding the distance may be calculated. However, for multi-run welding the situation is more complicated, and maximum sensitisation may occur very close to the root run fusion line, because the second weld run may sensitise the root run HAZ. To find out the effect of wall thickness a plot is shown in Figure 6-2. The majority of the cases are in wall thicknesses above 5 mm, which normally means more than one weld run. This may explain the large number of cracking very close to the fusion line.

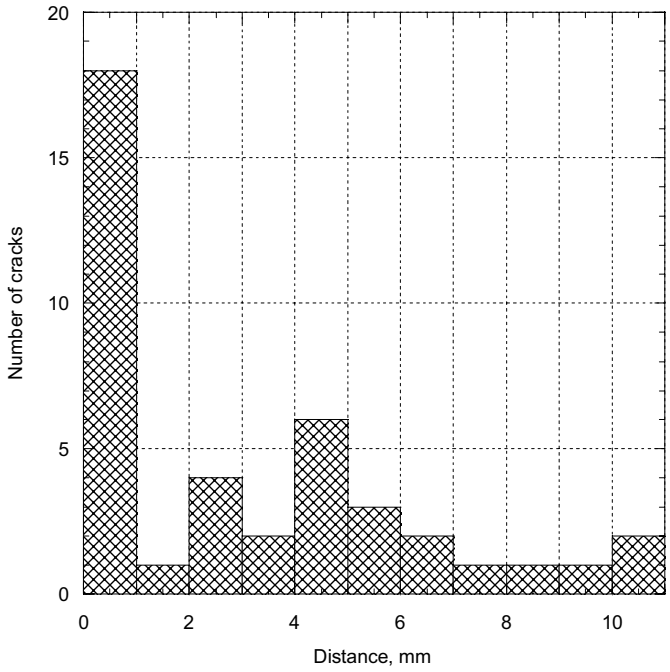

Figure 6-1 Distance from fusion line for IGSCC in weld sensitised austenitic stainless steels

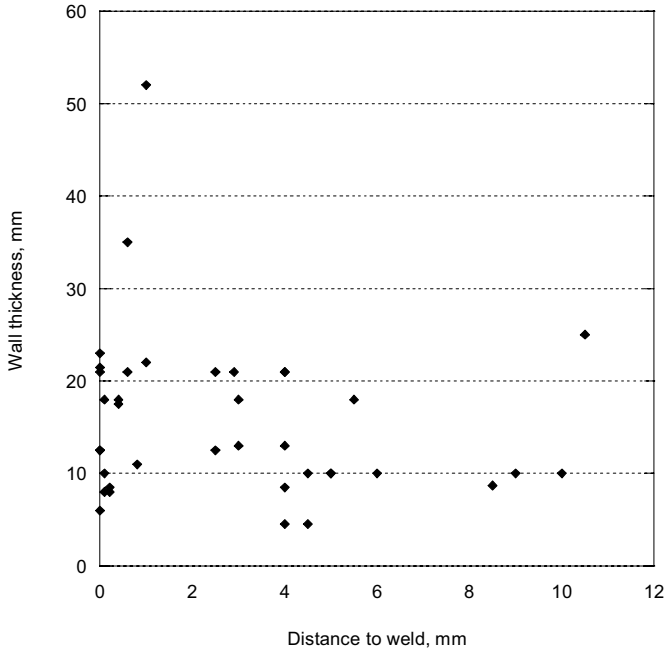

Figure 6-2 Wall thickness versus distance from fusion line for IGSCC in weld sensitised austenitic stainless steels

6.2.2 Orientation in surface direction (skew)

The crack orientation in surface direction is approximately parallel to the weld in those cases where the cracking is close to a weld. When the cracking occur in parent metal of pipes or pipe bends 8 cases show cracking transverse to the pipe axis and 4 show longitudinal cracking.

6.2.3 Shape in surface direction

Typical shape in surface direction is straight or winding, half of each among the evaluated cases. Most cases show a continuous crack running approximately at a constant distance from the weld. However, there are exceptions showing discontinuous cracking and cracks growing at various distances from weld. Examples of appearance in the surface direction are shown in Figures 6-3 and 6-4 and in the through thickness direction in Figures 6-4, 6-5 and 6-6.

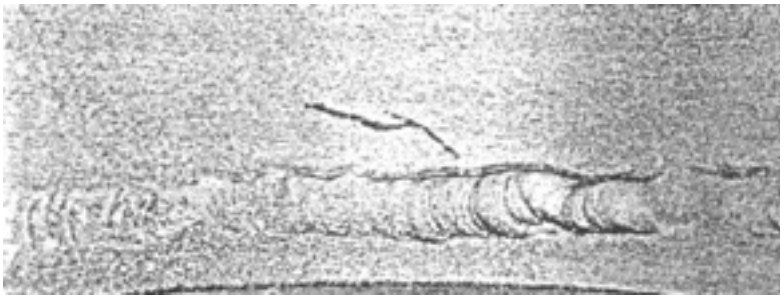

Figure 6-3 Example of IGSCC appearance on the surface

Typical location at weld and a typical crack appearance are shown by Figure 6-5. Another common location is shown by Figure 6-6 where the cracking is very close to the fusion line and the crack has grown abnormally into the weld metal.

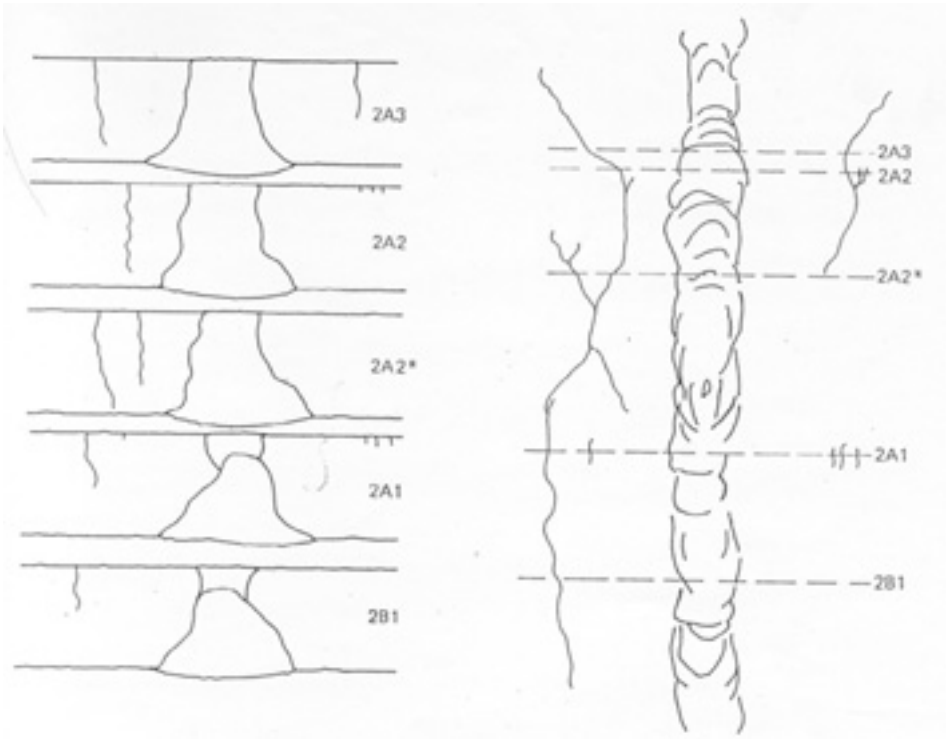

Figure 6-4 Example of IGSCC appearance on the surface and in five cross sections

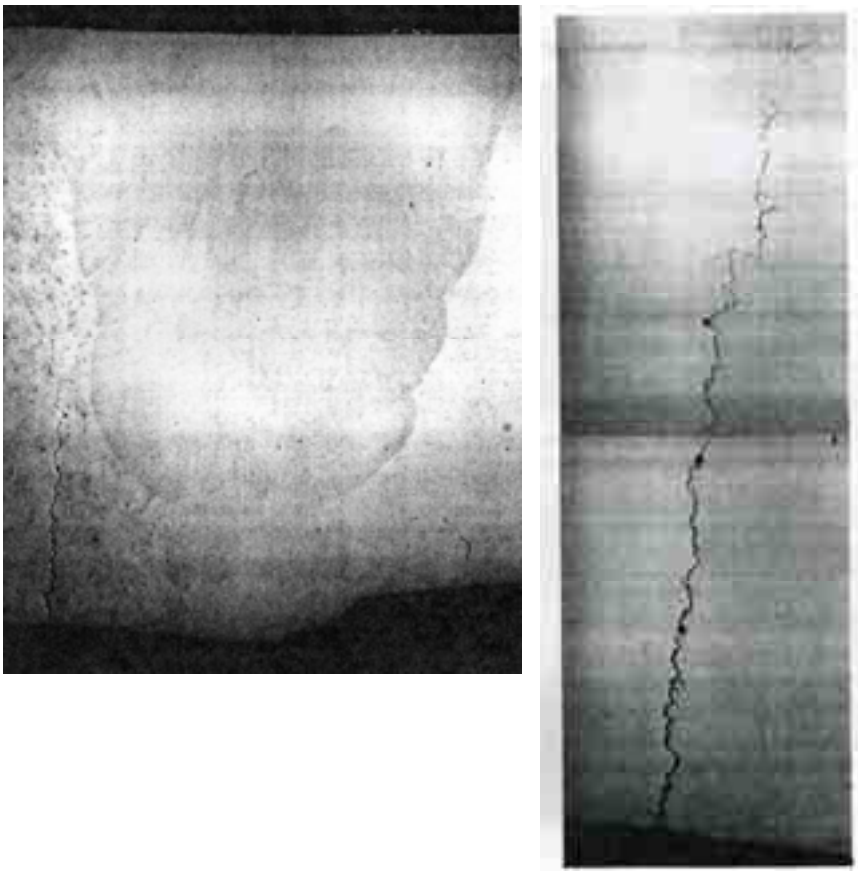

Figure 6-5 Typical location and appearance of IGSCC in austenitic stainless steels

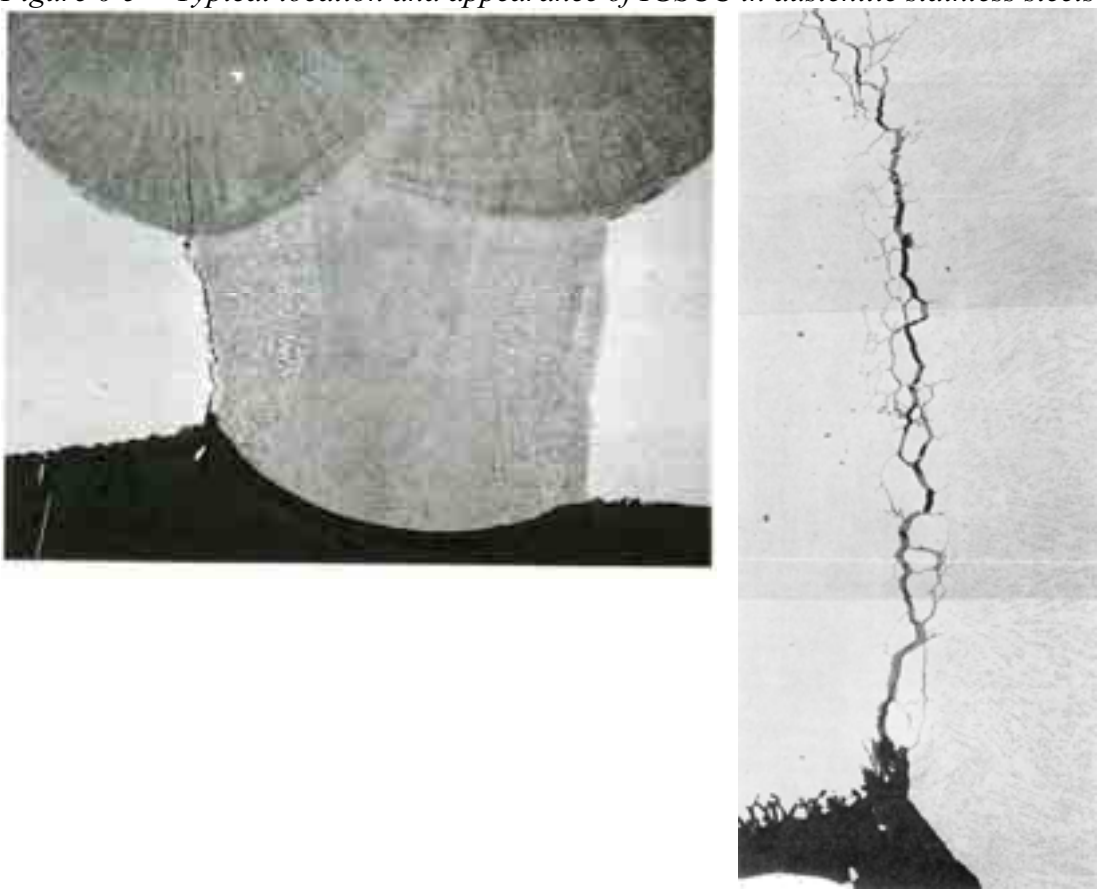

Figure 6-6 Typical location and appearance of IGSCC close to root run fusion line

6.2.4 Number of cracks

The number of cracks is typically one for each case. Sometimes one crack appears at each side of the weld root. Exceptionally up to 6 separate cracks were observed; see statistics in Table 6-1 and distribution in Figure 6-7.

	Number of cracks/case
Points	70
Minimum	1
Maximum	6
Mean	1,81
Median	1
RMS	2,27
Std Deviation	1,38
Variance	1,89

Table 6-1 Statistics on number of cracks formed by IGSCC in austenitic stainless

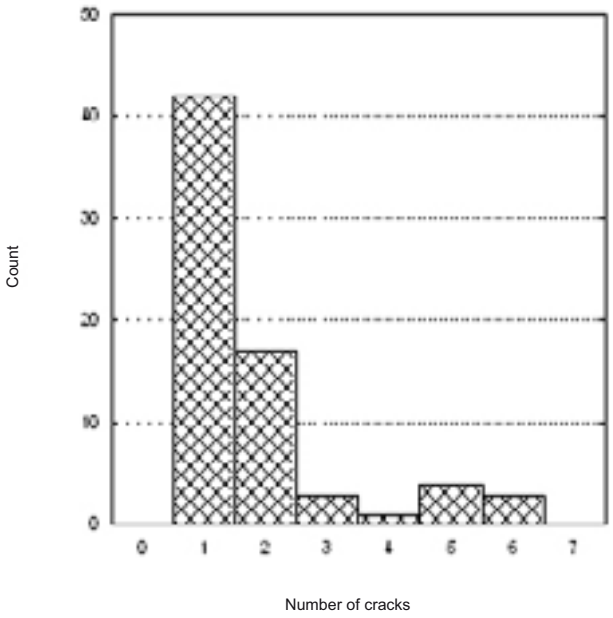

Figure 6-7 Distribution of number of cracks of IGSCC in austenitic stainless steels

6.3 Metallurgical parameters

6.3.1 Orientation in through thickness direction (tilt)

The orientation in the thickness direction is typically 90°, but cracks commonly tend to bend towards the weld metal, see Figure 6-8. The statistics are shown in Table 6-2 and the distribution in Figure 6-9.

Figure 6-8 Typical orientation in the through thickness direction of an IGSCC in austenitic stainless steels

	Tilt (°)
Data points	71
Minimum	40
Maximum	100
Mean	85,6
Median	90
RMS	86,0
Std Deviation	8,4
Variance	70,5

Table 6-2 Orientation in through thickness direction of IGSCC in austenitic stainless steels

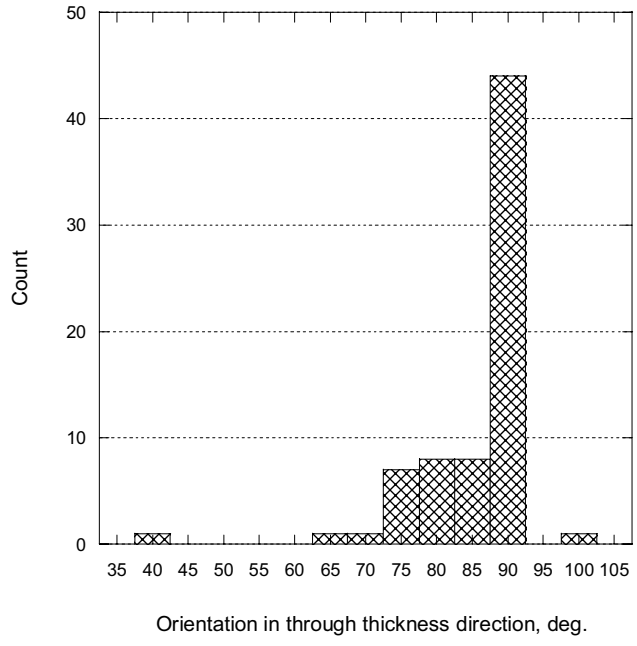

Fig 6-9 Crack orientation in the through thickness direction of IGSCC in austenitic stainless steels

6.3.2 Shape in through thickness direction

Typical shape in the through thickness directions is winding in high magnification, due to the inter-granular growth, and straight at low magnification. Curved cracks are common, where the crack growth tend to turn towards the weld, see Figure 6-8. Crack growth into the weld metal is very unusual and was only found in one case, see Figure 6-6.

6.3.3 Macroscopic branching in through thickness direction

A macroscopic branching is defined as minimum five grain diameters; i. e. 100-250 μm. Microscopic branching is common for IGSCC in austenitic stainless steels. A typical crack is shown in Figure 6-10, displaying several micro-cracks ranging between a half and one grain diameter. In contrary, macroscopic branching is rare. The evaluation was made as number of branches per depth of the crack, number/mm. The statistics are shown in Table 6-3 and a plot showing the number of branches versus crack depth in Figure 6-11.

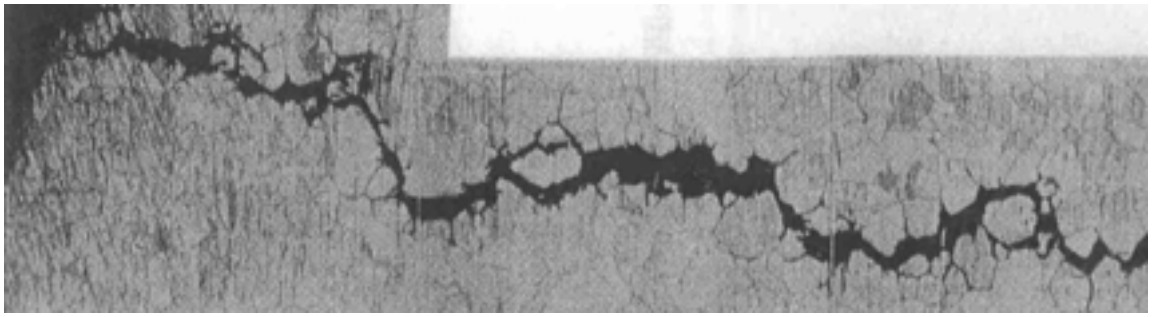

Figure 6-10 Typical micro branching of IGSCC in austenitic stainless steels

	Branching
Points	71
Minimum	0
Maximum	12
Mean	1,01
Median	0
RMS	2,38
Std Deviation	2,17
Variance	4,70

Table 6-3 Statistics of branching in through thickness direction of IGSCC in austenitic stainless steels

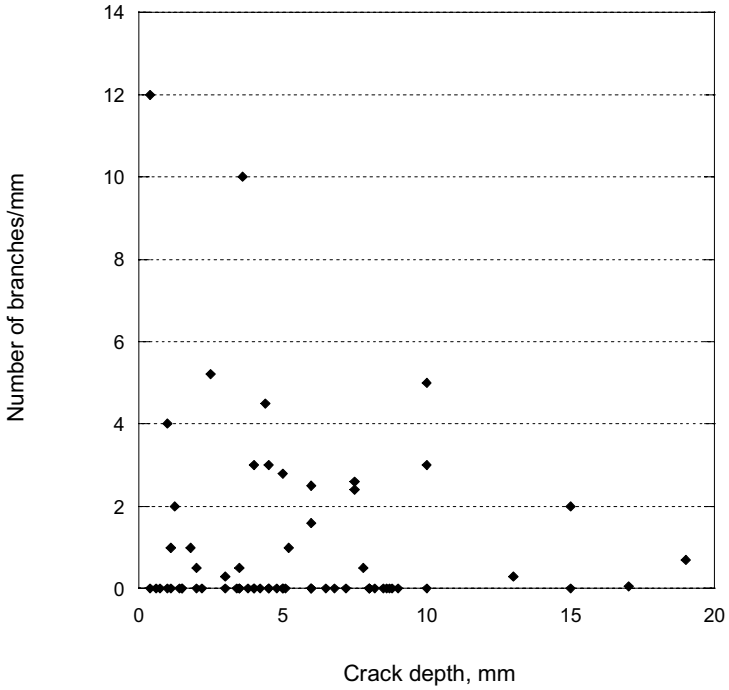

Figure 6-11 Macroscopic branching versus crack depth of IGSCC in austenitic stainless steels

6.3.4 Crack tip radius

A crack formed by IGSCC is initially very sharp and the crack tip radius is normally less than 1 micron. A majority of the cracks evaluated show crack tip radii less than 1 micron. In most cases the crack tip region was not documented at high magnification, thus, it was impossible to measure accurately the crack tip radius. In those cases the radius was set to 0.1 microns. However, some crack show more blunted crack tip and rarely radii above 1 micron were measured. The statistics are shown in Table 6-4.

In Figure 6-12 the crack tip radius is plotted versus crack depth. It is obvious that blunted crack tips were not found for very deep cracks. A reasonable explanation is that as long as the crack is continuously growing the tip is sharp. If the crack growth of some reason stops other corrosion processes than stress corrosion cracking may widen the crack and blunt the crack tip.

	Crack tip radius [μm]
Points	49
Minimum	0,1
Maximum	7
Mean	0,82
Median	0,1
RMS	1,56
Std Deviation	1,34
Variance	1,80

Table 6-4 Statistics on crack tip radius for IGSCC of austenitic stainless steels

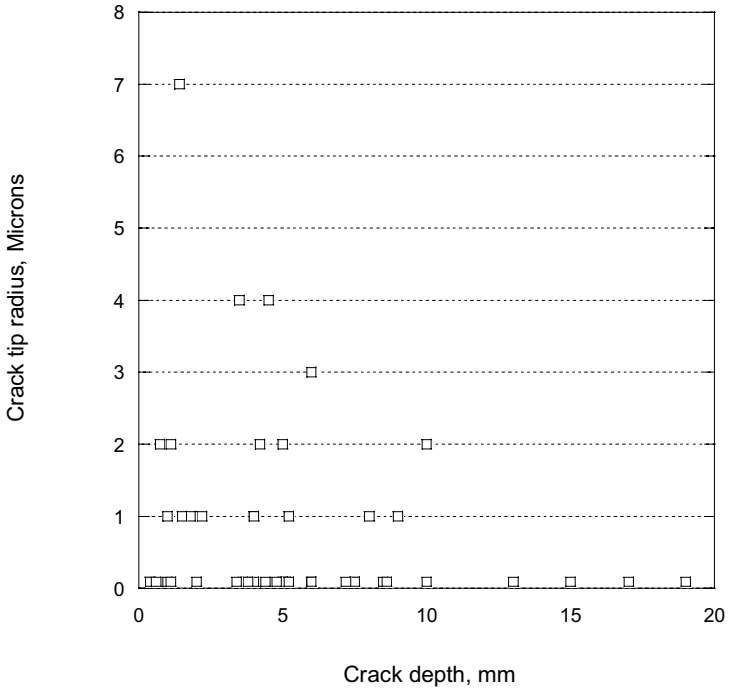

Figure 6-12 Crack tip radius versus crack depth of IGSCC in austenitic stainless steels

6.3.5 Crack surface roughness

The crack surface roughness was evaluated from crack profiles derived from micro-graphs in the reports. The roughness was measured as R_z, see definition in section 5.3. During the evaluation it was found that the evaluated roughness was strongly depending of the magnification of the micro-graph. Therefore micro-graphs with similar magnification were used for the evaluation, when possible. The aim was to use 50 times magnification and most photos ranges between 20 and 100 times magnification. The surface roughness statistics are shown in Table 6-5.

The average grain size of the austenitic stainless steels covered by this work ranges between 30 and 250 μm. Thus, when measuring the surface roughness of inter-granular cracks at a magnification in the same order as the grain size, the result is strongly influenced by the grain size. By plotting the surface roughness versus the average grain size a weak dependence may be indicated, see Figure 6-13. A similar plot is shown in Figure 6-14 for the correlation length versus grain size. The correlation length was evaluated similar to the surface roughness, see definition in section 5.3 and statistics in Table 6-5.

Besides, the surface roughness and correlation length, two other parameters were evaluated. When evaluating the correlation length a straight line is applied to the crack profile. The number of intersection between the crack profile and the straight line is determined. The correlation length is calculated from the formula: measuring length divided by 2 times the number of intersections. The result corresponds to a quarter of the wave length. A similar parameter that easily can be evaluated is the number of intersections divided by the measuring length, expressed in numbers of intersections per mm. The second parameter is number of turns per mm, where a turn is defined by a substantial change of the crack growth direction. Intersections/mm versus turns/mm are shown in Figure 6-15.

	Surface roughness [μm]	Correlation length [μm]	Grain size [μm]
Points	69	73	56
Minimum	8	3	15
Maximum	200	310	250
Mean	70,7	78,4	69,6
Median	68	71	50
RMS	80,9	96,8	86,5
Std Deviation	39,6	57,2	51,9
Variance	1568	3272	2690

Table 6-5 Statistics on surface roughness, correlation length and grain size of IGSCC in austenitic stainless steels

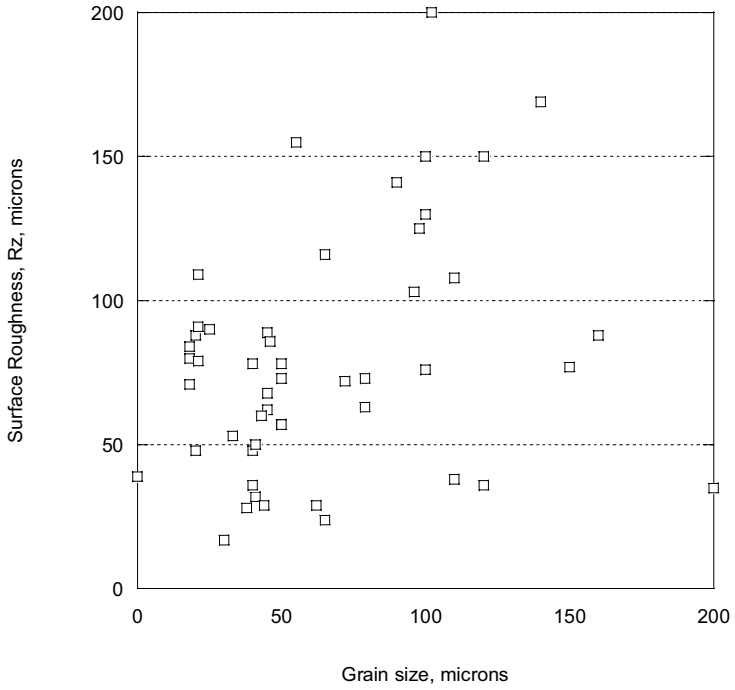

Figure 6-13 Surface roughness versus average grain size of IGSCC in austenitic stainless steels

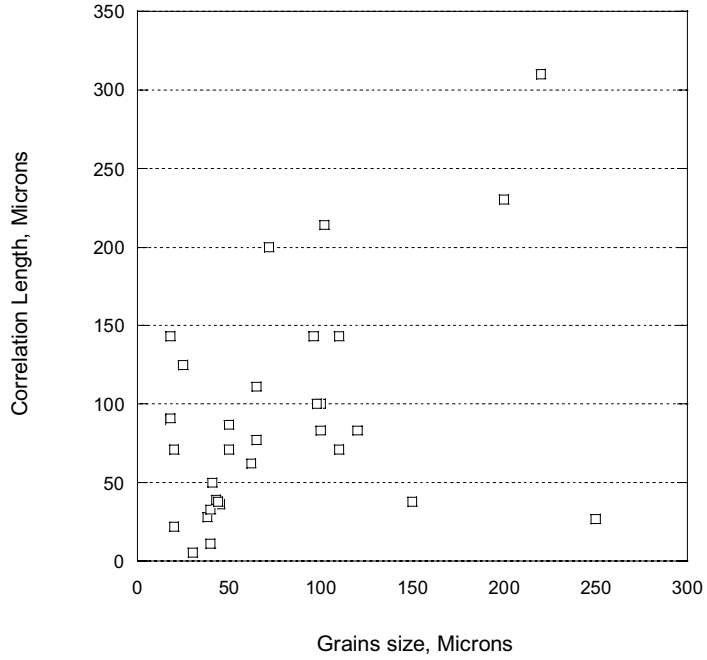

Figure 6-14 Correlation length versus average grain size of IGSCC in austenitic stainless steels

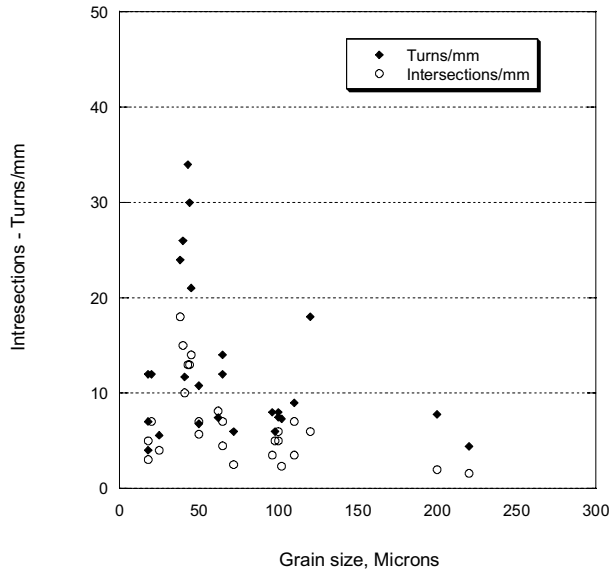

Figure 6-15 Crack profile intersections/mm and crack turns/mm versus grains size of IGSCC in austenitic stainless steels

6.3.6 Crack width

The crack width was measured at the crack intersection with the surface and midway between the surface and the crack tip. The statistics are shown in Table 6-6 and the crack width versus crack depth/wall thickness ratio in Figure 6-16.

	Crack width at surface [μm]	Crack width at midway [μm]	Crack width at tip [μm]
Points	65	65	57
Minimum	3	2	1
Maximum	160	133	25
Mean	37,7	22,5	4,7
Median	30	16	3
RMS	47,2	31,3	6,67
Std Deviation	28,7	22,0	4,74
Variance	822	485	22,4

Table 6-6 Statistics on crack width at surface and midway of IGSCC of austenitic stainless steels

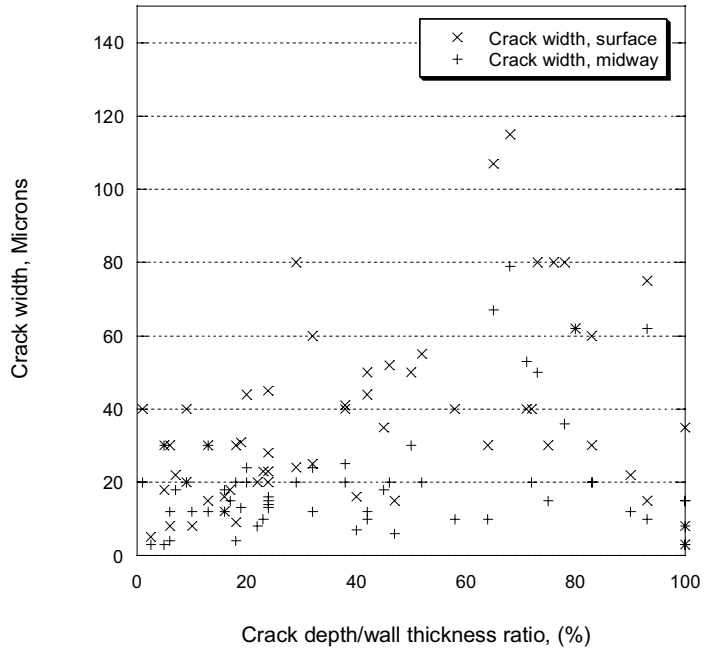

Figure 6-16 Crack width at surface and midway versus crack dept/wall thickness ratio of IGSCC in austenitic stainless steels

6.3.7 Discontinuous appearance

In this work discontinuous appearance was evaluated for all cracking mechanisms, although it is most common for IDSCC in nickel base alloy weld metal. Out of 38 evaluated cases of IGSCC in austenitic stainless steels discontinuous appearance was observed in 9. The statistics is shown in Table 6-7.

	Number of discontinuities	Mean discontinuity length [µm]	Mean partial crack length [mm]
Points	38	8	7
Minimum	0	20	0,06
Maximum	4	180	3
Mean	0,63	72,9	1,10
Median	0	50	1
RMS	1,41	89,3	1,42
Std Deviation	1,28	55,2	0,96
Variance	1,64	3051	0,926

Table 6-7 Statistics on discontinuity parameters of IGSCC in austenitic stainless steels

6.3.8 Weld repairs

Out of 38 evaluated cases weld repairs was recorded in two.

7 IGSCC in nickel base alloys

7.1 General comments

Only three cases were evaluated within this work. Sixteen cases were collected from /1/. All but two cases are cracking in Alloy 600. The exceptions are cracking in Alloy X-750 of reactor vessel internals.

7.2 Visually detectable parameters

7.2.1 Location, orientation and shape in surface direction

Out of 19 cases of cracking 13 are in pipes and the remaining in other components. Out of 13 cases in pipes two are located parallel to girth welds and 6 are located in parent metal not affected by welding. Out of 6 cases of parent metal cracking three are oriented transverse to the pipe and three parallel to the pipe axial direction. The shape in surface direction was evaluated in three cases only; two straight cracks and one winding.

7.2.2 Number of cracks

A single crack was found in 13 cases out of 19. In three cases two or three cracks were found and in two cases multiple cracking.

7.3 Metallurgical parameters

7.3.1 Orientation and shape in through thickness direction

The angle in through thickness direction was evaluated for 10 cases. The distribution is shown in Figure 7-1. A crack angle close to 90° is dominating, but two exceptions with

cracks in 60° angle were found. Due to the inter-granular growth all cracks show a winding shape.

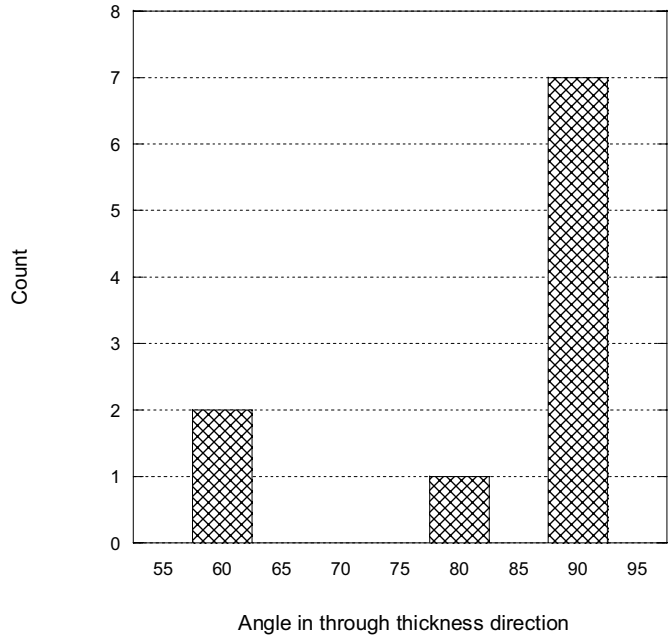

Figure 7-1 Distribution of crack orientation in through thickness direction of IGSCC in nickel base alloys

7.3.2 Macroscopic branching in through thickness direction

The branching was evaluated for 12 cases. The statistics are shown in Table 7-1 and the distribution in Figure 7-2. Compared to IGSCC in austenitic stainless steels branching is more frequent in nickel base alloys.

	Branches/mm
Points	12
Minimum	0
Maximum	7
Mean	1,57
Median	0,65
RMS	2,55
Std Deviation	2,11
Variance	4,44

Table 7-1 Statistics on branching of IGSCC in nickel base alloys

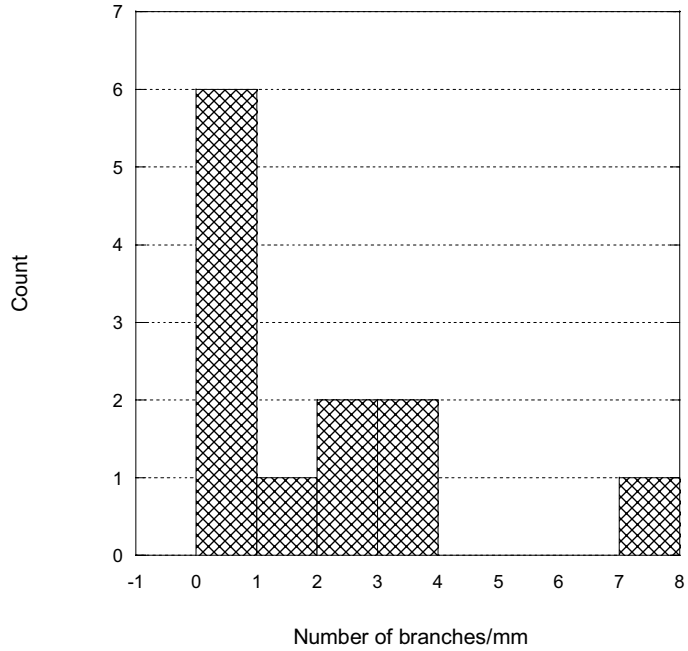

Figure 7-2 Distribution of branching of IGSCC in nickel base alloys

7.3.3 Crack tip radius

The crack tip radius was evaluated for 9 cases. Values close to zero is dominating but a few extreme values were measured, probably due to secondary corrosion. The distribution is shown by Figure 7-3.

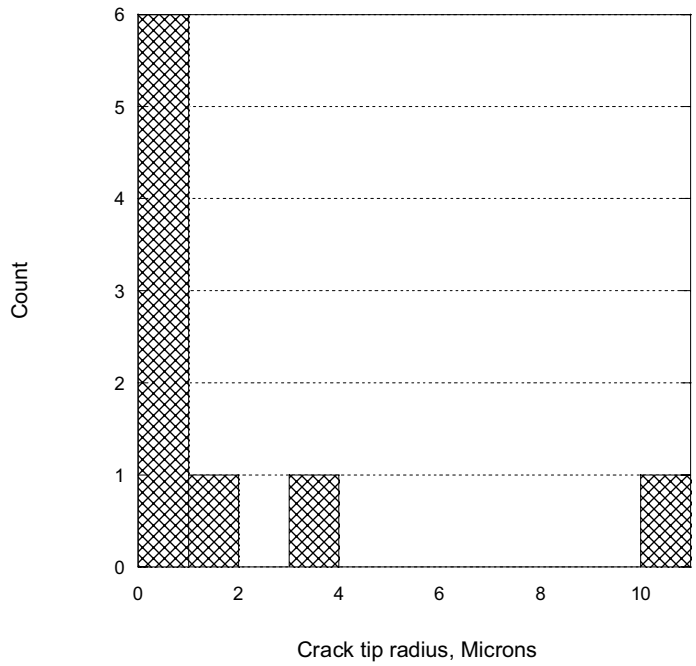

Figure 7-3 Distribution of crack tip radius for 9 cases of IGSCC in nickel base alloys.

7.3.4 Crack surface roughness

The crack surface roughness was evaluated for 19 cases and the correlation length for 17 cases. The number of intersections and turns were evaluated for three cases only. The statistics are shown in Table 7-2. The grain size of the cases covered varies

between 10 and 175 μm. A reasonably good correlation between the average grain size and the surface roughness/correlation length is shown in Figure 7-4.

	Surface roughness [μm]	Correlation length [μm]	Intersections/mm	Turns/mm
Points	19	17	3	3
Minimum	8	3,1	7	16
Maximum	142	150	72	128
Mean	42,8	34,9	37,3	65,7
Median	27	14	33	53
RMS	55,3	53,1	45,9	80,5
Std Deviation	36,0	41,3	32,7	57,1
Variance	1298	1700	1070	3256

Table 7-2 Statistics on crack surface roughness, correlation length, intersections/mm and turns/mm of IGSCC in nickel base alloys

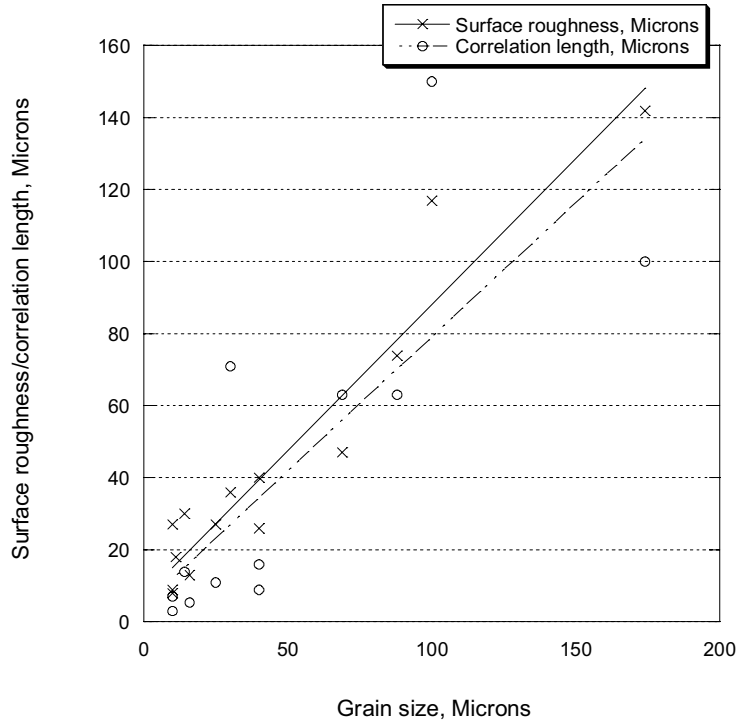

Figure 7-4 Surface roughness/correlation length versus average grain size of IGSCC in nickel base alloys.

7.3.5 Crack width

Crack width measurements were made on 14-17 cases. The statistics are shown in Table 7-3.

	Width, surface [μm]	Width, midway [μm]	Width, crack tip [μm]
Points	14	17	15
Minimum	4	2	1
Maximum	260	260	20
Mean	42,4	44,8	3,87
Median	17,5	7	1
RMS	77,8	91,9	6,58
Std Deviation	67,7	82,7	5,51
Variance	4582	6846	30,4

Table 7-3 Statistics on crack width at three locations of IGSCC in nickel base alloys

7.3.6 Discontinuous appearance and weld repairs

Discontinuous crack appearance or weld repairs were not observed in any of the evaluated cases.

8 IDSCC in nickel base alloys weld metal

8.1 General comments

The total number of evaluated crack cases is 30. Out of them 13 were collected from /1/. Out of the remaining 17 cases 12 were derived from /3/. Due to the specific morphology of IDSCC some additional parameters were evaluated, such as discontinuous appearance and repair welding.

8.2 Visually detectable parameters

8.2.1 Location

The designation Inter-Dendritic Stress Corrosion Cracking indicate that the cracking occur in weld metal only. Out of 30 cases 25 are in Alloy 182 and 5 in Alloy 82.

8.2.2 Orientation in surface direction

Typical orientation is transverse to the weld joint. Transverse cracking was documented in 24 cases. In the remaining cases the orientation was not specified. In 12 cases the orientation in surface direction was measured. As shown in Figure 8-1 an orientation close to 90º is dominating.

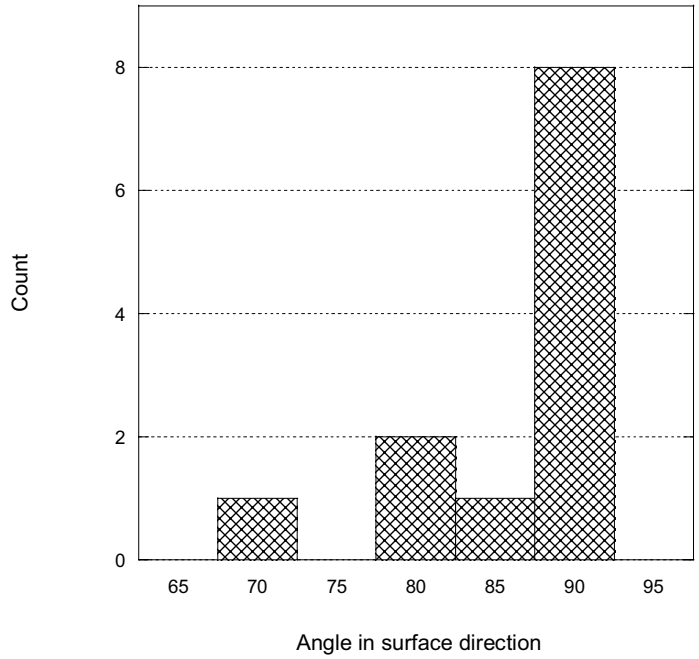

Figure 8-1 Distribution of orientation in surface direction of IDSCC in Nickel base alloy weld metal

8.2.3 Shape in surface direction

The shape was evaluated for 15 cracks. Eleven of them were straight and four showed a winding appearance on the surface.

8.2.4 Number of cracks

Out of 30 evaluated cases 25 showed single cracking. In two cases two separate cracks were found and three cases showed multiple cracking, that is, more than five cracks.

8.3 Metallurgical parameters

8.3.1 Orientation in through thickness direction

For the majority of the 19 cases which were evaluated an orientation in through thickness direction between 70 and 90° was recorded. The distribution is shown by Figure 8-2.

8.3.2 Shape in through thickness direction

The shape was evaluated in 24 cases. Out of them the crack shape was winding in 18 cases and straight in 6 cases.

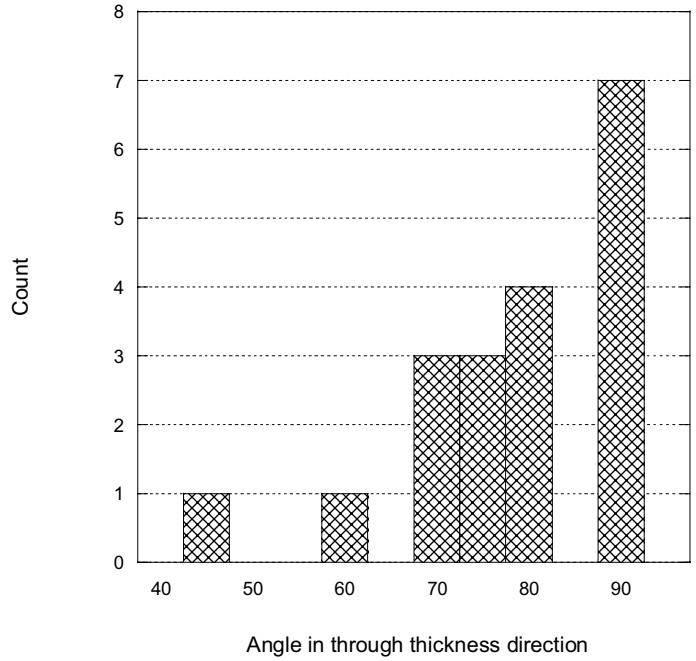

Figure 8-2 Distribution of orientation in through thickness direction of IDSCC in Nickel base alloy weld metal

8.3.3 Macroscopic branching in through thickness direction

Similar to IGSCC in austenitic stainless steels IDSCC in weld metal shows frequent micro-branching. However, macro-branching is less frequent. Out of 24 evaluated cases 17 show macro-branching between 0 and 0.5 branches/mm. The results are summarised in Figure 8-3. A plot of branching versus crack depths in Figure 8-4 shows the single values of 14 cracks.

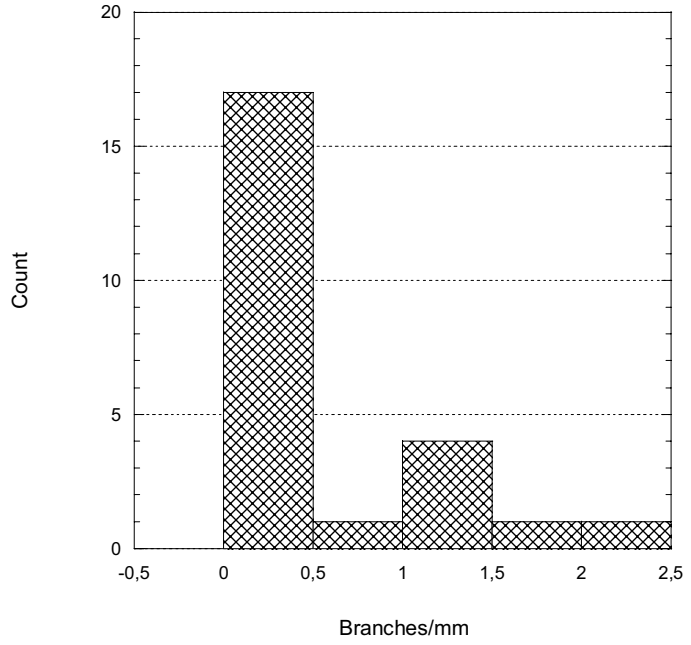

Figure 8-3 Distribution of branching of IDSCC in nickel base alloy weld metal

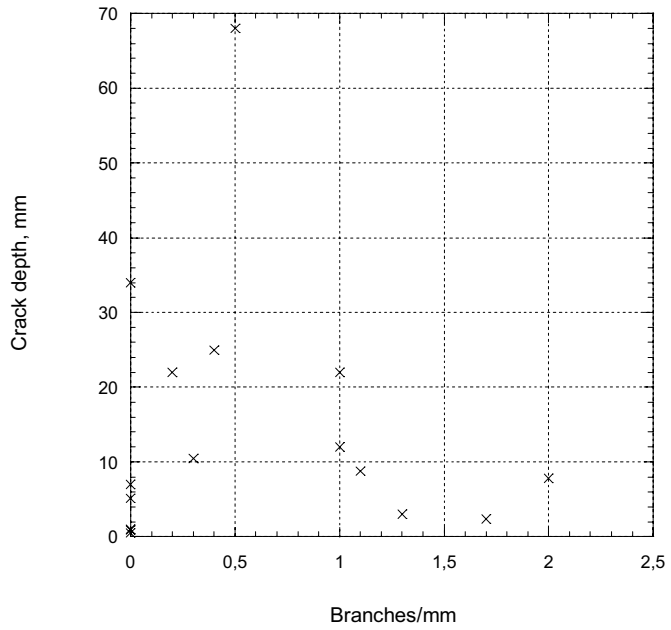

Figure 8-4 Crack depth versus branching of IDSCC in nickel base alloy weld metal

8.3.4 Crack tip radius

The crack tip radius was evaluated in 10 cases. Out of them a radius of 2 μm was found in 7 cases, 1 μm in 2 and a radius < 1 μm in one case. Stress corrosion cracking normally produce very sharp crack tips, typically < 1 μm, compare section 5 for IGSCC. The deviation indicates secondary corrosion within the crack and retarding crack growth.

8.3.5 Crack surface roughness

The crack surface roughness and correlation length were evaluated for 23 and 26 cases, respectively. The number of intersections/mm and turns/mm were only evaluated for 5 cases. The statistics are shown in Table 8-1.

The majority show a surface roughness between 20 and 90 μm. Four extreme cases show values between 250 and 300 μm. They all are from test specimens, which may not be representative for real cracking. The distribution of crack surface roughness and correlation length is shown in Figures 8-5 and 8-6. The number of turns/mm is plotted versus intersections/mm in Figure 8-7.

	Surface roughness, Rz, [μm]	Correlation length, λ_0, [μm]	Intersections/mm	Turns/mm
Points	23	26	5	5
Minimum	20	17	1	2,7
Maximum	288	500	5	8,5
Mean	111	150	2,74	5,7
Median	80	113	2	7
RMS	138	193	3,13	6,14
Std Deviation	84,3	124	1,68	2,55
Variance	7110	15500	2,84	6,50

Table 8-1 Statistics on crack surface roughness of IDSCC in nickel base alloy weld metal

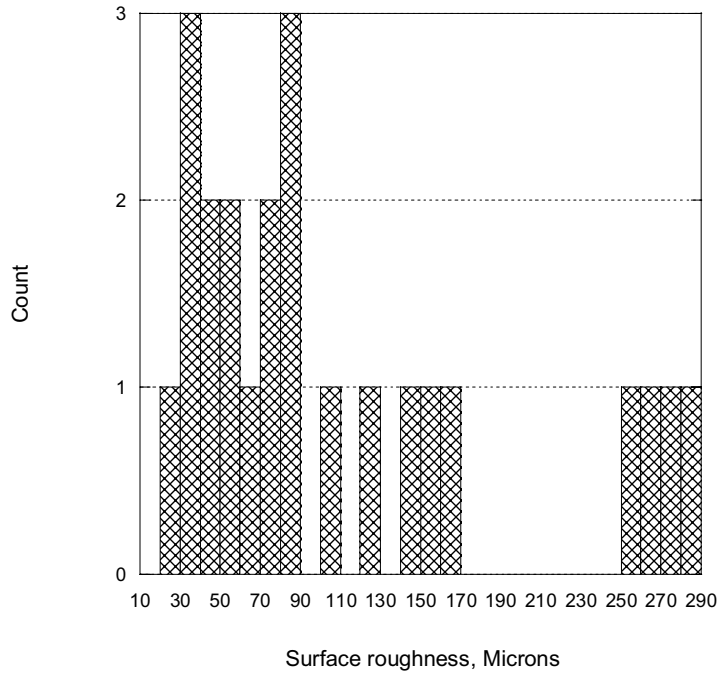

Figure 8-5 Distribution of crack surface roughness of IDSCC in nickel base alloy weld metal

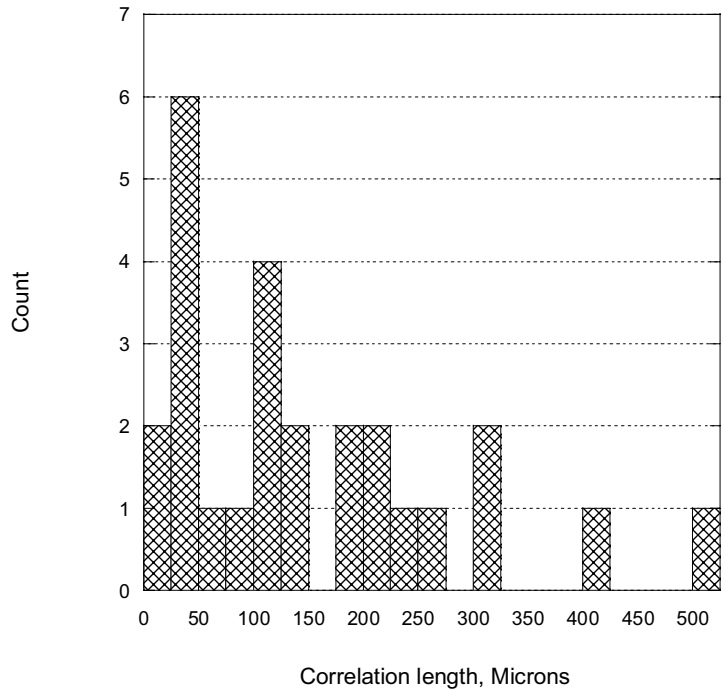

Figure 8-6 Distribution of correlation length of IDSCC in nickel base alloy weld metal

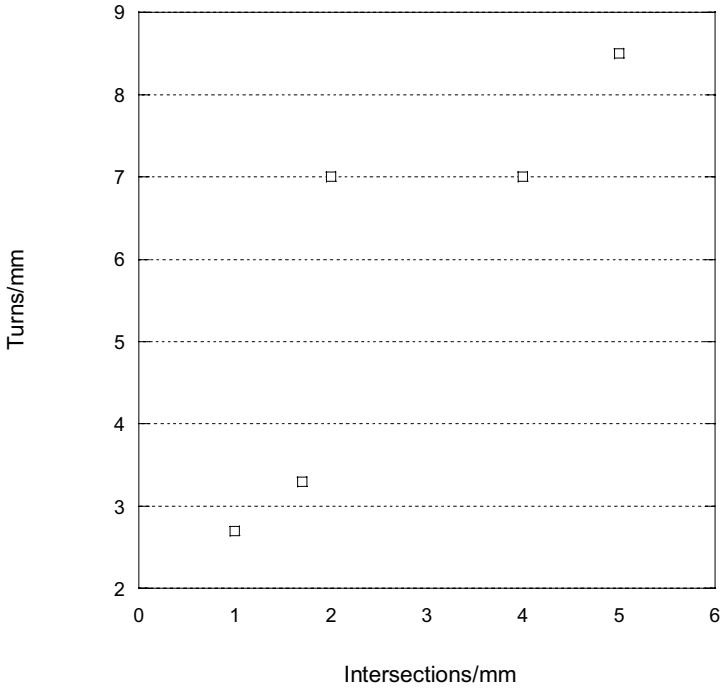

Figure 8-7 Number of turns versus intersections of IDSCC in nickel base alloy weld metal

8.3.6 Crack width

The crack width at the intersection with surface, at midway between surface and crack tip and close to the tip was measured for 20 cracks. The statistics are shown in Table 8-2. It is obvious that the crack width don't necessarily decrease with increasing distance from the surface. This is shown in more detail by the width distribution of each region which is given in Figure 8-8. In Figure 8-9 this is shown in another way by plotting the crack width versus the distance from crack tip for seven cracks with a depth between 8 and 25 mm.

This appearance is typical for IDSCC in weld metal. The crack width is varying considerable more along the crack in through thickness direction compared with other crack mechanisms. It is also common that the crack width at the surface is considerably smaller than further below. A crack width close to zero at the intersection with the surface was measured for three cracks, see also section 6.3.7.

	Crack width, surface [μm]	Crack width, midway [μm]	Crack width, crack tip [μm]
Points	16	20	15
Minimum	0	4	1
Maximum	120	180	45
Mean	31	47,2	10,2
Median	20	35,5	5
RMS	45,6	67,3	16,6
Std Deviation	34,6	49,2	13,6
Variance	1196	2420	184

Table 8-2 Statistics on crack width of IDSCC in nickel base alloy weld metal

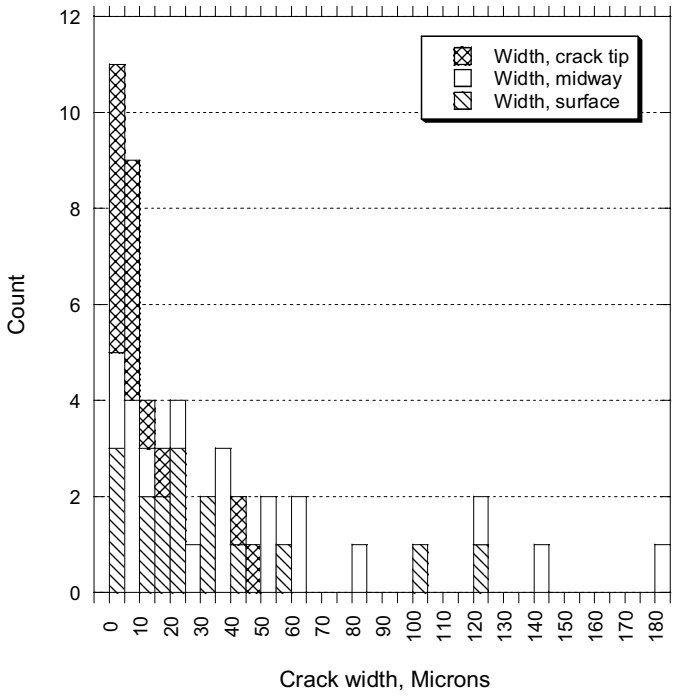

Figure 8-8 Distribution of crack width at three locations of IDSCC in nickel base alloy weld metal

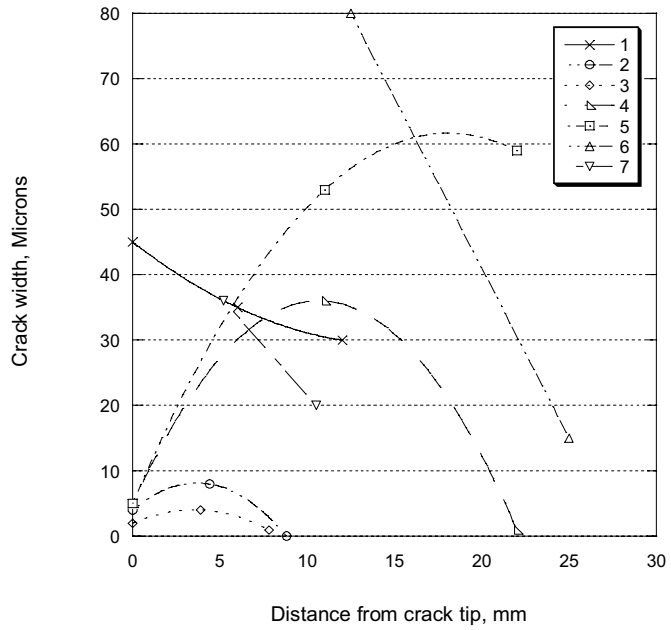

Figure 8-9 Crack width versus distance from crack tip for seven IDSCC in nickel base alloy weld

8.3.7 Discontinuous appearance

Due to the three-dimensional dendritic micro-structure of weld metal, an IDSC crack often appears to be discontinuous, when looking at a cross-section. A reasonable explanation is that the growing crack can not pass through dendrites oriented perpendicular to the crack plane. The crack front must split when it meets the dendrite and is rejoining after having passing it. Everywhere the cross-section coincides with such dendrites the crack appears to be discontinuous. To characterise such discontinuities three morphology parameters were used, namely, the number of discontinuities, the mean length of discontinuity, i.e. the distance between the partial cracks and finally the mean length of the partial cracks between them. A typical crack appearance is shown by Figure 8-10.

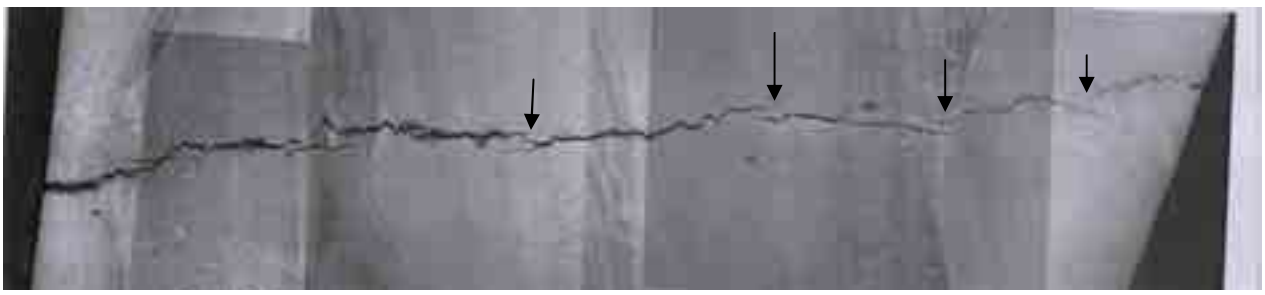

Figure 8-10 Typical appearance of a cross-section of an IDSCC in nickel base alloy weld metal. Crack growth is from left to right. Areas of apparent discontinuities are marked by arrows.

Discontinuity parameters were evaluated for 9 cases, where more than one discontinuity was observed. The statistics on those cases are shown in Table 8-3. For three cases a discontinuity coincides with the surface. However, a few IDSCC without

discontinuities were found. In Figure 8-11 the number of discontinuities is shown from 13 cases.

	Number of discontinuities	Mean discontinuity length [μm]	Mean partial crack length [mm]
Points	9	9	9
Minimum	2	0,96	95
Maximum	12	6,66	330
Mean	7	2,60	190
Median	6	1,8	170
RMS	7,82	3,15	205
Std Deviation	3,71	1,87	78,9
Variance	13,8	3,50	6228

Table 8-3 Statistics on discontinuity parameters of IDSCC in nickel base alloy weld metal

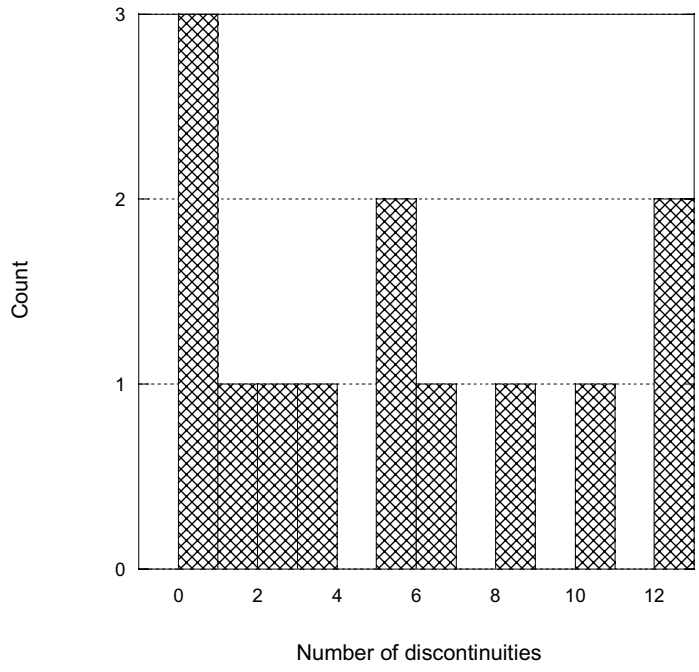

Figure 8-11 Number of discontinuities of IDSCC in nickel base alloy weld metal

8.3.8 Weld repairs

Especially, for IDSCC in nickel base alloys weld metal, weld repairs seems to be of great influence for cracking to develop. Out of 30 evaluated cases weld repairs close to the cracking was detected in 10. In 7 cases there were no weld repairs in the cracked region and in 13 cases information was lacking.

9 TGSCC in austenitic stainless steels

9.1 General comments

The number of evaluated cracks in this work is 5, while 26 were collected from /1/. Among those 26 cases 7 are from the non-nuclear area. Nowadays, TGSCC in austenitic stainless steels in Swedish nuclear power plants is rare. The reason is that the chloride content of the reactor water is extremely low and contamination from other sources, such as gaskets, mostly has been eliminated.

9.2 Visually detectable parameters

9.2.1 Location, orientation and shape in surface direction

Out of 31 cracks 11 are located close to welds, < 5 mm, oriented both parallel and transverse to the weld direction. Three cracks are located 5 – 10 mm from a weld and 9 did develop in parent metal not affected by welding. In the remaining 8 cases the crack location was not specified.

Out of 11 cracks located close to a weld two were oriented 90° to the weld, two parallel to it and two at an angle of approximately 45°. Out of 9 cracks in parent metal of tubular components three were oriented 90° to the pipe axis, three parallel to it and three at an angle of 45°.

The shape was evaluated for 15 cracks. Nine of them showed a straight appearance, two were winding, two bend and two branched.

9.2.2 Number of cracks

The number of cracks was evaluated for 30 cases. The result is shown in Table 9-1.

Number of cracks	Number of cases
1	7
2	2
3	4
> 5	16

Table 9-1 Number of cracks of TGSCC in austenitic stainless steels

9.3 Metallurgical parameters

9.3.1 Orientation in through thickness direction

The orientation in through thickness direction was evaluated for 27 cases. The result is shown in Figure 9-1.

An orientation of 90° is dominating but several cracks with angles between 60 and 75° occur. Typical for TGSCC is that the main crack is oriented close to 90 but the branches have deviating orientation.

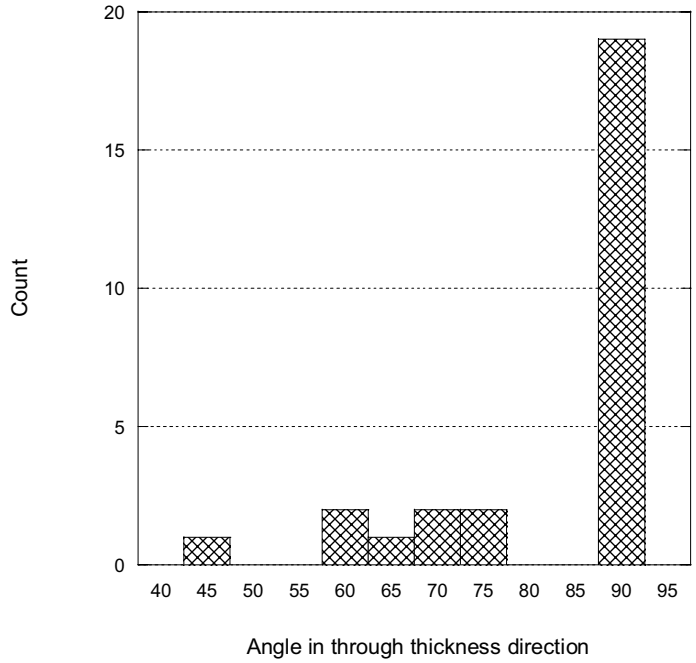

Figure 9-1 Distribution of crack orientation in through thickness direction of TGSCC in austenitic stainless steels

9.3.2 Shape in through thickness direction

The typical shape in through thickness direction is branched. Out of 30 evaluated cases, 20 show branched shape. Out of the remaining 10 four show straight, three bend, two winding and one biliniar shape. A typically branched crack is shown by Figure 9-2

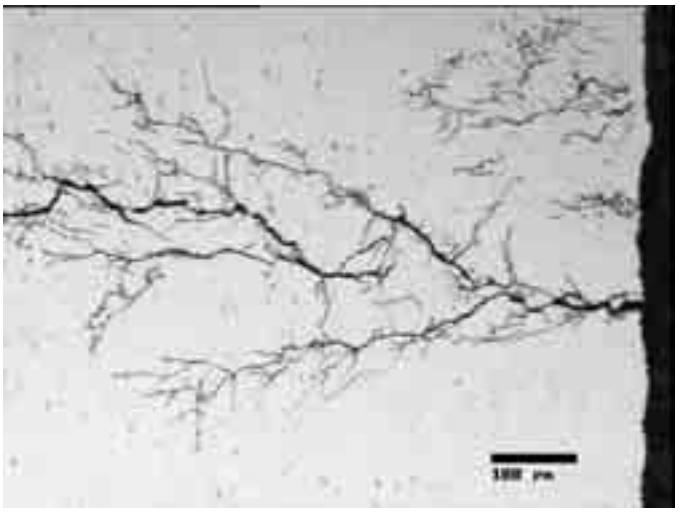

Figure 9-2 Typically branched shape of TGSCC in austenitic stainless steels

9.3.3 Macroscopic branching in through thickness direction

The branching in through thickness direction was measured for 28 cases. Although, TGSCC in austenitic steel is typically heavily branched there are cases with almost no branches at all. Six cases with 0 macroscopic branching was found in this work. The statistics are shown in Table 9-2 and the distribution in Figure 9-3. A plot of branches/mm versus the crack depth is shown in Figure 9-4.

	Branching
Points	28
Minimum	0
Maximum	16
Mean	2,725
Median	2
RMS	4,23
Std Deviation	3,30
Variance	10,9

Table 9-2 Statistics on branching of TGSCC in austenitic stainless steels

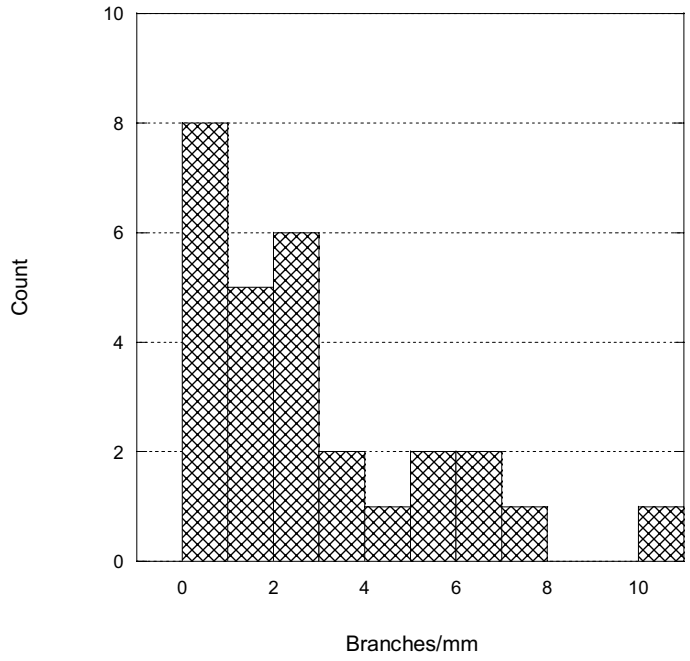

Figure 9-3 Branching in through thickness direction of TGSCC in austenitic stainless steels

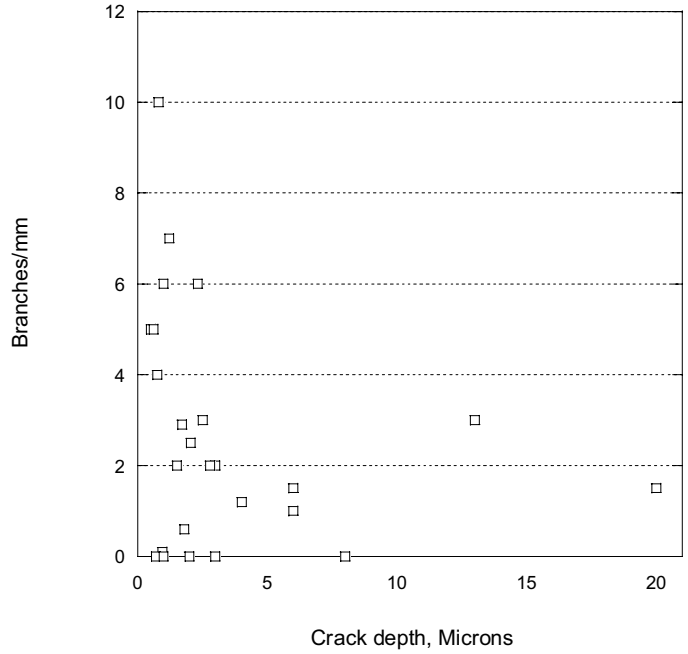

Figure 9-4 Branching versus crack depth of TGSCC in austenitic stainless steels

9.3.4 Crack tip radius

The crack tip radius was evaluated for 20 cases. Out of them 13 showed very sharp tips, < 1 μm. A few exceptions showed blunted crack tips due to secondary corrosion. The crack tip radius distribution is shown in Figure 9-5.

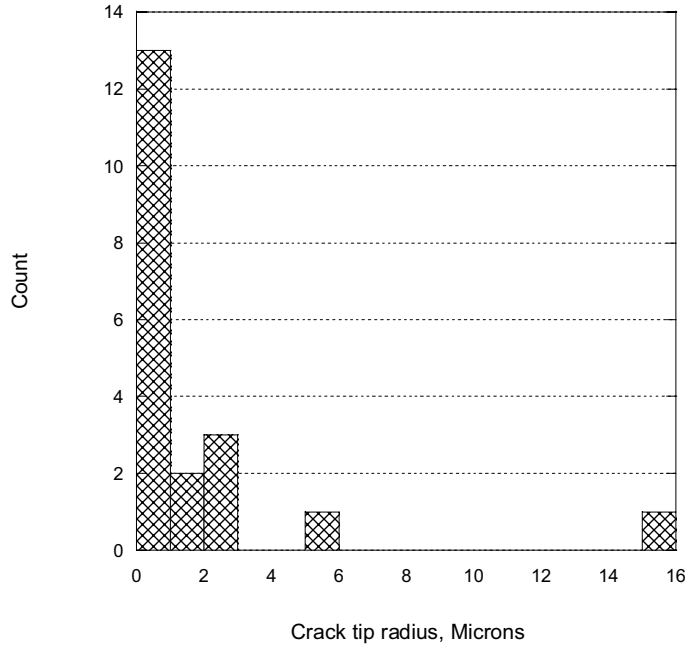

Figure 9-5 Distribution of crack tip radius for 20 cases of TGSCC in austenitic stainless steels

9.3.5 Crack surface roughness

Crack surface roughness was evaluated for 29 cases and correlation length for 17. The number of intersections and turn/mm were evaluated for 5 cases. The statistics are shown in Table 9-3. The distribution of crack surface roughness and correlation length is shown in Figure 9-6 and a plot of turns versus intersections in Figure 9-7.

	Surface roughness, Rz [μm]	Correlation length, λ_0 [μm]	Intersections/mm	Turns/mm
Points	29	17	5	5
Minimum	10	7	3	5
Maximum	90	160	10	16
Mean	37,1	38,9	6,88	10,32
Median	36	21	8,10	8
RMS	42,7	56,8	7,44	11,2
Std Deviation	21,6	42,6	3,18	4,88
Variance	465	1817	10,1	23,8

Table 9-3 Statistics on crack surface roughness, correlation length, intersections and turns of TGSCC in austenitic stainless steels

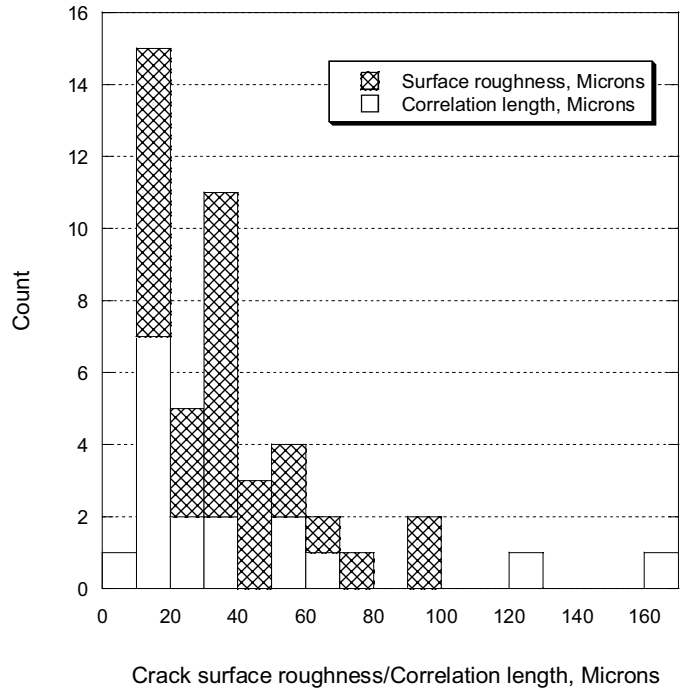

Figure 9-6 Distribution of crack surface roughness and correlation length of TGSCC in austenitic stainless steels

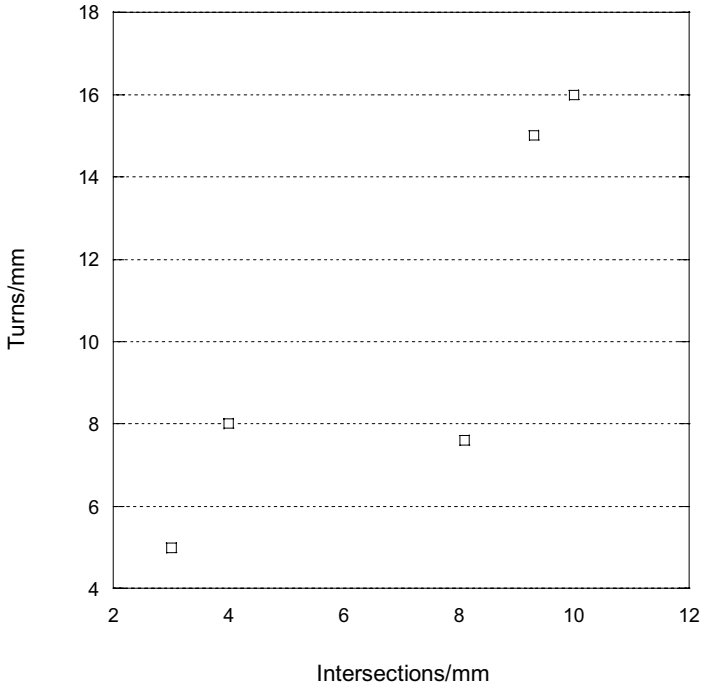

Figure 9-7 Number of crack turns/mm versus number of intersection of TGSCC in austenitic stainless steels

9.3.6 Crack width

The crack width was evaluated for 24 – 29 cracks. The results are displayed in Table 9-4 and in Figure 9-8.

	Crack width, surface [µm]	Crack width, midway [µm]	Crack width, crack tip [µm]
Points	24	28	23
Minimum	3	1	0
Maximum	150	125	10
Mean	31,1	19,6	3,56
Median	20	9	3
RMS	45,9	32,0	4,64
Std Deviation	34,5	25,8	3,04
Variance	1188	665	9,26

Table 9-4 Statistics on crack width of TGSCC in austenitic stainless steels

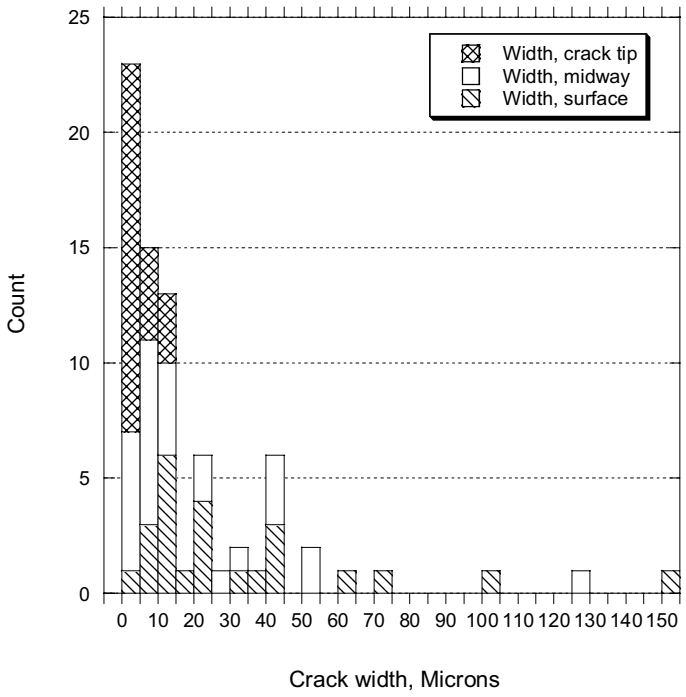

Figure 9-8 Distribution of crack width at three locations of TGSCC in austenitic stainless steels

9.3.7 Discontinuous appearance and weld repairs

Out of six evaluated cracks discontinuities were found only in one case. The number was 12, the mean discontinuity length was 25 μm and of the mean length of partial cracks were 350 μm. Weld repairs were not recorded in any case.

10 Thermal fatigue of austenitic stainless steels

10.1 General comments

The total number of cases covered by this report is 37. Out of them 16 were evaluated during this work and 21 were collected from /1/. All cases are from the nuclear area.

Cracking due to thermal fatigue needs sufficiently high thermal gradients to occur. Such conditions may develop where fluids of different temperatures are mixed. Typical locations are T-joints. Out of those cases the temperature difference were known for 12. The difference is between 100 and 130 °C for 10 cases. One is as low as 55 °C and two as high as 215 and 225°C, respectively.

10.2 Visually detectable parameters

10.2.1 Location

The location of all evaluated cases is given in Table 10-1. In 19 cases the cracking was found close to or at a distance less than 500 mm from a mixing point, where fluids of different temperatures meet. Some of the 8 cases designated as piping may also be close to a T-joint, but detailed information is missing.

Location	Number	Comments
T-joint	19	Distance to T-joint < 500 mm
Piping	8	Distance to T-joint unknown
Valve or pump housing	4	Distance to nozzles unknown
Thermal protective sleeve	2	
Others	4	

Table 10-1 Location of thermal fatigue cracking of austenitic stainless steels

10.2.2 Orientation and shape in surface direction

Pure thermal loading on a flat metal surface normally result in randomly oriented cracking. Crossing cracks is common and are as such designated "cobble stone" cracking. If other loads exist simultaneously a crack pattern of many parallel straight cracks may develop. The shape of the 37 evaluated cases is summarised in Table 10-2. Due to the large number of cracks the orientation is less meaningful to evaluate and the angle in surface direction was measured only for 6 cases. In four cases the majority of the crack was parallel with a girth weld and in two cases they were perpendicular. A typical surface crack pattern is shown in Figure 10-1.

Shape	Number
Cobble stone	14
Straight	8
Winding	6
Not evaluated	9
Total number	37

Table 10-2 Typical shape of thermal fatigue cracking of austenitic stainless steels

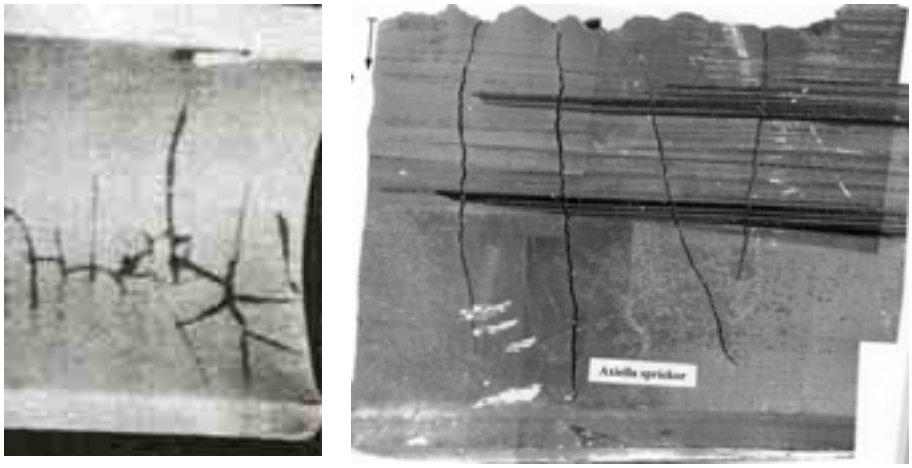

Figure 10-1 Cobble stone pattern to the left and straight crack pattern to the right

10.2.3 Number of cracks

Out of 37 cases the number of cracks was evaluated in 32 cases. The result is plotted in Figure 10-2. The bin of 6 cracks represents cases where more than 5 cracks were observed. It is obvious that the majority of the cases produced multiple cracking. The other group of data is one or two cracks. 18 of the multiple cracking cases were located

close to mixing points and the location of two were not specified (close to a mixing point can not be excluded). Out of 12 single/double cracking cases 4 were located close to a mixing point and 8 were not specified. One reasonable conclusion may be that local thermal loads at a mixing point mostly produce multiple cracking but single cracking can not be excluded. If the thermal loads act on a more global scale, fatigue cracking more similar to mechanical fatigue may be anticipated.

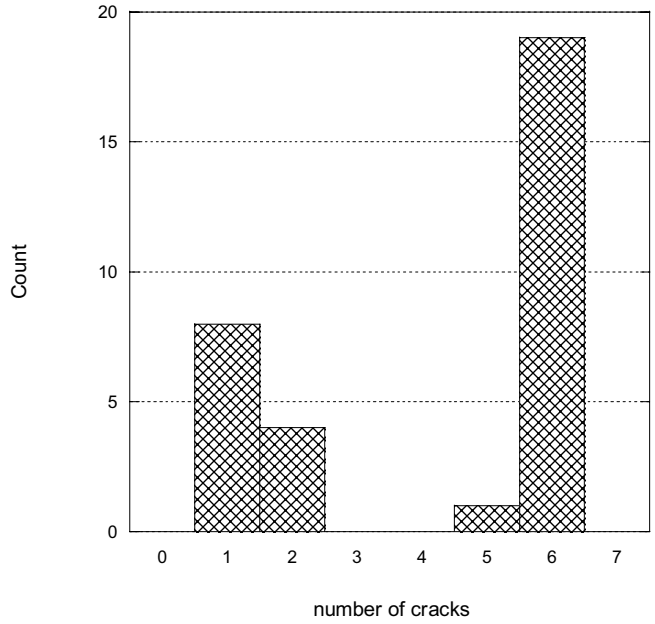

Figure 10-2 The number of cracks for each case of thermal fatigue in austenitic stainless steels

Out of the 20 cases where multiple cracking were observed the average distance between the cracks were evaluated in 9 cases. The result is shown in Figure 10-3. The average distance was calculated as 8.5 mm. For comparison 5 cases of thermal fatigue multiple cracking in carbon steel from /1/ are shown in Figure 10-3. The average distance for carbon steels were calculated as 0.8 mm. It is obvious that the crack pattern are considerable more dense in the carbon steel cases.

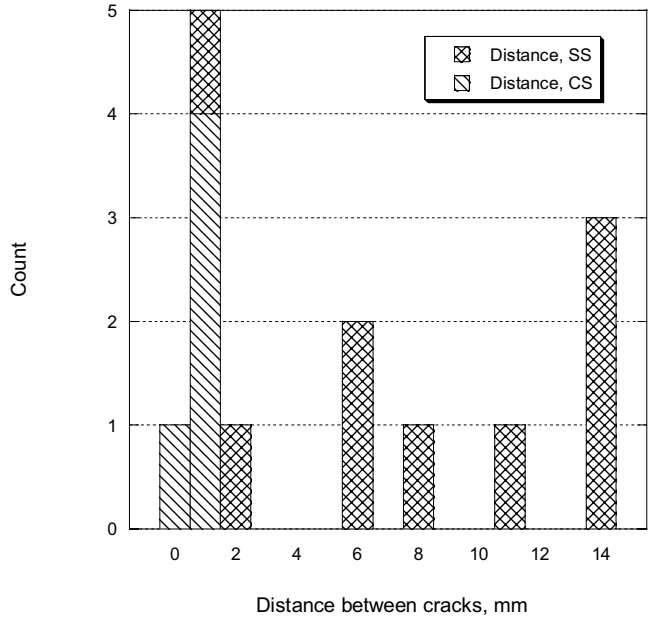

Figure 10-3 Distance between cracks in 9 cases of multiple cracking of thermal fatigue in austenitic stainless steels compared with five similar cases in carbon steels.

10.3 Metallurgical parameters

10.3.1 Orientation in through thickness direction

The orientation in through thickness direction was measured for 29 cases. Angles close to 90° dominates, see distribution in Table 10-4.

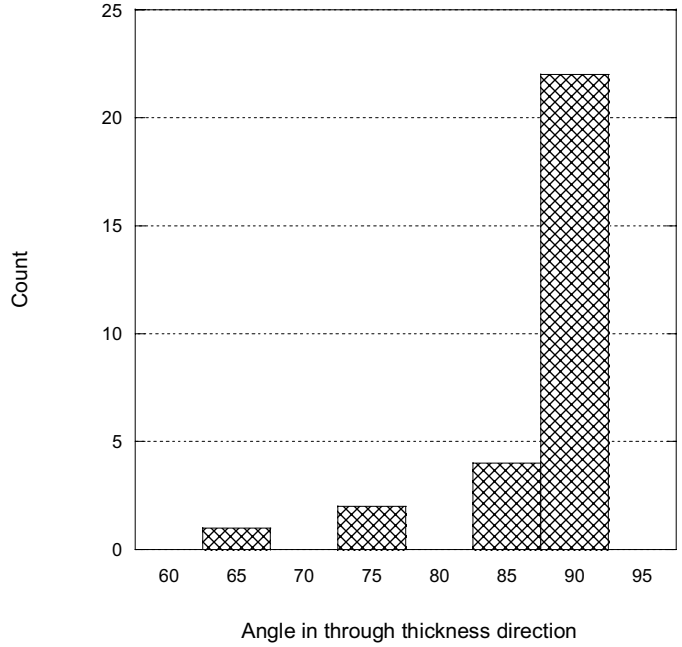

Table 10-4 Distribution of crack orientation in through thickness direction of thermal fatigue in austenitic stainless steels

10.3.2 Shape in through thickness direction

The shape in through thickness direction was evaluated for 32 cases. The dominating shape is straight, but winding cracks are frequent. The results are shown in Table 10-3.

Shape	Number
Straight	19
Winding	8
Lightly bend	4
Bi-liniear	1

Table 10-3 Shape in through thickness direction of thermal fatigue cracking in austenitic stainless steels

10.3.3 Macroscopic branching in through thickness direction

The degree of branching in the through thickness direction was measured for 36 cases. No branches is dominating, 27 cases. Occationally, up to one branch/mm was observed. The statistics are shown in Table 10-4 and a plot of branches verus crack depth in Figure 10-5.

	Branching
Points	36
Minimum	0
Maximum	1,7
Mean	0,197
Median	0
RMS	0,442
Std Deviation	0,401
Variance	0,161

Table 10-4 Statistics on degree of branching of thermal fatigue cracking in austenitic stainless steels

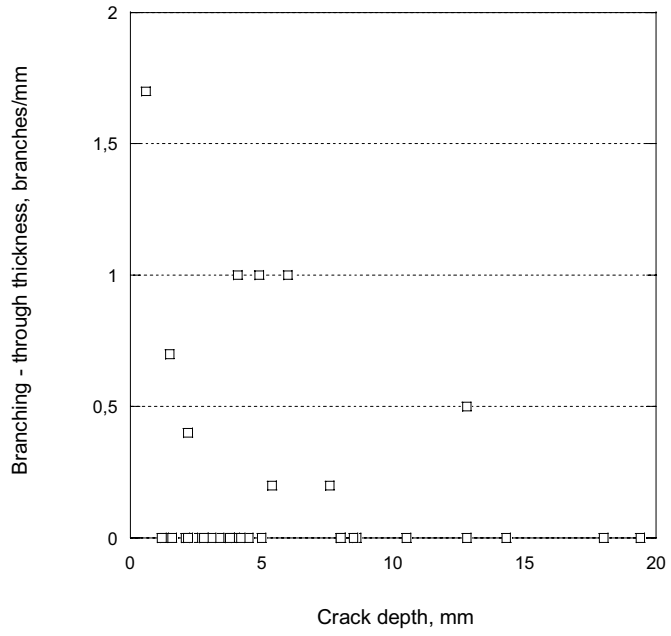

Figure 10-5 Branching in the through thickness direction versus crack depth

10.3.4 Crack tip radius

The crack tip radius was measured for 13 cases. Out of them 8 showed values below 1 micron. Two extreme values, 5 and 9 microns, also were recorded, see Figure 10-6.

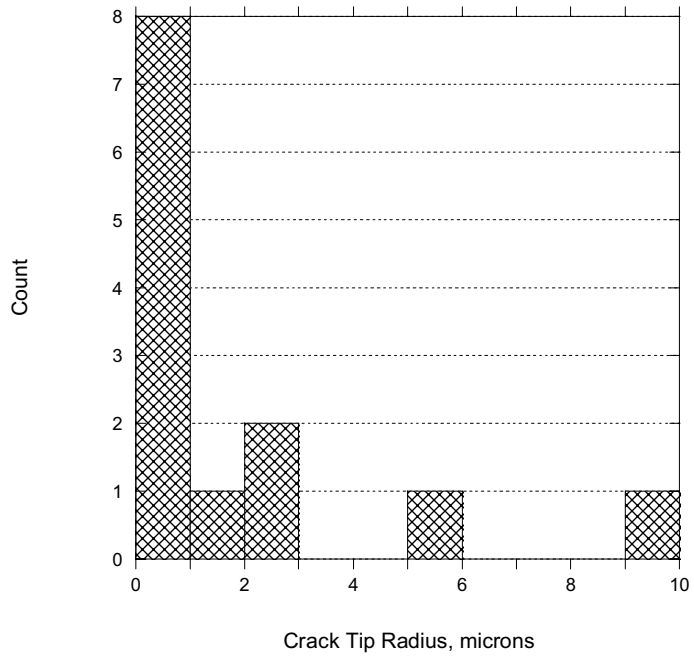

Figure 10-6 Distribution of crack tip radius of thermal fatigue cracking in austenitic stainless steels

10.3.5 Crack surface roughness

Surface roughness and correlation length were evaluated for 14 cases in this work. Data from 20 cases were collected from /1/. Intersections between the crack profile and the measuring line and number of turns were evaluated in this work but not in /1/. The statistics are summarised in Table 10-5. The distribution of surface roughness and correlation length are shown in Figures 10-7 and 10-8, respectively. The recorded intersections/mm is plotted versus number of turns/mm in Figure 10-9.

	Surface roughness, Rz [μm]	Correlation length, λ_0 [μm]	Intersections/mm	Turns/mm
Points	34	33	14	14
Minimum	6	27	1	0,700
Maximum	140	500	12	55
Mean	54,8	136	3,61	9,76
Median	45	106	3	5,5
RMS	64,2	172	4,54	16,4
Std Deviation	34,0	106	2,87	13,7
Variance	1156	11300	8,24	189

Table 10-5 Statistics on surface roughness, correlation length, intersections/mm and number of turns/mm of thermal fatigue cracking in austenitic stainless steels

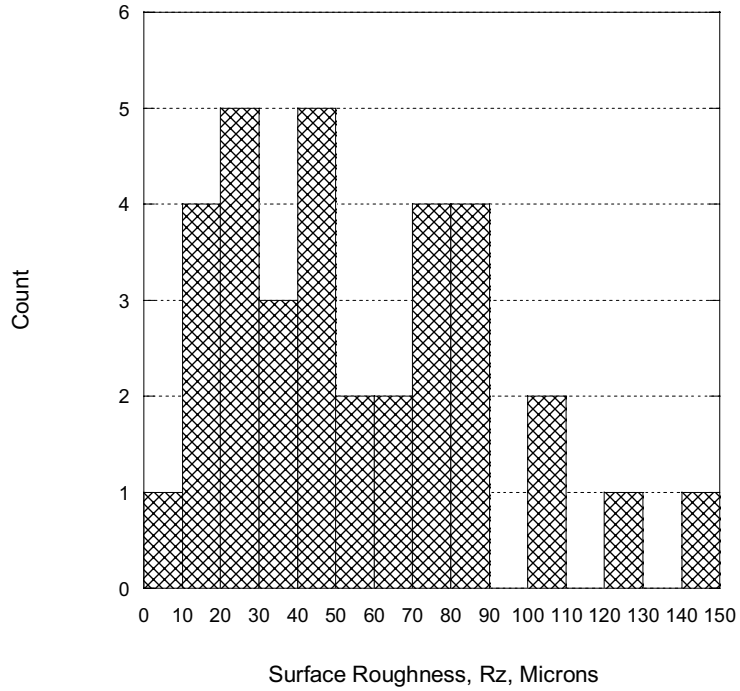

Figure 10-7 Distribution of surface roughness of thermal fatigue cracking in austenitic stainless steels

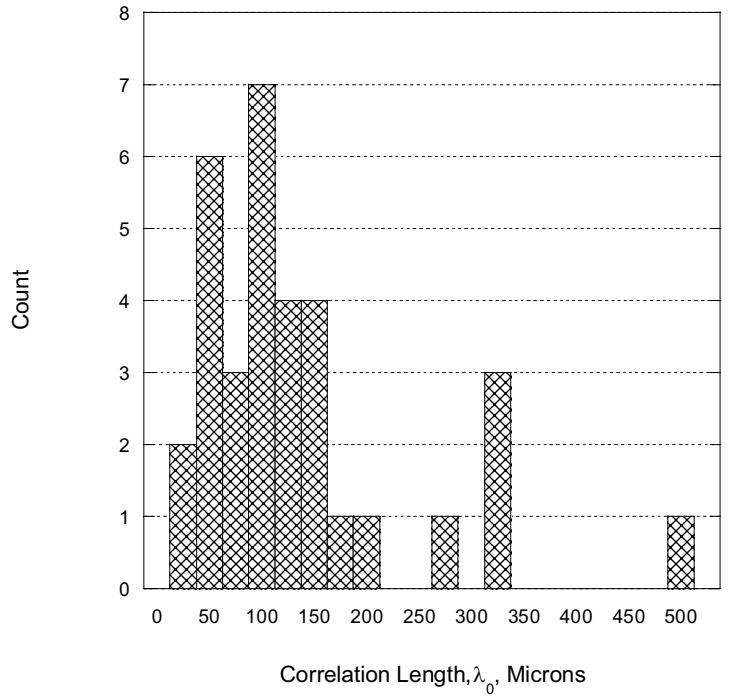

Figure 10-8 Distribution of correlation length of thermal fatigue cracking in austenitic stainless steels

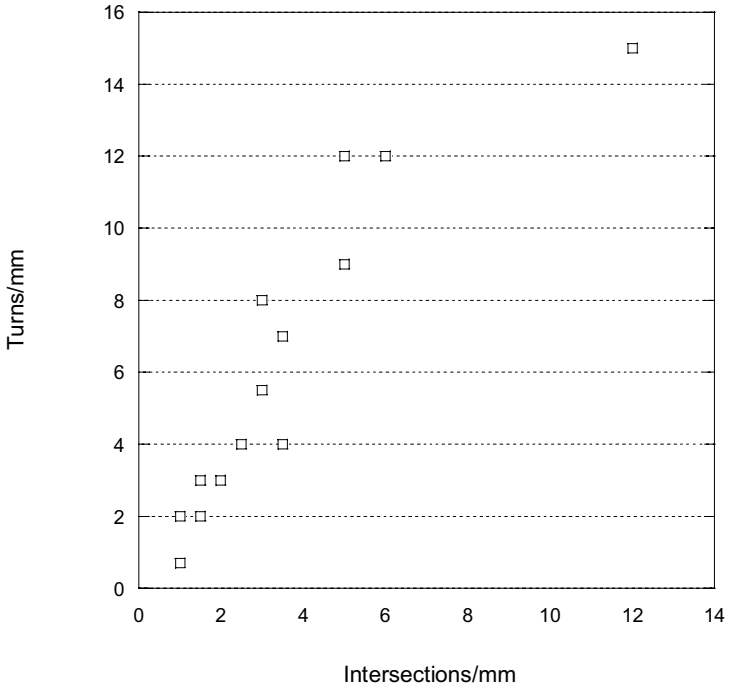

Figure 10-9 Intersections/mm versus turns/mm of thermal fatigue cracking in austenitic stainless steels

10.3.6 Crack width

Data from 30 cases are summarised in Table 10-6. The crack width is plotted versus crack depth/wall thickness ratio in Figure 10-10.

	Crack width at surface [μm]	Crack width at midway [μm]	Crack width at crack tip [μm]
Points	28	30	29
Minimum	5	2	1
Maximum	125	80	25
Mean	39,7	26	7,6
Median	28,5	20	7
RMS	48,9	32,2	9,33
Std Deviation	29,0	19,4	5,42
Variance	843	376	29,4

Table 10-6 Statistics on crack width of thermal fatigue cracking in austenitic stainless steels

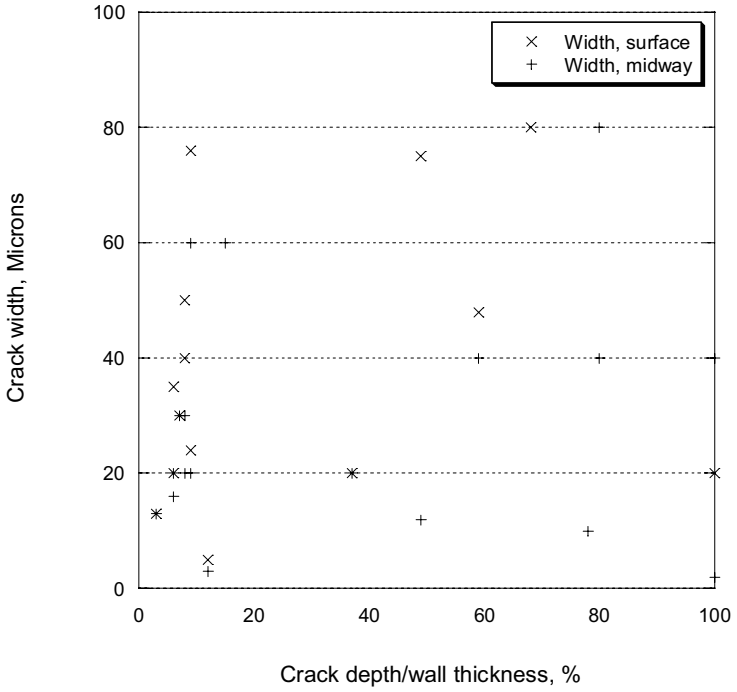

Figure 10-10 Crack width at surface and midway versus crack depth/wall thickness ratio of thermal fatigue cracking in austenitic stainless steels

10.3.7 Discontinuous appearance and weld repairs

Discontinuous appearance was not recorded for any of 16 evaluated casaes. Weld repairs was found in one case out of 16. The remaining cases were not evaluated for discontinuous appearance or weld repairs.

11 Mechanical fatigue

11.1 General comments

In this work three cases of mechanical fatigue in austenitic stainless steels were evaluated. Four cases were collected from /1/. To extend the data basis 11 cases of mechanical fatigue cracking in carbon and low alloy steels were added from /1/.

11.2 Visually detectable parameters

11.2.1 Location, orientation and shape in surface direction

Out of 18 cracks 10 started close to the weld fusion line. In 6 cases the crack started from another geometric stress raiser than a weld. The crack location of the two remaining cases was not recorded. Out of 10 cracks starting at the weld fusion line 9 are parallel to the weld direction and one is oriented in 45°. Out of 18 cracks 14 show a straight shape in the surface direction. In the remaining cases the shape was not recorded.

11.2.2 Number of cracks

Out of 18 cases a single crack was found in 11. In three cases five or more cracks were recorded. All cases with multiple cracking are located at other stress raisers than welds. The distribution of data is shown in Figure 11-1.

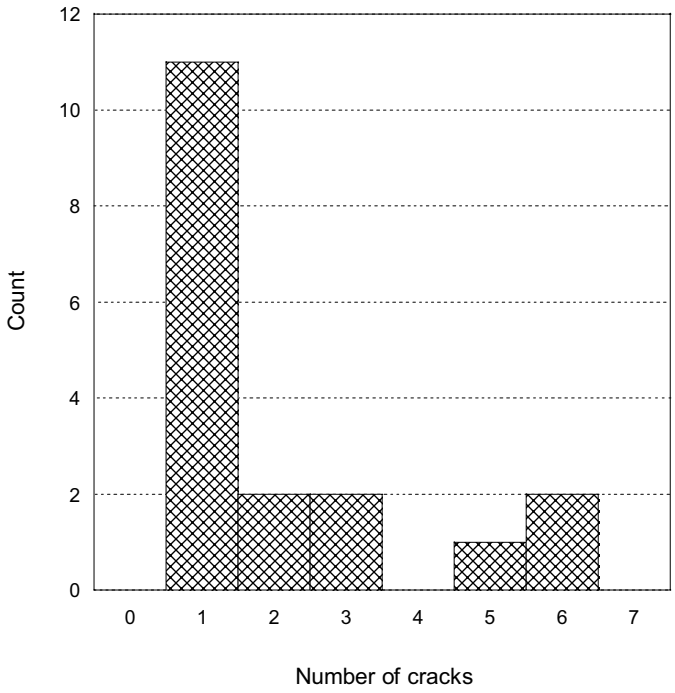

Figure 11-1 Distribution of number of cracks of mechanical fatigue cracking

11.3 Metallurgical parameters

11.3.1 Orientation and shape in through thickness direction

The angle in through thickness direction was evaluated in five cases. Two of them showed cracks oriented 90°. In two cases the angle was 75° and one case 65°.

The shape was evaluated in six cases. Four showed straight cracks and two winding cracks.

11.3.2 Macroscopic branching in through thickness direction

The branching was evaluated in all 18 cases. No macroscopic branching was found in any of those cases.

11.3.3 Crack tip radius

The crack tip radius was evaluated in five cases. It was measured as 2 μm in two cases, 3 μm in one and 15 μm in one case. From cracking due to fatigue very sharp crack tips are expected. The results indicate considerable influence of secondary corrosion within the crack tips.

11.3.4 Crack surface roughness

Crack surface roughness and correlation length were evaluated in seven cases. The number of intersections and turns were evaluated for three cases only. The statistics are shown in Table 11-1 and the distribution of surface roughness and correlation length in Figure 11-2. The number of turns/mm is plotted versus the number of intersections/mm in Figure 11-3. With few exceptions the fatigue cracks show low values of surface roughness and high correlation length, that is, smooth crack profiles with long wave length.

	Surface roughness, Rz [μm]	Correlation length, λ_0 [μm]	Intersections/mm	Turns/mm
Points	7	7	3	3
Minimum	8	36	1	1
Maximum	212	1000	6	6
Mean	43,6	312	3	3,33
Median	13	250	2	3
RMS	81,8	443	3,70	3,92
Std Deviation	74,8	340	2,65	2,52
Variance	5597	115600	7	6,33

Table 11-1 Statistics on crack surface roughness, correlation length, number of intersections and turns of mechanical fatigue cracking

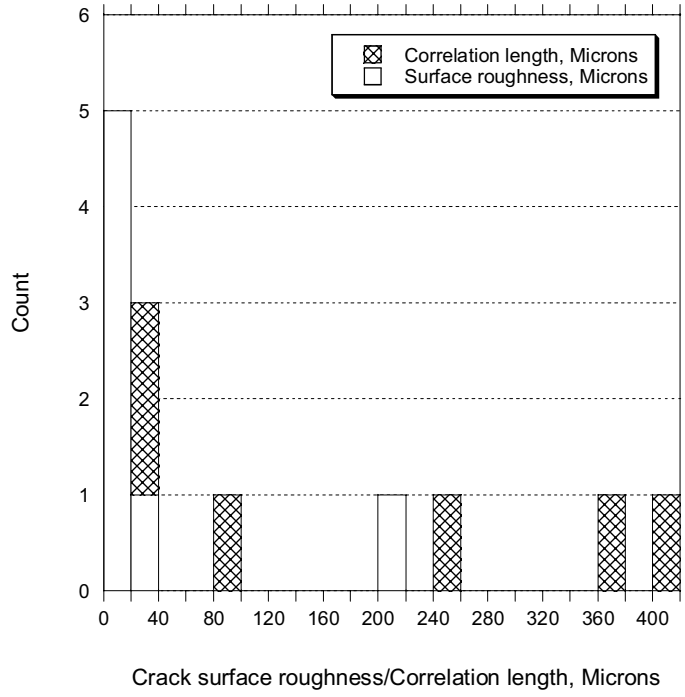

Figure 11-2 Distribution of crack surface roughness and correlation length of mechanical fatigue cracking

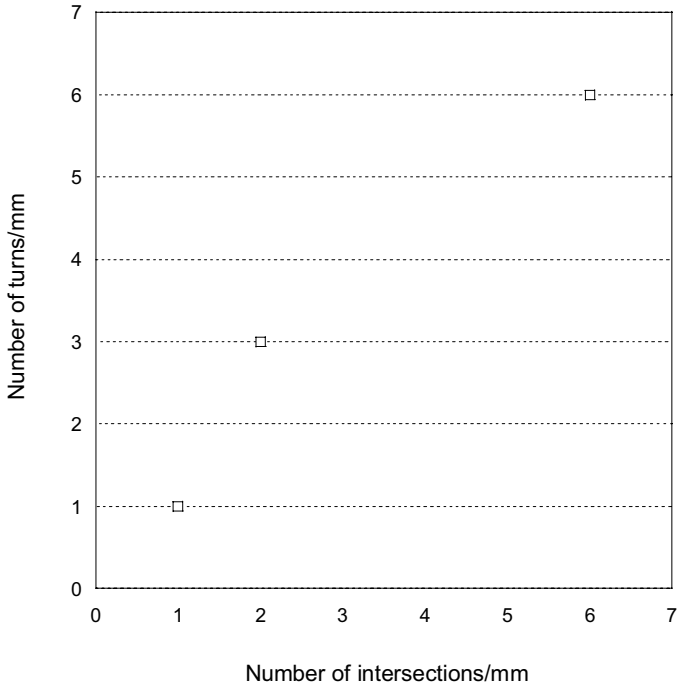

Figure 11-3 Number of turns versus number of intersection of mechanical fatigue cracking

11.3.5 Crack width

The crack width was evaluated in six cases. The statistics are shown in Table 11-2. Two cracks out of six were extremly wide, probably due to secondary corrosion. The remaining cases showed normal width, < 50 μm. The crack width distribution is shown in Figure 11-4.

	Crack width, surface [μm]	Crack width, midway [μm]	Crack width, crack tip [μm]
Points	6	5	4
Minimum	10	8	4
Maximum	450	250	30
Mean	130	108	12,2
Median	28	20	7,5
RMS	211	158	16,1
Std Deviation	182	130	12,1
Variance	33100	16900	147

Table 11-2 Statsitics on crack width of mechanical fatigue cracking.

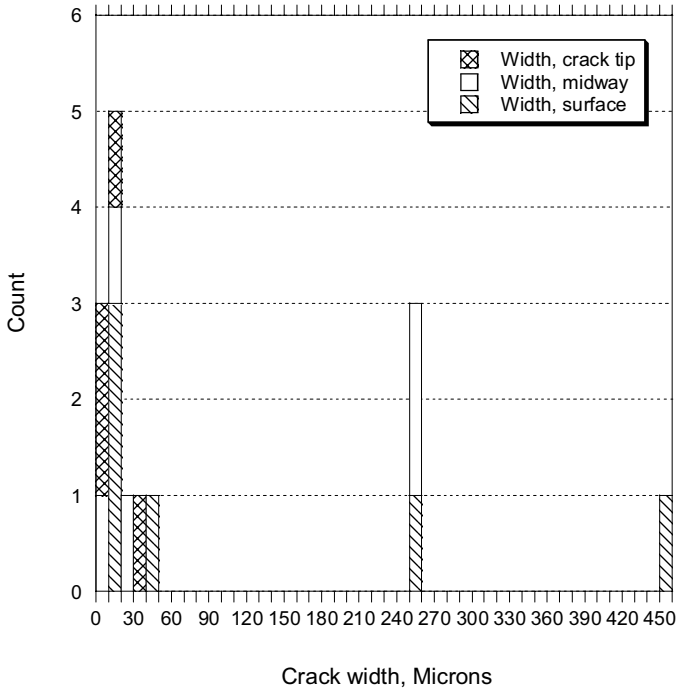

Figure 11-4 Distribution of crack width at thre locations of mechanical fatigue cracking

11.3.6 Discontinuous appearance and weld repairs

Discontinuous appearance or weld repairs was not recorded for any of the evaluated casaes.

12 Solidification cracking (hot cracking)

12.1 General comments

Totally 17 cases are covered in this section. Out of them 14 were evaluated in this work and 3 are from /1/. The 17 cases cover four weld metal groups; six are in austenitic stainless steels, four in nickel base alloys, five in cobalt base alloys and two in carbon steels.

Especially, in nickel base alloys, an established opinion is that solidification cracking is difficult to distinguish from IDSCC. The four cases in this section were definitely identified as solidification cracking in the failure analysis reports. In case of an uncertain identification statement in the report the case was evaluated as IDSCC in section 8.

12.2 Visually detectable parameters

12.2.1 Location, orientation and shape in surface direction

In all 17 cases the cracking is located within the weld metal. Eleven cases are located in but-welds and six in overlay welding. Out of 11 but-welds the cracks are oriented parallel to the weld in 4 cases and transversal in 5 cases. In two cases the orientation was not recorded. The shape in surface direction was documented in five cases. Four showed straight shape and one winding. Typical appearance on the surface and the through thickness direction is shown by Figure 12-1.

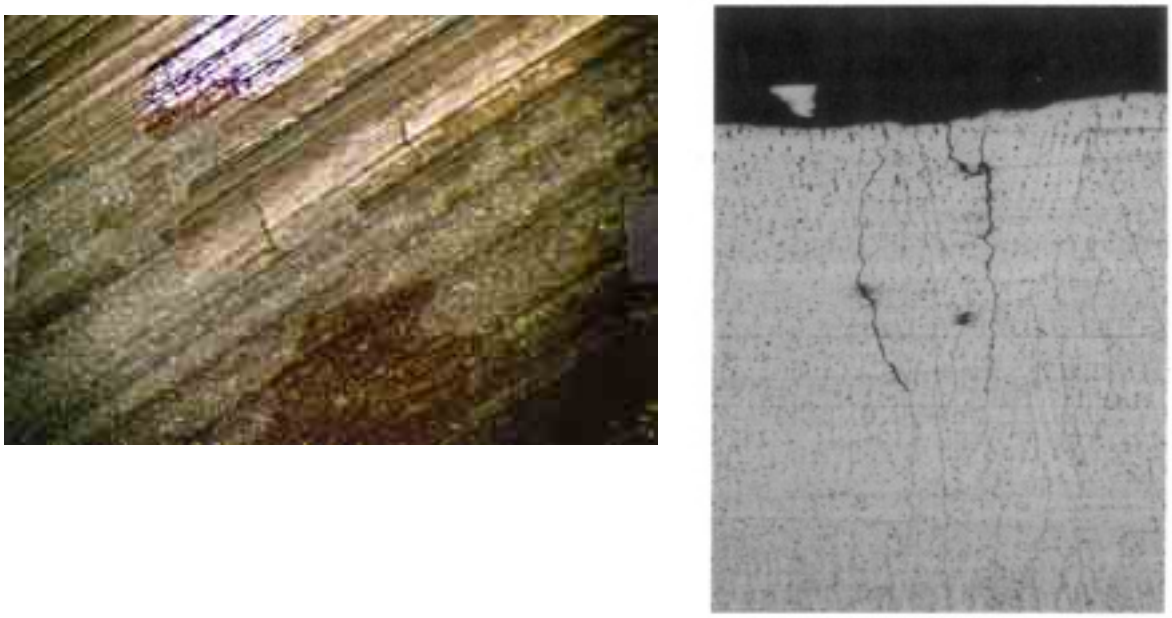

Figure 12-1 Typical appearance on the surface and in through thickness direction of solidification cracking in weld metal

12.2.2 Number of cracks

The number of cracks in the cracked region was evaluated in all 17 cases. The distribution is shown by Figure 12-2. Out of 17 cases five cracks or more were found in 11. The stack of 6 in Figure 12-2 represents > 5 cracks. Single cracking was found in three cases.

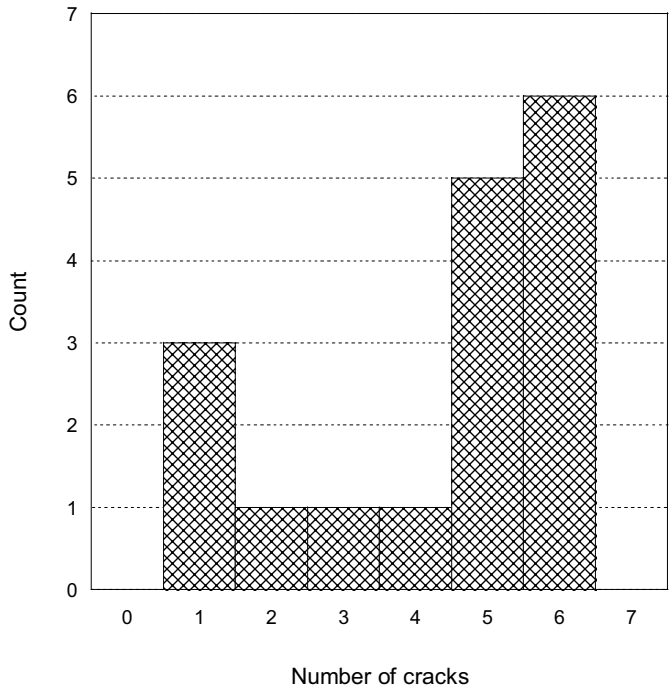

Figure 12-2 Distribution of number of cracks of solidification cracking in weld metal

12.3 Metallurgical parameters

12.3.1 Orientation in through thickness direction

The crack orientation was evaluated in 12 cases. An angle close to 90° was found in all, but one case. The distribution is shown in Figure 12-3.

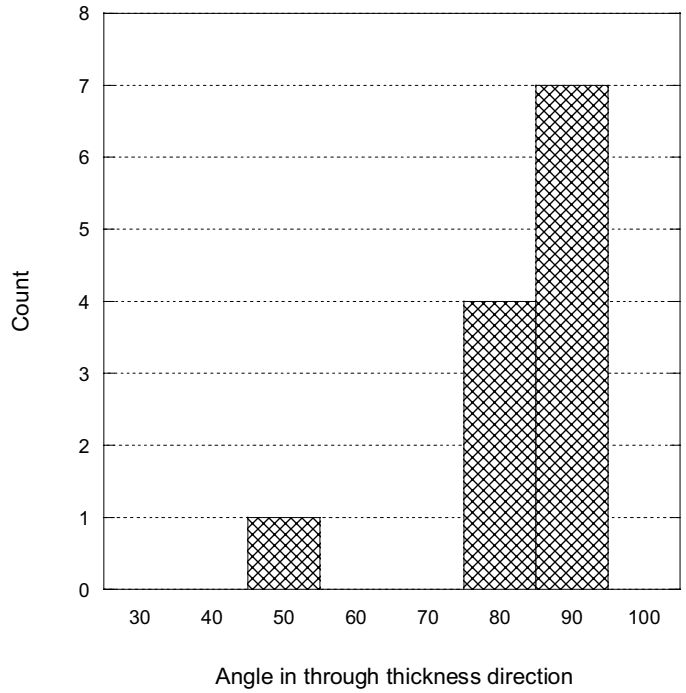

Figure 12-3 Distribution of crack orientation in through thickness direction of solidification cracking in weld metal

12.3.2 Shape in through thickness direction

The shape in through thickness direction was evaluated for all, but one case. Winding cracks were found in 12 cases, straight in three and bilinear in one case.

12.3.3 Macroscopic branching in through thickness direction

Macroscopic branching was evaluated in 16 cases. No branching was found in 13 cases and heavy branching in two. The distribution is given by Figure 12-4.

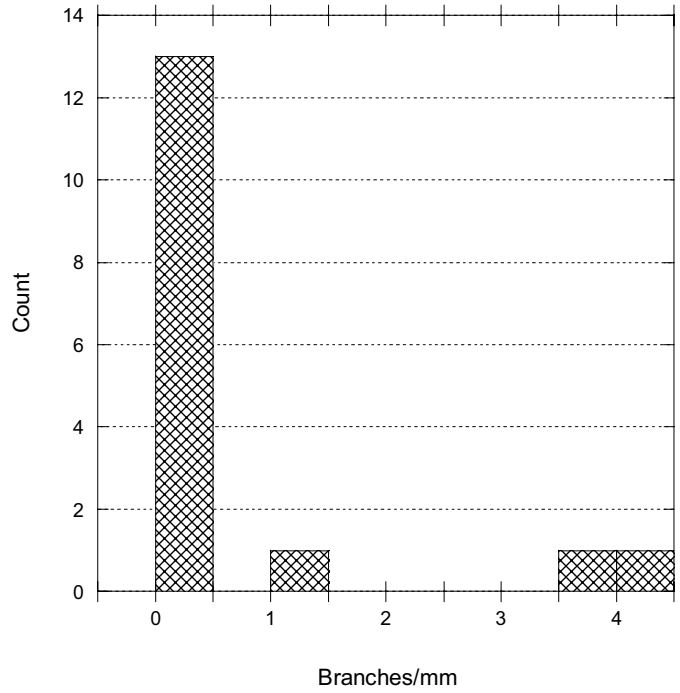

Figure 12-4 Distribution of branching of solidification cracking in weld metal

12.3.4 Crack tip radius

The crack tip radius was evaluated in 14 cases. The majority showed radii ≤ 1 μm, see Figure 12-5.

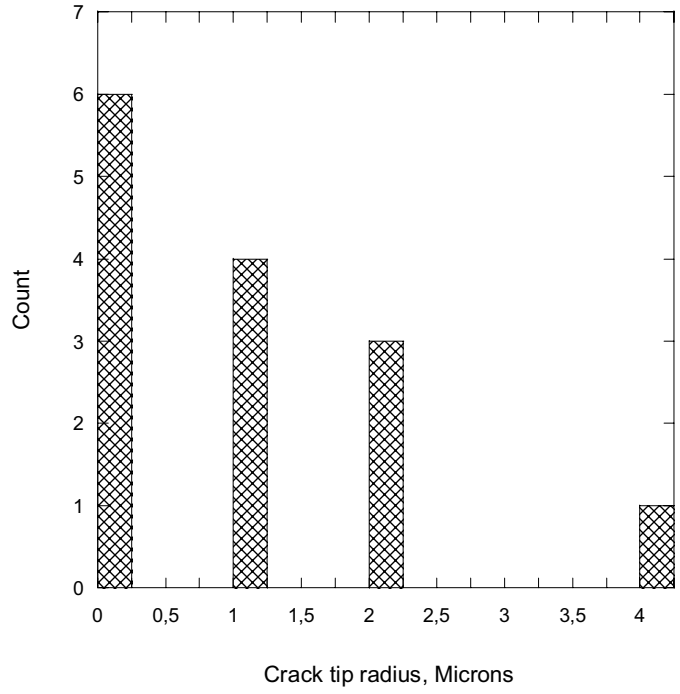

Figure 12-5 Distribution of crack tip radius of solidification cracking in weld metal

12.3.5 Crack surface roughness

The crack surface roughness was evaluated for 17 and the correlation length for 14 cases. The statistics are shown in Table 12-1. The distribution of crack surface

roughness and correlation length is shown in Figure 12-6 and a plot of crack turns/mm versus intersections/mm is shown in Figure 12-7. Two extreme values, 500, are excluded from Figure 12-6.

	Surface roughness, Rz [μm]	Correlation length, λ_0 [μm]	Intersections/mm	Turns/mm
Points	17	14	14	14
Minimum	6	23	1	1
Maximum	155	500	22	46
Mean	43,1	154	6,37	12,6
Median	30	105,5	4,75	9,5
RMS	57,5	213	8,30	17,0
Std Deviation	39,2	154	5,51	11,8
Variance	1535	23620	30,4	139

Table 12-1 Statistics on crack surface roughness, correlation length, crack intersections and turns of solidification cracking in metal

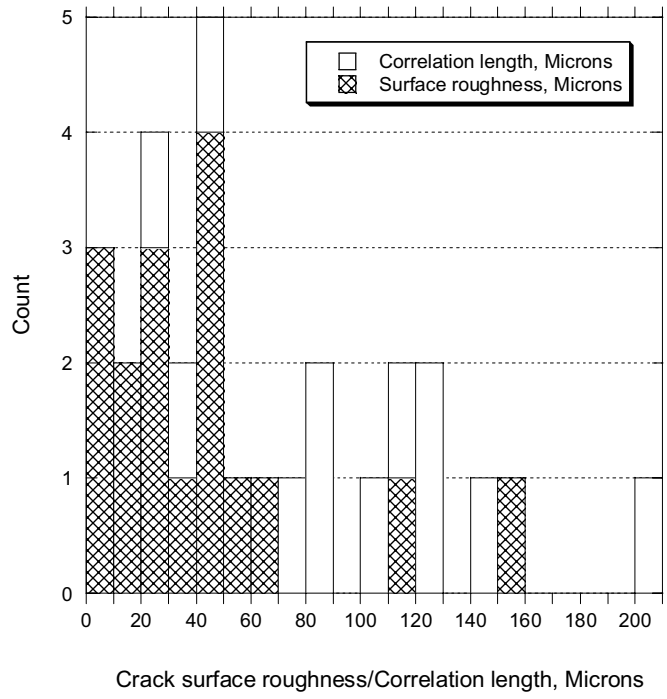

Figure 12-6 Distribution of crack surface roughness and correlation length of solidification cracking in weld metal

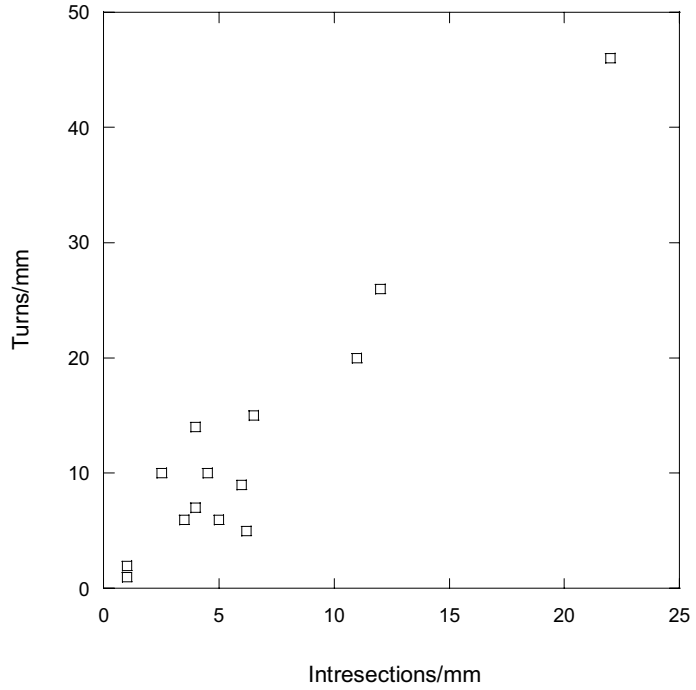

Figure 12-7 Number of turns/mm versus intersections/mm of solidification cracking in weld metal

12.3.6 Crack width

The crack width was evaluated in 17 cases. The statistics are shown in Table 12-2 and the distribution in Figure 12-8, where the most exreme crack width values are excluded.

	Crack width, surface [μm]	Crack width, midway [μm]	Crack width, crack tip [μm]
Points	17	16	16
Minimum	2	2	1
Maximum	250	110	70
Mean	38,6	21,6	7,12
Median	25	15,5	2
RMS	67,3	32,9	17,9
Std Deviation	56,8	25,6	16,9
Variance	3231	656	287

Table 12-2 Statistics on crack width at three locations of solidification cracking in weld metal

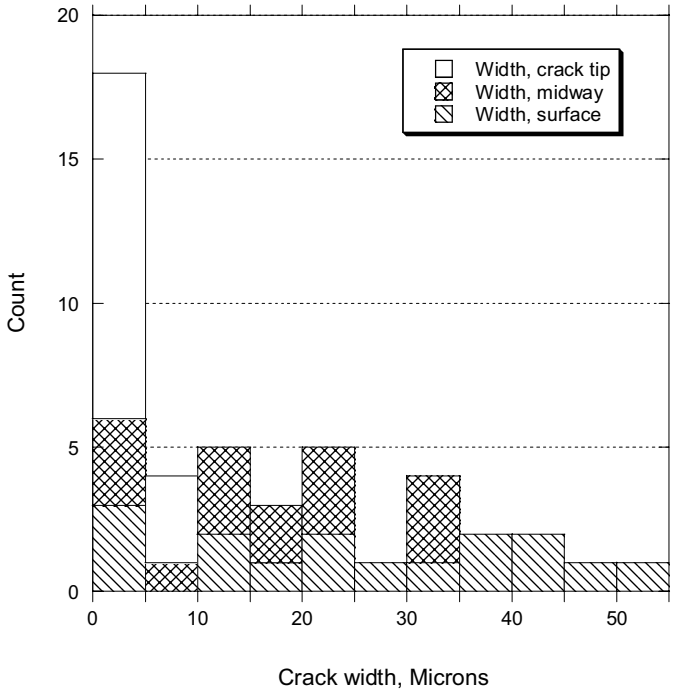

Figure 12-8 Crack width at three locations of solidification cracking in weld metal. One extreme is excluded.

12.3.7 Discontinuous appearance and weld repairs

Discontinuous appearance was not recorded for any of 14 evaluated cases. Weld repairs was found in three cases out of 14.

13 Data comparisons

13.1 General comments

The statistics for each evaluated parameter discussed in section 5-11 is compared similar as in /1/. The result is shown as statistics in tables and for an overview in plots. Two types of plots are used to give statistical information, such as median values and scatter, for comparison see Figure 13-5 and 13-6. The first, called box plot put 50 % of the data within the box. The top limit represents the upper quartile and the bottom limit the lower quartile. The lines extending from the box mark the 95 % limits in each direction. The remaining data are marked as individual points, outliners.

The second type of graph, called percentile plot, gives 90 % of the data within the box. The top limit is 95 % and the bottom 5 % confidence. The median value is marked as an unbroken line and the upper and lower quartile as dashed lines. Outliners above 95 % or below 5 % confidence are not shown.

13.2 Visually detectable parameters

13.2.1 Location

The crack location is highly depending on the cracking mechanism. For mechanisms such as IDSCC and solidification cracking all cracks are located to weld metal only. For stress corrosion cracking mechanisms cracks within and close to welds are common due to high weld residual stresses and in some cases due to weld sensitisation. Cracking

by mechanical fatigue often occurs at the weld fusion line where geometrical stress raisers and weld residual stresses are contributing factors, while thermal fatigue only occasionally is located close to welds. The frequency of cracking close to welds was evaluated for each cracking mechanism covered by this work, see Figure 13-1.

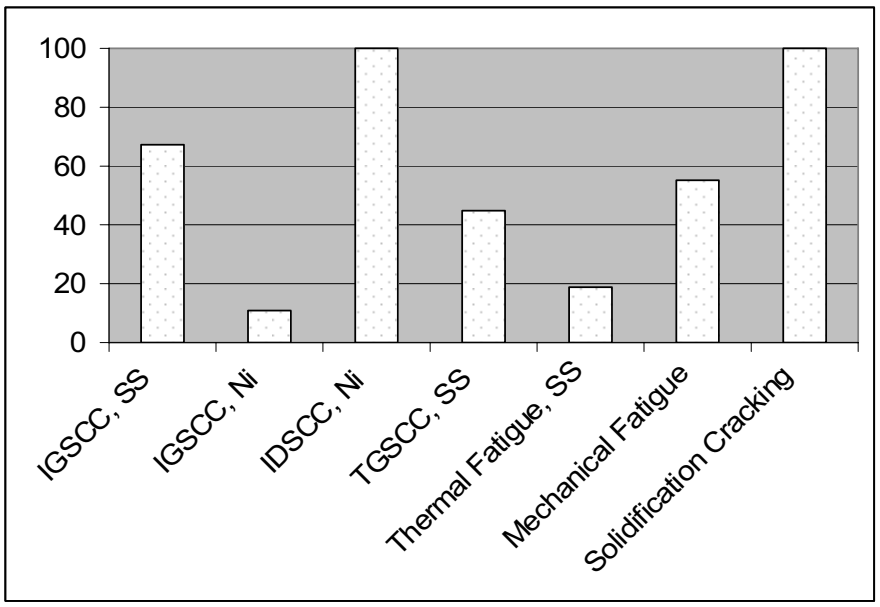

Figure 13-1 Frequency of cracking close to welds. All mechanism/material group combinations compared.

13.2.2 Orientation in surface direction (skew)

The orientation for cracking close to welds was compared for five crack mechanism/ material group combinations. Thermal fatigue and IGSCC in nickel base alloys were excluded due to lack of recorded data. The statistics is shown in Table 13-1 and in Figure 13-2. It is clearly shown that IGSCC and mechanical fatigue cracking mostly produce cracking parallel to the welds, while IDSCC mostly growth transverse to welds. Cracking due to TGSCC or solidification cracking are more randomly oriented.

	Crack orientation [º]				
	IGSCC, SS	IDSCC, Ni	TGSCC, SS	Mechanical Fatigue	Solidification Cracking
Points	26	12	6	10	9
Minimum	0	0	0	0	0
Maximum	20	90	90	45	90
Mean	1,65	78,8	45	4,5	50
Median	0	90	45	0	90
RMS	5,37	82,4	58,1	14,2	67,1
Std Deviation	5,21	25,6	40,2	14,2	47,4
Variance	27,1	655	1620	202	2250

Table 13-1 Statistics on crack orientation close to welds. Five cracking mechanism/-material group combinations are compared.

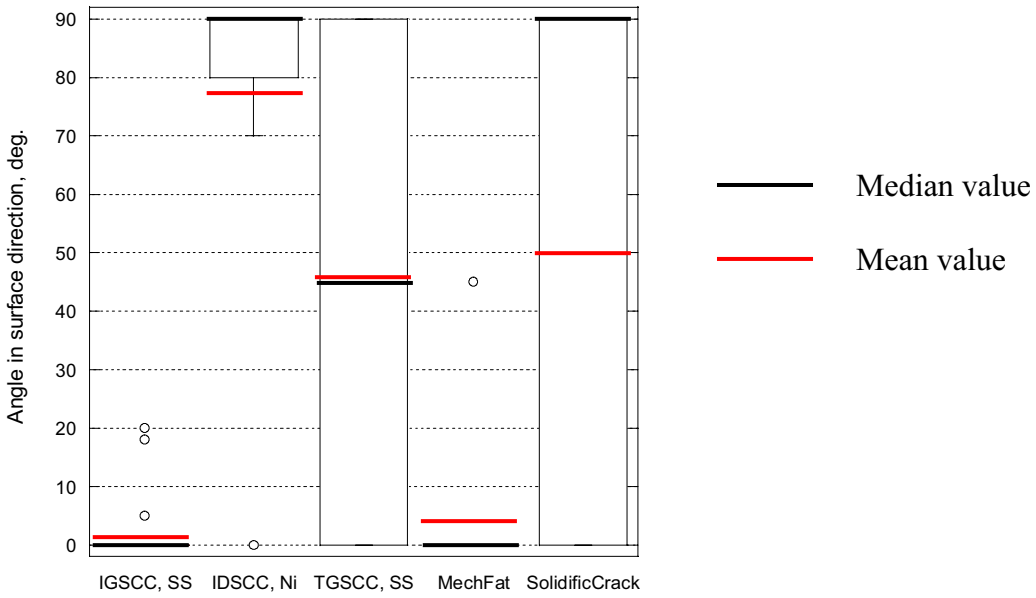

Figure 13-2 Crack orientation in surface direction for cracking close to welds. Five mechanism/material group combinations are compared. Box plot

13.2.3 Shape in surface direction

Generally, the most common shape in surface direction is straight and winding is the second most common. For mechanical fatigue only straight cracking was found and it is the most common shape for IGSCC, IDSCC, TGSCC and solidification cracking. TGSCC is the only mechanism showing branched shape and thermal fatigue is the only mechanism showing cobble stone pattern. The shape in surface direction is summarised in Figure 13-3.

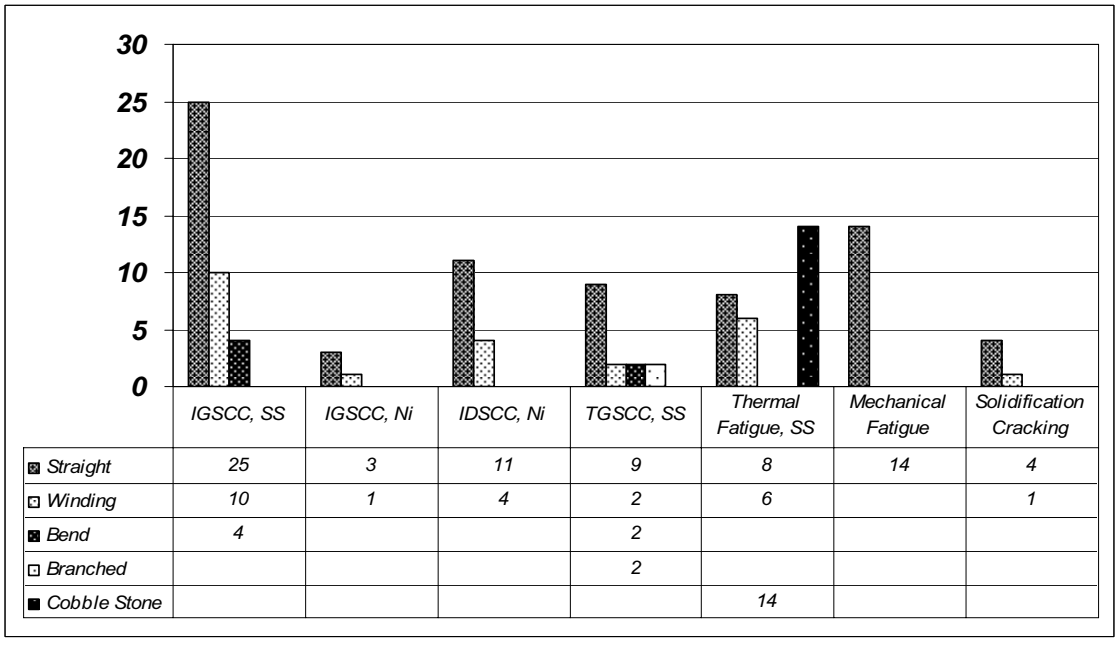

	IGSCC, SS	IGSCC, Ni	IDSCC, Ni	TGSCC, SS	Thermal Fatigue, SS	Mechanical Fatigue	Solidification Cracking
Straight	25	3	11	9	8	14	4
Winding	10	1	4	2	6		1
Bend	4			2			
Branched				2			
Cobble Stone					14		

Figure 13-3 Comparison of shape in surface direction between seven cracking mechanism/material group combinations

13.2.4 Number of cracks

The number of cracks in the cracked area was compared between the cracking mechanism/material group combinations covered by this work. The result is displayed in Table 13-2 and Figure 13-4. In cases where more than five cracks were found the number of cracks was set as 6, which affects the mean value and the statistical scatter factors.

It is obvious that TGSCC, thermal fatigue and solidification cracking mostly produce more than five cracks, while the remaining mechanisms result in single cracking or occasionally two or more cracks.

	Number of cracks in the cracked area						
	IGSCC, SS	IGSCC, Ni	IDSCC, Ni	TGSCC, SS	Thermal Fatigue	Mechanical Fatigue	Solidification Cracking
Points	70	18	30	30	32	18	17
Minimum	1	1	1	1	1	1	1
Maximum	6	6	6	6	6	6	6
Mean	1,87	1,83	1,57	4,03	4,25	2,11	4,29
Median	1	1	1	6	6	1	5
RMS	2,40	2,44	2,17	4,59	4,82	2,73	4,68
Std Deviation	1,52	1,65	1,52	2,22	2,31	1,78	1,93
Variance	2,32	2,74	2,32	4,93	5,35	3,16	3,72

Table 13-2 Comparison of number of cracks for all covered cracking mechanism/ material group combinations

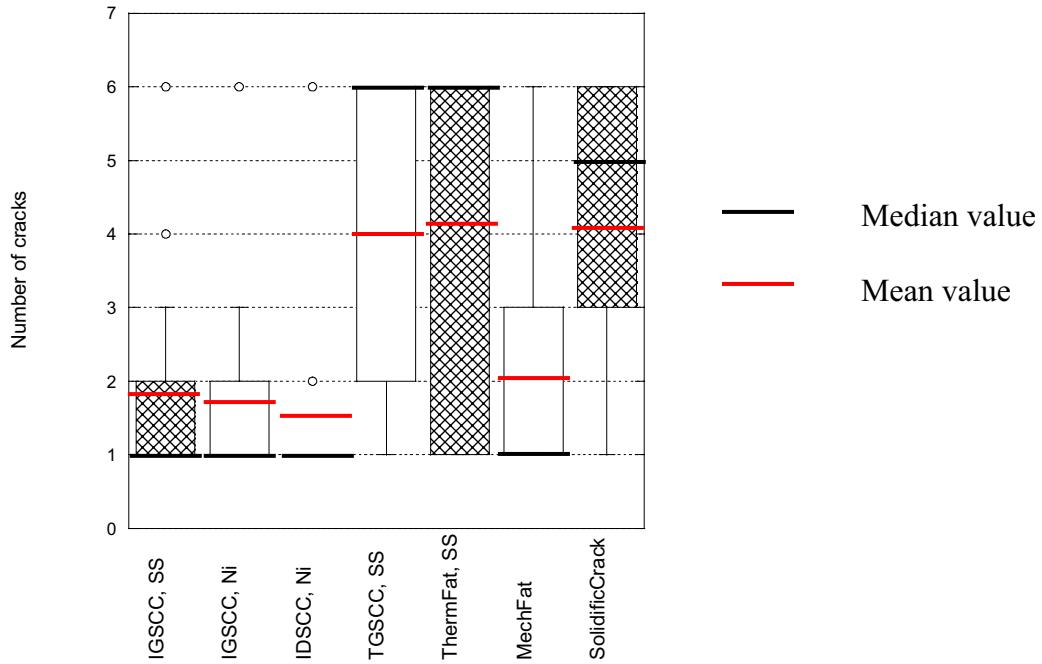

Figure 13-4 Comparison of number of cracks for seven cracking mechanism/material group combinations. Box plot

13.3 Metallurgical parameters

13.3.1 Orientation in through thickness direction (tilt)

The crack orientation in the through thickness direction was compared for the cracking mechanism/material group combinations covered by this work. The result is shown by Table 13-3 and Figures 13-5, and 13-6. All data groups end up with median angles as 90°, but IDSCC which show 80°. Thermal fatigue shows largest scatter.

	Crack orientation [º]						
	IGSCC, SS	IGSCC, Ni	IDSCC, Ni	TGSCC, SS	Thermal Fatigue	Mechanical Fatigue	Solidification Cracking
Points	71	14	19	27	20	16	12
Minimum	40	60	45	45	16	60	45
Maximum	100	90,6	90	90	90	90	90
Mean	85,6	85,0	78,4	82,6	82,7	81,9	82,9
Median	90	90	80	90	90	90	90
RMS	86,0	85,7	79,3	83,5	84,4	82,6	83,8
Std Deviation	8,39	10,9	12,1	12,7	17,1	11,7	12,9
Variance	70,5	120	147	162	294	136	166

Table 13-3 Orientation in through thickness direction for seven cracking mechanism/material group combinations

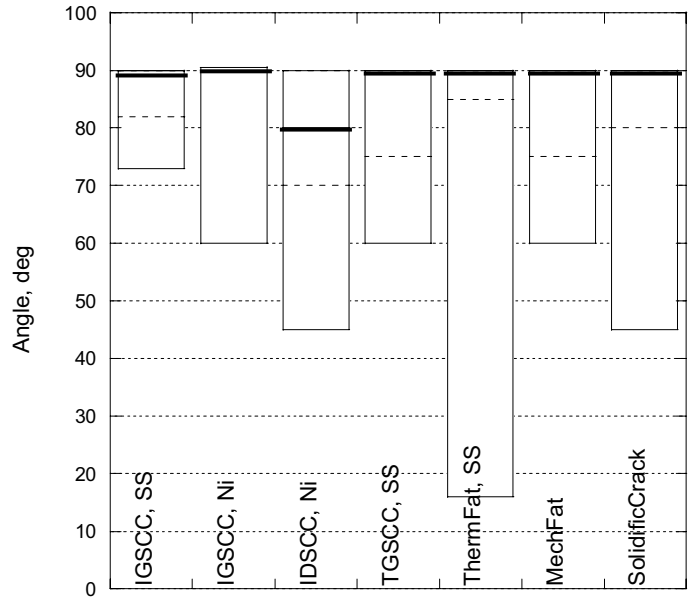

Figure 13-5 Orientation in through thickness direction for seven cracking mechanism/ material group combinations. Percentile plot.

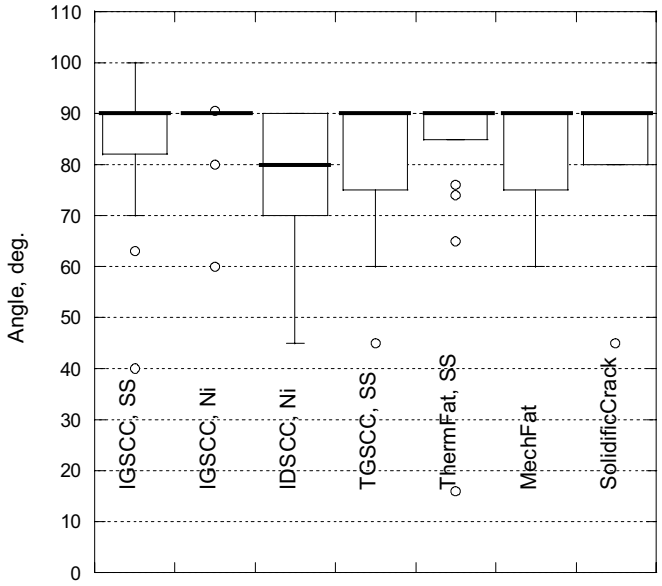

Figure 13-6 Crack orientation in through thickness direction for IGSCC in austenitic stainless steels. Box plot.

13.3.2 Shape in through thickness direction

The crack shape in through thickness direction was compared between all cracking mechanism/material group combinations covered by this work. The result is shown by Figure 13-7. A winding shape is dominating the inter-granular, inter-dendritic and solidification cracking mechanisms, while straight cracking is most common for fatigue mechanisms. Branched cracking is the most common shape for TGSCC in austenitic stainless steels.

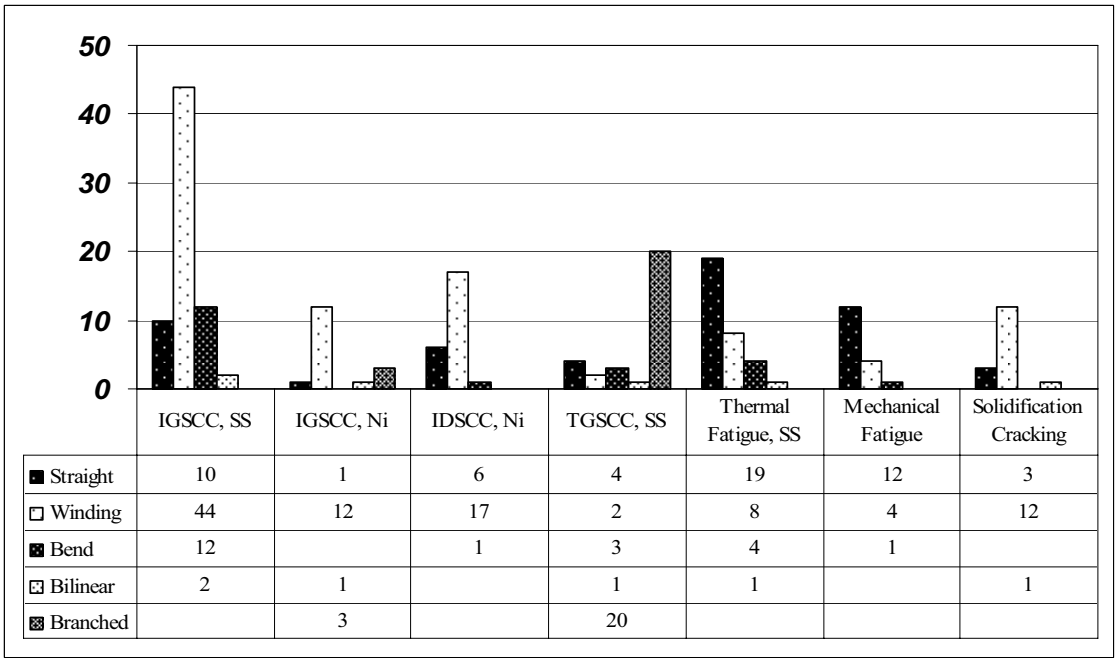

	IGSCC, SS	IGSCC, Ni	IDSCC, Ni	TGSCC, SS	Thermal Fatigue, SS	Mechanical Fatigue	Solidification Cracking
Straight	10	1	6	4	19	12	3
Winding	44	12	17	2	8	4	12
Bend	12		1	3	4	1	
Bilinear	2	1		1	1		1
Branched		3		20			

Figure 13-7 Comparison of shape in through thickness direction between seven cracking mechanism/material group combinations

13.3.3 Macroscopic branching in through thickness direction

Macroscopic branching was compared, se Table 13-4 and Figures 13-8 and 13-9. TGSCC in austenitic stainless steels is the cracking mechanism/material combination that shows the highest values. Due to a few extreme values IGSCC in nickel base alloys almost reaches similar values. Thermal fatigue show low tendency to branching, while mechanical fatigue does not show any branching at all.

	Number of macroscopic branches per mm of crack depth						
	IGSCC SS	IGSCC Ni	IDSCC Ni	TGSCC SS	Thermal Fatigue	Mechanical Fatigue, SS	Solidification Cracking
Points	71	17	24	28	30	18	16
Minimum	0	0	0	0	0	0	0
Maximum	2,5	8	2	10	1,7	0	4
Mean	0,353	2,04	0,396	2,51	0,17	0	0,55
Median	0	1	0	2	0	0	0
RMS	0,742	3,22	0,717	3,51	0,435	0	1,40
Std Deviation	0,657	2,56	0,610	2,50	0,407	0	1,33
Variance	0,432	6,57	0,373	6,26	0,166	0	1,77

Table 13-4 Macroscopic branching in through thickness direction for seven cracking mechanism/material group combinations

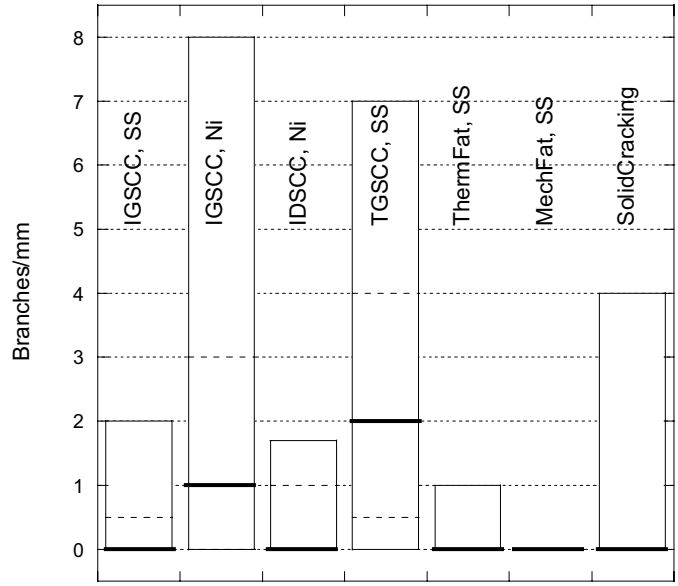

Figure 13-8, Comparison of branching tendency of seven cracking mechanism/material group combinations. Percentile plot.

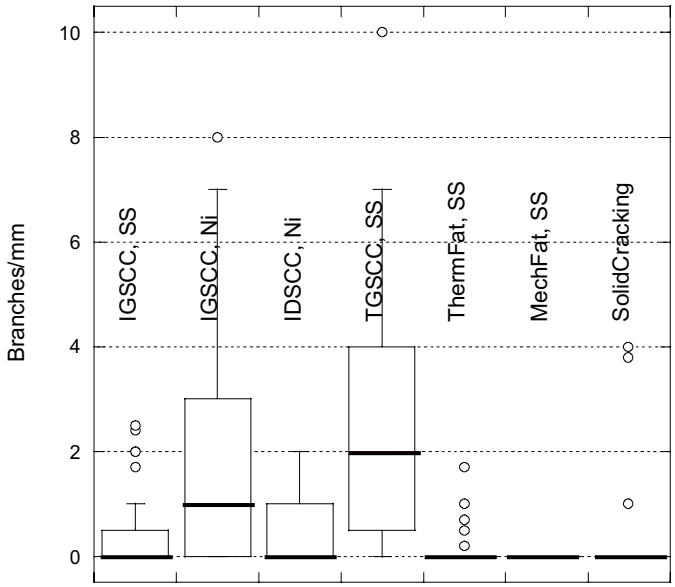

Figure 13-9 Comparison of branching tendency of seven cracking mechanism/material group combinations. Box plot.

13.3.4 Crack tip radius

A comparison of crack tip radius is shown in Table 13-5 and in Figure 13-10. A crack tip radius < 1 μm normally was not measurable, and was given the value of 0.1 μm during the statistical evaluation. All mechanisms, but two, show a typical crack tip radius close to 1 μm. The exceptions are mechanical fatigue and solidification cracking, showing radii close to 4 μm. The influence of secondary corrosion must be considered independent of cracking mechanism.

	Crack tip radius [μm]						
	IGSCC SS	IGSCC Ni	IDSCC Ni	TGSCC SS	Thermal Fatigue	Mechanical Fatigue	Solidification Cracking
Points	49	14	10	20	13	15	17
Minimum	0,1	0,1	0,1	0,1	0,1	0,1	1
Maximum	7	10	2	15	9	15	6
Mean	0,82	1,08	1,61	1,46	1,52	3,89	4,29
Median	0,1	0,1	2	0,1	0,1	3	5
RMS	1,56	2,80	1,73	3,63	2,97	5,58	4,68
Std Deviation	1,34	2,69	0,67	3,41	2,66	4,15	1,93
Variance	1,80	7,22	0,45	11,6	7,08	17,2	3,72

Table 13-5 Comparison of crack tip radius between seven cracking mechanism/material group combinations

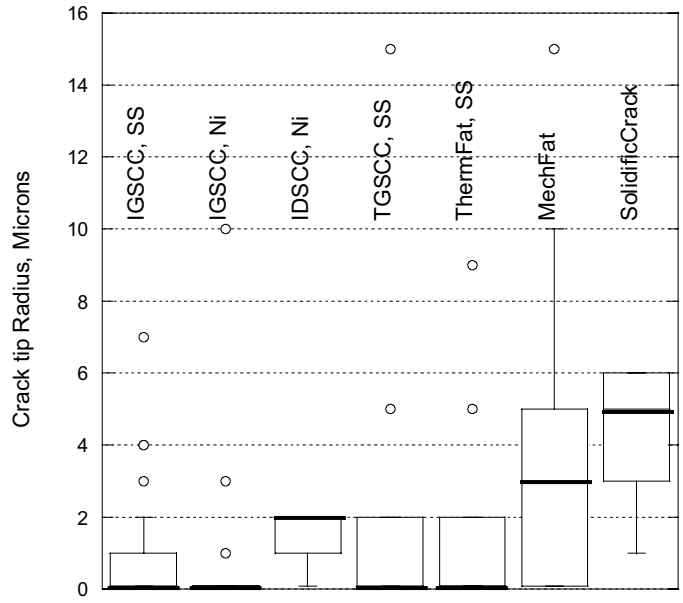

Fig 13-10 Comparison of crack tip radius of seven cracking mechanism/material group combinations. Box plot.

13.3.5 Crack surface roughness

A comparison of crack surface roughness parameters of all evaluated crack mechanism/material group combinations was made. The evaluated parameters are crack surface roughness, R_z, correlation length, λ_0, number of intersections/mm and number of turns/mm, as defined in section 5. The resulting statistics on crack surface roughness is shown in Table 13-6, by a box plot in Figure 13-11 and by a percentile plot in Figure 13-12. The most significant deviations are the high values measured for IDSCC and the low for mechanical fatigue. Both were expected and can easily be explained. The coarse solidification structure of a nickel base weld metal is expected to produce a crack profile with high top to valley distance. On the contrary, a fatigue crack growth process normally produces smooth crack surfaces with low top heights, which is verified by the results of this work. Solidification cracking is expected to show similar surface roughness as IDSCC. However, this was not verified.

The correlation length, representing the wave length of the crack profile, was compared in a similar way. The result is shown by statistics in Table 13-7 and by plots in Figures 13-13 and 13-14. The largest values were found for mechanical fatigue, which is expected.

Another parameter representing the wave length is the number of intersections between the crack profile and the median line. A comparison of this parameter is shown by statistics in Table 13-8 and by box plots in Figures 13-15 and 13-16. The results from IGSCC of nickel base alloys strongly deviates from the remaining groups, which is the reason why two graphs are used, one with and the other without showing IGSCC of nickel base alloys.

Finally, the number of turns of the crack profile is shown by statistics in Table 13-9 and by plots in Figures 13-17 and 13-18. Of the same reasons as above IGSCC in nickel base alloys is included in the first plot but excluded in the second. It was noted that both fatigue cracking mechanisms show low values, which was expected. Also IDSCC in nickel base alloys show low values, which may be explained by coarse weld metal micro-structure.

	Crack surface roughness, R_z [µm]						
	IGSCC SS	IGSCC Ni	IDSCC Ni	TGSCC SS	Thermal Fatigue	Mechanical Fatigue	Solidification Cracking
Points	69	19	24	29	34	16	17
Minimum	8	8	5	10	6	8	4
Maximum	200	142	288	90	140	212	155
Mean	70,7	42,8	106	37,1	54,8	30,4	43
Median	68	27	79,5	36	45	15	30
RMS	80,9	55,3	135	42,7	64,2	56,6	57,5
Std Deviation	39,6	36,0	85,2	21,6	34,0	49,3	39,3
Variance	1568	1299	7267	465	1156	2434	1545

Table 13-6 Comparison of crack surface roughness, R_z, between seven cracking mechanism/material group combinations

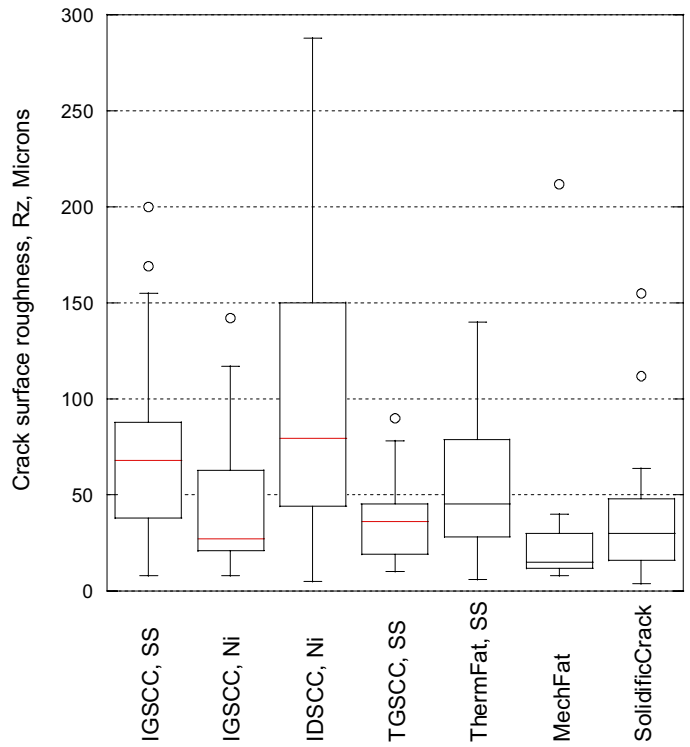

Figure 13-11 Comparison of crack surface roughness, R_z, between seven cracking mechanism/material group combinations. Box plot.

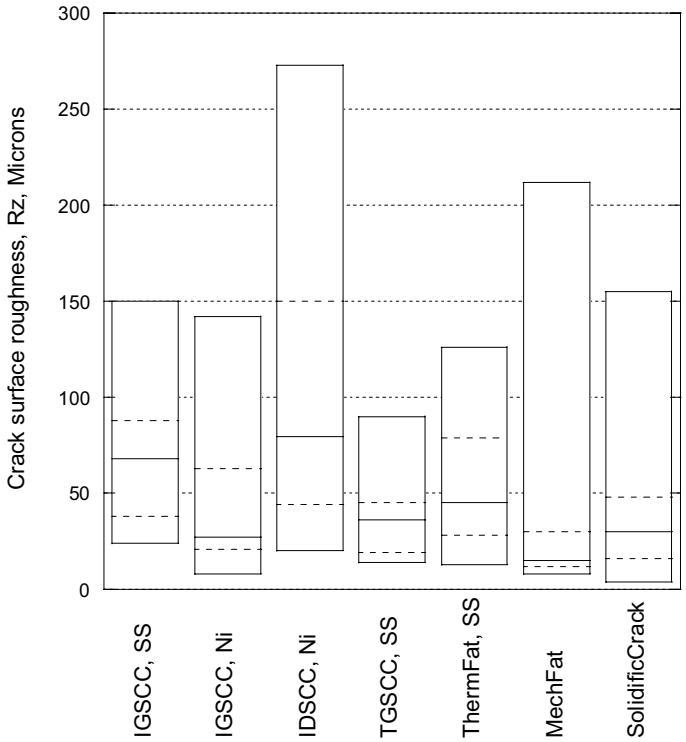

Figure 13-12 Comparison of crack surface roughness, R_z, between seven cracking mechanism/material group combinations. Percentile plot

	Correlation length, λ_0 [μm]						
	IGSCC SS	IGSCC Ni	IDSCC Ni	TGSCC SS	Thermal Fatigue	Mechanical Fatigue	Solidification Cracking
Points	72	17	26	12	33	14	14
Minimum	5	3,1	17	15	27	25	23
Maximum	310	150	500	160	500	1000	500
Mean	79,5	34,9	150	50,6	136	330	154
Median	71	14	113	31	106	265	105,5
RMS	97,5	53,1	193	67,2	171,7	438	213
Std Deviation	56,9	41,3	124	46,2	106	299	154
Variance	3240	1710	15500	2140	11300	89700	23620

Table 13-7 Comparison of correlation length, λ_0, between seven cracking mechanism/material group combinations

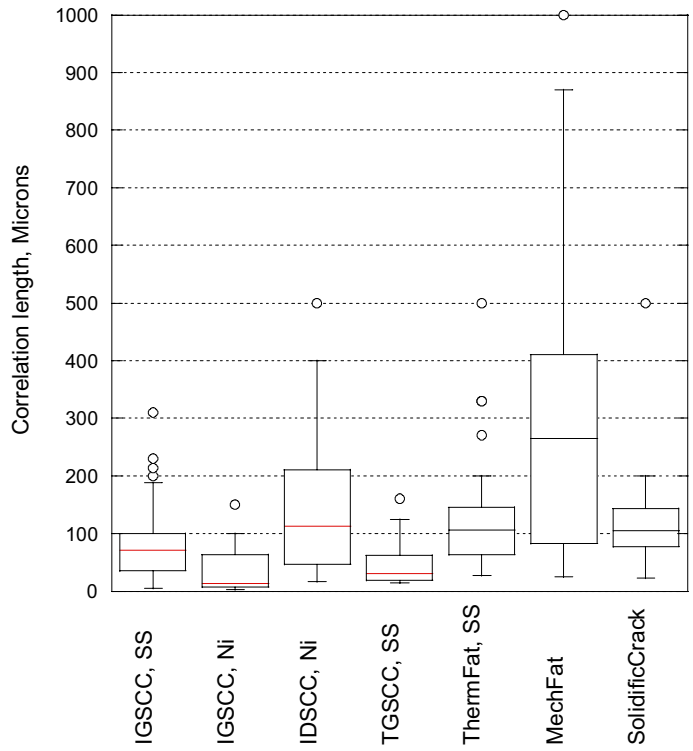

Figure 13-13 Comparison of correlation length, λ_0, between seven cracking mechanism/material group combinations. Box plot.

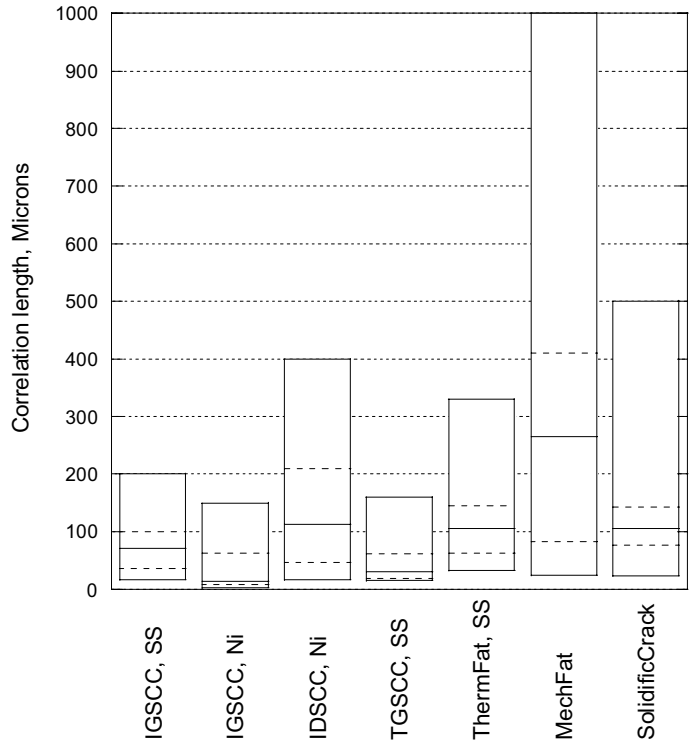

Figure 13-14 Comparison of correlation length, λ_0, between seven cracking mechanism/material group combinations. Percentile plot.

	Number of intersections/mm						
	IGSCC SS	IGSCC Ni	IDSCC Ni	TGSCC SS	Thermal Fatifue	Mechanical Fatigue	Solidification Cracking
Points	38	3	5	5	14	4	14
Minimum	1,6	7	1	3	0,08	1	1
Maximum	18	72	5	10	1	6	22
Mean	7,01	37,3	2,74	6,88	0,44	3,25	6,37
Median	6	33	2	8,1	0,33	3	4,75
RMS	8,15	45,9	3,13	7,44	0,52	3,77	8,30
Std Deviation	4,21	32,7	1,68	3,18	0,29	2,22	5,51
Variance	17,8	1070	2,84	10,1	0,086	4,92	30,4

Table 13-8 Statistics on number of intersection/mm between seven cracking mechanism/material group combinations

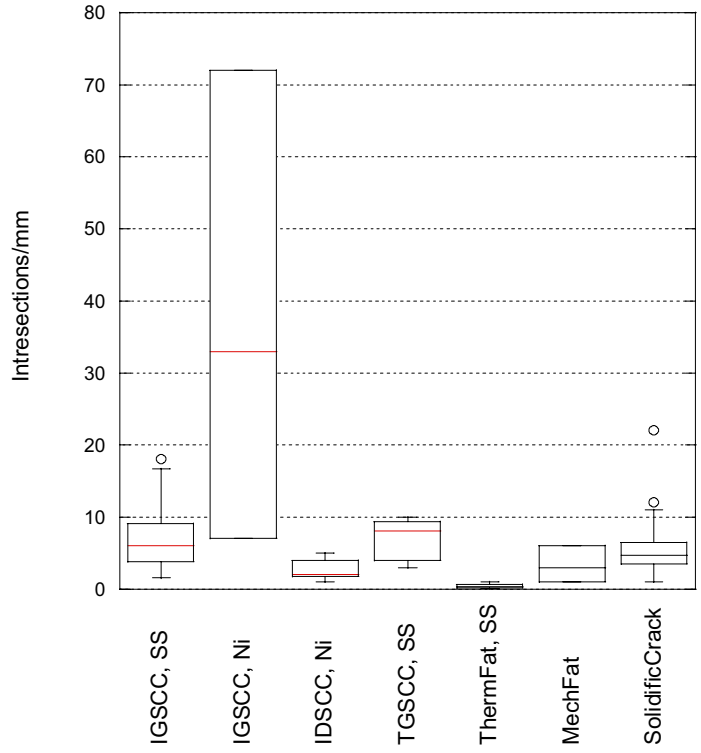

Figure 13-15 Comparison of number of intersection between seven cracking mechanism/material group combinations. Box plot.

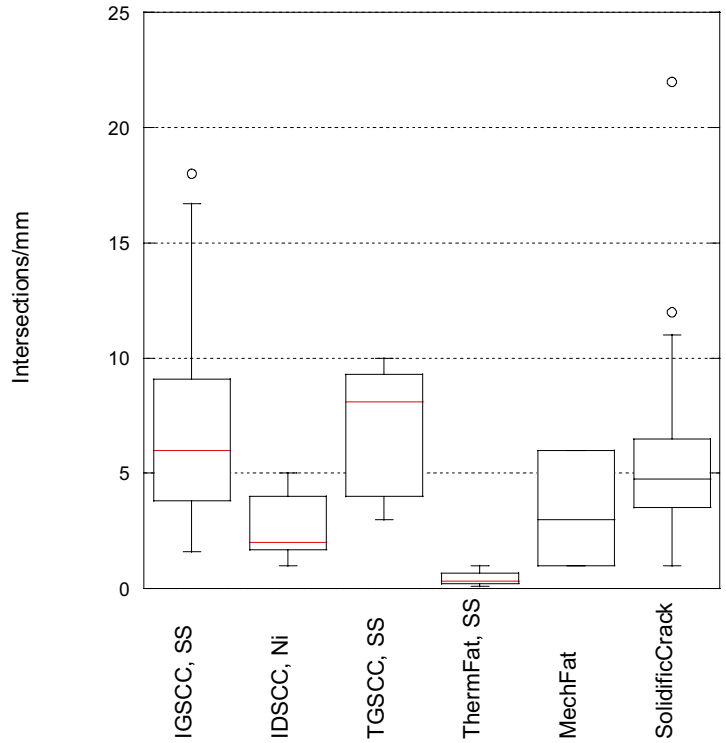

Figure 13-16 Comparison of number of intersection between six cracking mechanism/material group combinations (IGSCC in Nickel base alloys is excluded). Box plot.

	Number of turns/mm						
	IGSCC SS	IGSCC Ni	IDSCC Ni	TGSCC SS	Thermal Fatigue	Mechanical Fatigue	Solidification Cracking
Points	38	3	5	5	14	4	14
Minimum	4	16	2,7	5	1	1	1
Maximum	40	128	8,5	16	12	6	46
Mean	12,7	65,7	5,7	10,3	3,61	4	12,6
Median	9,9	53	7	8	3	4,5	9,5
RMS	15,2	80,5	6,14	11,2	4,54	4,53	17,0
Std Deviation	8,51	57,1	2,55	4,88	2,87	2,45	11,8
Variance	72,5	3256	6,49	23,8	8,24	6	139

Table 13-9 Statistics on number of turns/mm between seven cracking mechanism/material group combinations

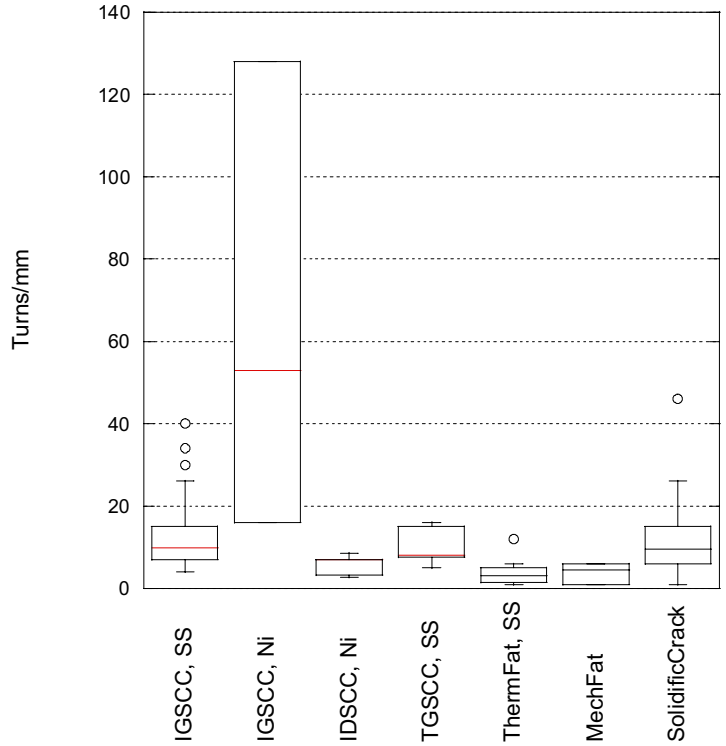

Figure 13-17 Comparison of number of turns/mm between seven cracking mechanism/material group combinations. Box plot.

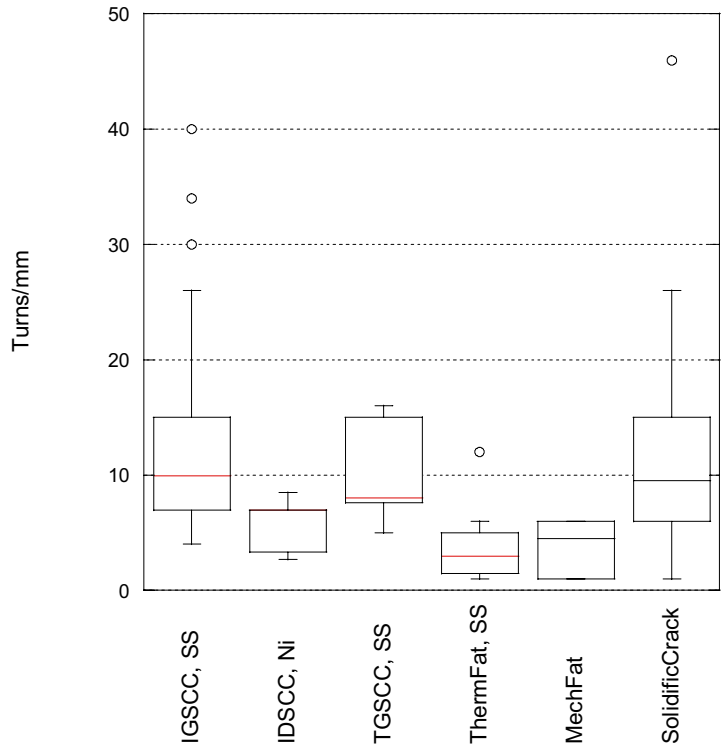

Figure 13-18 Comparison of number of turns/mm between six cracking mechanism/material group combinations (IGSCC in Nickel base alloys is excluded). Box plot.

13.3.6 Crack width

A comparison of crack width at surface and midway was made for all evaluated cracking mechanism/material group combinations. The statistics on stress corrosion cracking mechanisms are shown in Table 13-10 and on fatigue and solidification cracking in Table 13-11. All results are also shown in a box plot in Figure 13-19. This plot show outliners, which make the median region compressed. In Figure 13-20 the most extreme outliners are excluded and the median region less compressed

	Crack width [µm]							
	IGSCC, SS, surface	IGSCC, SS, midway	IGSCC, Ni, surface	IGSCC, Ni, midway	IDSCC, Ni, surface	IDSCC, Ni, midway	TGSCC, SS, surface	TGSCC, SS, midway
Points	65	65	14	17	14	18	25	29
Minimum	3	2	4	2	0	4	3	1
Maximum	160	133	260	260	120	180	500	200
Mean	37,7	22,5	42,4	44,8	33,4	51,7	49,9	25,8
Median	30	16	17,5	7	21	36	20	10
RMS	47,2	31,3	77,8	91,9	48,5	70,9	110	48,7
Std Deviation	28,7	22,0	67,7	82,7	36,4	49,9	99,6	42,0
Variance	821	485	4582	6846	1327	2493	9932	1763

Table 13-10 Comparison of crack width between four stress corrosion cracking mechanism/material group combinations

	Crack width [µm]					
	Thermal Fatigue, surface	Thermal Fatigue, midway	Mechanical Fatigue, surface	Mechanical Fatigue, midway	Solidification Cracking, surface	Solidification Cracking, midway
Points	29	31	15	15	17	16
Minimum	5	2	3	3	2	2
Maximum	380	190	450	250	250	110
Mean	51,4	31,3	79,4	54,5	38,6	21,6
Median	30	20	16	14	25	15,5
RMS	85,4	46,6	144	98,1	67,3	32,9
Std Deviation	69,3	35,1	125	84,4	56,8	25,6
Variance	4800	1230	15600	7125	3230	656

Table 13-11 Comparison of crack width between three fatigue cracking mechanism/material group combinations

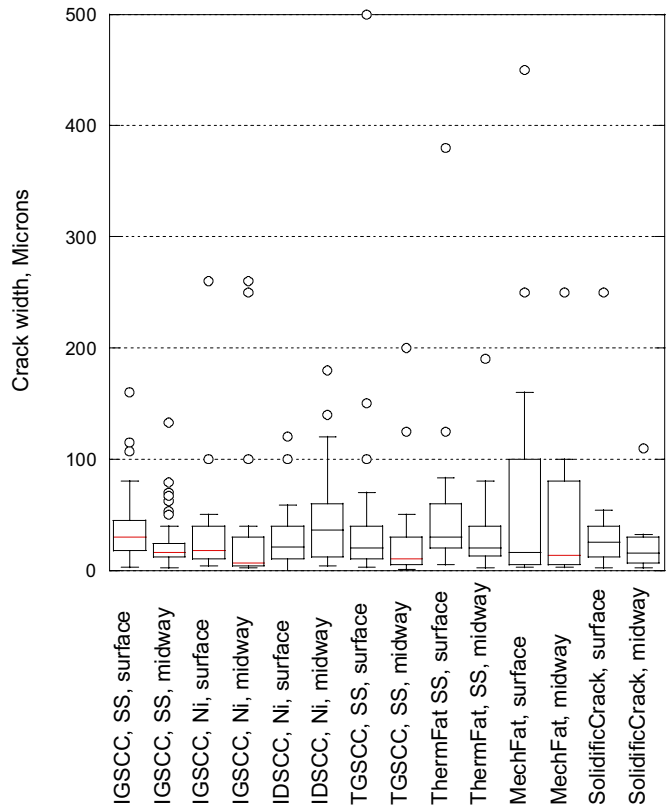

Figure 13-19 Comparison of crack width of seven cracking mechanism/material group combinations. Box plot.

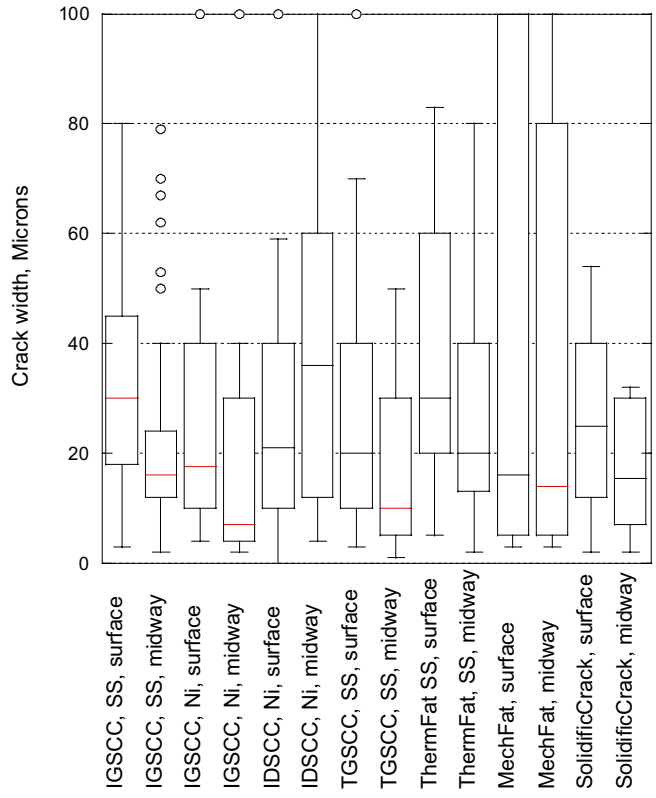

Figure 13-20 Comparison of crack width of seven cracking mechanism/material group combinations. Extreme outliners excluded. Box plot.

13.3.7 Comments on crack width measurements

One factor to consider when dealing with crack width measurements on cut out specimens is that the crack width is affected when the test piece is cut out, especially, if it is cut out from a weld or close to a weld. Weld residual stresses is expected to be redistributed when the piece is cut out, which will affect the crack width.

During recent years the replica technique has been used as a complement to visual inspection. A replica offer a permanent documentation of the crack features, such as crack width along the intersection with the surface. To find out the effect on the crack width by cutting out a sample, replicas were used as reference. The crack width was measured from replicas taken on cracks evaluated in this work and compared with the values measured on cross-sections of small specimens.

Example 1

A crack was detected in a pipe bend. The pipe outer diameter was 114 mm and the wall thickness 10 mm. The crack was located in the heat affected zone of a longitudinal weld close to a crossing girth weld. The distance from the longitudinal weld fusion line was measured as 0.75 mm. The crack was oriented parallel with longitudinal weld. The crack length was measured as 13 mm and the depth was 1.7 mm. Initially the crack width was measured as 5 μm on a replica taken from a ring formed piece. After an axial cut was made the ring expanded and the crack width decreased to 1 μm when measured on another replica. Subsequently, a small specimen was cut out and prepared by conventional metallography. When measuring the crack width on the small specimen it was found to be 12 μm. The example indicates that residual stresses may have significant influence on the crack width when measured on a cross-section of a small specimen /4/.

Example 2

A leakage was detected in a T-joint, where two piping systems meet. The leakage was caused by a through wall crack located in the incoming pipe nozzle close to a girth weld. The pipe outer diameter was 42 mm and the wall thickness 4.5 mm. The crack was oriented 50° to the girth weld. The distance to the weld was found to be in the range of 6 to 17 mm. The crack length was measured as 19 mm. The crack was recorded by the replica technique before small specimens were cut out. The crack width at the surface was measured from a photo taken of the replica. The magnification of the photo was 10 times, which means that the accuracy of the measurement was low. The crack width was measured as 60 – 110 μm. When measuring on small specimens two cross-sections were used. In one the crack depth was 3 mm and in the other 3.5 mm. The crack width was measured as 62 and 75 μm, respectively.

Example 3

A leakage was detected in a nozzle. The leakage was caused by a through wall crack located close to a girth weld. The crack was oriented parallel with the weld. The crack length and the distance to the weld were measured as 100 mm and 16 mm, respectively. The outer diameter of the nozzle was 114 mm and the wall thickness 7.1 mm. The crack features was recorded by means of a replica before cutting out small specimens. When measuring the crack width on a photo of the replica it was found to be 220 –

450 μm. Corresponding measurement on a cross-section of a small specimen cut out from the nozzle resulted in a crack width of 250 μm.

Example 4

The effect on crack width by cutting out small specimens was studied by Finite Element analysis in a project addressing NDT qualification of IDSCC in nickel base weld metal /5/. The assumption was a transverse crack in a pipe girth weld. The crack depth and size of the small specimen were varied to study the effect on the crack width before and after cutting out of the specimen. The results indicate that the crack width is reduced by a factor of 2.3 – 5.4 when the specimen is cut out. The crack width reduction was found to decreases with increasing size of the cut out specimen.

By reflecting the four examples it is obvious that several parameters are involved when considering the effect on crack width and in some cases it is even difficult to predict if the crack width will increase or decrease after cutting out a small specimen. However, a few reliable conclusions may be drawn:

- For cracking far away from welds (>10 mm) the crack width is only marginally affected.
- Cracking oriented parallel to welds is less affected compared to cracking transverse to welds.

To fully understand how the crack width is affected a considerably more detailed study is necessary. The most important factors to be considered are listed below.

- The dimensions of the cracked component; diameter and wall thickness.
- The dimensions of the crack; length and depth.
- The crack location, especially, relating to welds
- The crack orientation, especially, relating to welds.
- If the weld is a longitudinal weld or a girth weld.

14 Comments and conclusions

Typical characteristics for each cracking mechanism/material group combination are summarised below:

IGSCC in austenitic stainless steels

Most IGSCC develop next to welds with straight cracks oriented almost parallel to the weld. Single cracking is most common but occasionally two cracks are formed. In the through thickness direction IGSCC is typically straight or lightly bend and macroscopic branching is rare. The surface roughness is normally on a grain size magnitude and the cracks are particularly narrow providing secondary corrosion is small.

IGSCC in nickel base alloys

Similar characteristics to IGSCC in austenitic stainless steels may be expected. However, cracking close to weld are less frequent and macroscopic branching is more common for IGSCC in nickel base alloys compared to austenitic stainless steels.

IDSCC in nickel base alloy weld metal

Typically IDSCC is straight, single cracking in the weld metal transverse to the weld. In the through thickness direction IDSCC cause typically winding, non-branched cracks with large surface roughness due to course solidification micro-structure. The crack width often shows large variation along the crack and a width close to zero at the surface intersection is common.

TGSCC in austenitic stainless steels

Typically, TGSCC is branched both in surface and through thickness direction. The crack orientation shows a random distribution and the number of cracks is large. The crack surface roughness show low values and the crack width is typically medium range compared with the other groups.

Thermal fatigue in austenitic stainless steels

A large number of randomly oriented cracks are typical for thermal fatigue. However, single or few cracks with similar orientation occur. In the through thickness direction straight, non-branched cracking oriented in right angle to the surface is most common. The crack surface roughness is of medium range and larger than for mechanical fatigue.

Mechanical fatigue

Typically straight, single cracking oriented parallel with stress raisers is common for mechanical fatigue. In the through thickness direction most cracks are straight, non-branched and oriented in right angle to the surface. The crack surface roughness is the smallest and the correlation length the highest of all groups.

Solidification cracking

Solidification cracks occur equally frequent parallel as well as transversal to the weld. A large number of cracks are common. In the through thickness direction the cracks seldom show branching and is most often oriented close to 90º to the surface. The crack surface roughness is in the medium range and far below the one for IDSCC, which was not expected.

15 Suggested procedure for future evaluations

During the evaluation of morphology parameters from failure analysis reports it was found quite obvious that the majority of the failure investigations did not aim to measure the type of parameters needed for this work. Although, some of the parameters are used to diagnose the failure mechanism, several of them are of less importance when performing a failure analysis. Some reports did not even provide documentation, micro-graphs etc., sufficiently accurate for further evaluation.

To establish a more comprehensive and reliable database it is necessary to perform extended investigations on future failure cases, aiming to accurately determine the morphology parameters. A number of 20 - 30 cases for each data group is probably sufficient to provide statistical significance. The ordinary failure investigation pro-

cedure, thus, need to be extended with supplementary evaluations to determine all major morphology parameters given in section 4. Compared to the amount of work necessary to conduct an ordinary failure analysis the suggested supplementary evaluations probably would be a minor effort.

A procedure to perform such an extended failure investigation is suggested below.

- Record material grade and condition, heat treatment, cold forming etc.
- Record design and service conditions.
- Record component dimensions.
- Record crack length, crack location, crack surface orientation and macroscopic crack features.
- Measure crack width at the surface inter-section at several points along the crack.
- Sectioning should be done midway between the surface crack tips and when necessary at other points along the crack.

On the cross-section(s) the following parameters should be evaluated:

- Through thickness orientation (angle between crack and surface)
- Macroscopic shape
- Macroscopic branching and crack tip branching
- Crack tip radius
- Crack width at several points along the crack depth
- Surface roughness in terms of top height and wave length.
- The amount of non-metallic oxides inside the crack

16 References

/1/ Crack Characterisation for In-service Inspection, Ekström P., Wåle J. SKI Report 95:70, 1995

/2/ Cracking of Swedish nuclear power plants between 1972 and 2000 (Skador i svenska kärnkraftsanläggningars mekaniska anordningar 1972-2000) (in Swedish), Gott K, SKI Report 02:50, 2000

/3/ Characterising of IDSCC in Alloy 182 (Karakterisering av IDSCC i Alloy 182, Delmål 1 i projekt DAS182) (in Swedish), Wåle J, DNV Rapport Nr 10521100-1, 2001

/4/ Metallurgical exaination of piping components of SPRINT (Metallografisk undersökning av rördelar från SPRINT – 97, Ringhals 1) (in Swedish): Claesson B., Studsvik Material, Technical Note M-99/46

/5/ Project DAS 182, Final Report (in Swedish), Sundberg R., SQC Rapport 021/02

17 Acknowledgement

This work was made possible by fundings and support from the Swedich Nuclear Power Inspectorate.

www.ski.se

STATENS KÄRNKRAFTINSPEKTION
Swedish Nuclear Power Inspectorate

POST/POSTAL ADDRESS SE-106 58 Stockholm
BESÖK/OFFICE Klarabergsviadukten 90
TELEFON/TELEPHONE +46 (0)8 698 84 00
TELEFAX +46 (0)8 661 90 86
E-POST/E-MAIL ski@ski.se
WEBBPLATS/WEB SITE www.ski.se